MECHANICAL AND MOLECULAR CONTRIBUTION OF AIRWAY SMOOTH MUSCLE TO AIRWAY HYPERRESPONSIVENESS IN ASTHMA

by

CHRISTOPHER DANIEL PASCOE

B.Sc., The University of the Fraser Valley, 2010

A THESIS SUBMITTED IN PARTIAL FULFILLMENT OF THE REQUIREMENTS FOR THE DEGREE OF

DOCTOR OF PHILOSOPHY

in

THE FACULTY OF GRADUATE AND POSTDOCTORAL STUDIES

(Experimental Medicine)

THE UNIVERSITY OF BRITISH COLUMBIA

(Vancouver)

January 2015

Abstract

This thesis focuses on the mechanical and molecular role of airway smooth muscle (ASM) in asthma with the aim to determine the contribution of ASM to both asthma and airway hyperresponsiveness (AHR). The first three chapters involve studies probing the mechanical properties of tracheal ASM strips and how these may contribute to the development of AHR. They will aim to show that ASM can contribute to AHR without fundamental changes to the tissue. Specifically, the first chapter investigated the ASMs response to force oscillations mimicking breathing maneuvers under levels of activation that induce force adaptation, a phenomenon potentially seen in asthmatics. It shows that force adaptation can persist under conditions that mimic breathing maneuvers and therefore could contribute to AHR and ASM hypercontractility. The second chapter investigated the role of tone in limiting the strain imposed on ASM by breathing maneuvers and the subsequent response of ASM to those strains. The stiffening of muscle in response to agonist precedes force development and acts to decrease the strain applied to the ASM. As strain decreased, the effect on the muscle contractility was blunted. Interestingly, a prior history of oscillations induced a bronchoprotective effect in the strip and caused a two times greater decline in force than would normally be expected by the small strains indicating that prior DIs are effective in limiting the responsiveness of the ASM to agonist. The third chapter investigated whether the ASM is intrinsically responsible for the bronchoprotective effect of deep inspirations (DIs). This study showed that simulated prior DIs can increase the compliance of the muscle to subsequent DIs, and although the effect on a single strip of muscle is small, the effect at the whole lung level may be sufficient to explain the bronchoprotective effect of DIs. The final chapter describes the molecular phenotype of ASM in asthma at both the gene and protein level. Proteins involved in contraction were found not to be significantly altered in asthmatics; however a host of proteins involved in cytoskeletal structure were changed and could explain why asthmatic ASM is stiffer and less responsive to DIs.

Preface

This thesis is based on experiments performed by myself in the laboratory of Dr. Paré and Dr. Seow.

Chapter 1 is based on a published review: Pascoe CD, Wang L, Syyong HT, Pare PD. A Brief History of Airway Smooth Muscle's Role in Airway Hyperresponsiveness. *J Allergy* 2012. Reprinted with permission from Hindawi publishing group. The review was written in collaboration with lab members with certain sections being written by myself.

Chapter 2 is based on published research: C Pascoe, Y Jiao, CY Seow, PD Paré, Y Bossé. 2012. Force Oscillations Simulating Breathing Maneuvers do not Prevent Force Adaptation. *American Journal of Respiratory Cell and Molecular Biology.* Vol. 47, pp. 44-49. Reprinted with permission of the American Thoracic Society. Copyright © 2014 American Thoracic Society. The experiments were designed by Dr. Bossé and me. Experiments were performed by me and data were analyzed with help from Dr. Bossé, Dr. Paré and Dr. Seow. The muscle lever program was developed by Dr. Seow with help from Jiao Y. The muscle lever lab is maintained by Dr. Seow. Published manuscript was written by me with help from co-authors Dr. Paré, Dr. Seow, Dr. Bossé.

Chapter 3 is based on published research: A version of this chapter has been published. Pascoe CD, Seow CY, Paré PD, Bossé Y. Decrease of airway smooth muscle contractility induced by simulated breathing maneuvers is not simply proportional to strain. *J Appl Physiol* 114: 335–343, 2013. Reprinted with permission from American Physiological Society Journals ©. The experiments were designed by Dr. Bossé and me. Experiments were performed by me and data were analyzed with help from Dr. Bossé, Dr. Paré and Dr. Seow. The muscle lever program was developed by Dr. Seow with help from Jiao Y. The muscle lever lab is maintained by Dr. Seow. Published manuscript was written by me with help from co-authors Dr. Paré, Dr. Seow, Dr. Bossé.

Chapter 4 is based on published research: Pascoe CD, Donovan GM, Bossé Y, Seow CY, Paré PD. Bronchoprotective effect of simulated deep inspirations in tracheal smooth muscle. *J Appl Physiol* (EPub). Reprinted with permission from American Physiological Society Journals ©. The experiments were designed by Dr. Paré and me. Experiments and data analysis were performed by me. Computational modeling was performed by Dr. Donovan. Muscle lever program was developed by Dr. Seow with help from Jiao Y. Muscle lever lab is maintained by Dr. Seow. Published manuscript was written by me with help from co-authors Dr. Donovan, Dr. Bossé, Dr. Seow and Dr. Paré.

Chapter 5 is based on work carried out primarily by me. Sample collection and RNA isolation was performed by me. Morphometric measurements were collected by Arsenault B. Gene expression was run on Nanostring nCounter system by Nanostring®. Gene expression data were analyzed by me. Statistical consultation and tests were performed by the Center for Health Evaluation and Outcome Sciences (CHEOS). Tissue preparation and immunnohistochemical (IHC) staining were done by Samra A and Elliott M. IHC analysis was performed by Xia I and me. All data analysis, manuscript writing and figures creation were done by me. Dr Paré and Dr. Seow provided lab space, expertise, manuscript editing and funds to perform experiments.

The work presented in this thesis is covered under the Human Ethics Board of UBC certificate number H12-02487, project title “Plasticity in airway smooth muscle”

Table of Contents

List of Tables

List of Figures

List of Abbreviations and Symbols

AC - Adenylate cyclase

ACh – Acetylchoine

ACTA – α-smooth muscle actin

ADAM33 – A disintegrin and metalloproteinase domain-containing protein 33

AHR – Airway hyperresponsiveness

ANOVA – Analysis of variance

ASM – Airway smooth muscle

ATP - Adenosine triphosphate

BHR – Bronchial hyperresponsiveness

Ca^{2+} - Calcium ions

$CaCl_2$ – Calcium chloride

cADPR – Cyclic adenosine diphosphoribose

CAM - Calmodulin

cAMP – Cyclic adenosine monophosphate

CCh – Carbachol

CD38 - Cyclic ADP ribose hydrolase

CHEOS - Center for Health Evaluation & Outcome Sciences

CNS – Central nervous system

CO_2 – Carbon dioxide

COPD - Chronic obstructive pulmonary disease

CPI-17 - C-kinase potentiated protein phosphatase-1 inhibitor

CV – Coefficient of variation

DAG – Diacylglycerol

DI – Deep inspiration

DRS – Dose response slope

EFS – Electrical field stimulation

F_{CCh} – Force produced in response to carbachol

FEV_1 – Forced expiratory volume in 1 second

FFPE – Formalin fixed paraffin embedded

FLNA – Filamin alpha

FLNB – Filamin beta

FLNC – Filamin gamma

F_{max} – Maximal force produced in response to electrical field stimulation

FRC – Functional residual capacity

F_{RT} – Force of the resting tension

FVC – Forced vital capacity

$G\alpha_{12/13}$ – G protein alpha subunit 12/13

$G\alpha_{s}$ – G protein alpha subunit S

$G\alpha_{q/11}$ – G protein alpha subunit q/11

GM-CSF - Granulocyte macrophage colony-stimulating factor

GNB2L1 - Guanine nucleotide-binding protein subunit beta-2-like 1

GTP - Guanosine-5'-triphosphate

GUSB - Beta-glucuronidase

GWAS – Genome wide association study

η – Dynamic viscosity

H&E – Hematoxylin and eosin

Hz – Hertz

IHC – Immunohistochemistry

IIAM – International institute for the Advancement of Medicine

IL-1β – Interleukin 1 beta

IL-13 – Interleukin 13

IP_3 – Inositol triphosphate

KCl – Potassium chloride

kDa – Kilodalton

KEGG – Krypto Encyclopedia of Genes and Gemones

kPa – Kilopascal

L – length

l_O – Operating length

L_{Ref} – Reference length

L-T – Length tension

MCh – Methacholine

$MgSO_4$ – Magnesium sulfate

MLC_{20} – Myosin light chain 20 kilodalton

MLCK – Myosin light chain kinase

MLCP – Myosin light chain phosphatase

mm – Millimeter

mM – Millimolar

mN – Millinewton

mRNA – Messenger ribonucleic acid

MVA – Motor vehicle accident

MYH11 – Smooth muscle myosin heavy chain

NaCl – Sodium chloride

NAD^+ - Nicotinamide adenine dinucleotide

$NaHCO_3$ – Sodium bicarbonate

NaH_2PO_4 – Sodium phosphate monobasic

nM – Nanomolar

O_2 – Oxygen

P_{bm} – Basement membrane perimeter

PC_{20} – Provocative concentration of methacholine causing a 20% reduction in FEV_1

PCLS – Precision cut lung slices

P_i – Internal perimeter

PIP_2 - Phosphatidylinositol 4,5-bisphosphate

PKC – Protein kinase C

PLC - Phospholipase C

POLR2A - DNA-directed RNA polymerase II subunit RPB1

PPD – Packs per day

R – Airflow resistance

r – Radius

Raw – Airway resistance

RNA - Ribonucleic acid

ROCK – Rho-associated protein kinase

RPL19 - 60S ribosomal protein L19

RSV – Respiratory syncytial virus

SD – Standard deviation

SEM – Standard error of the mean

SM1 – Smooth muscle myosin heavy chain isoform 1

SM2 – Smooth muscle myosin heavy chain isoform 2

SM22 – Transgelin (alternative name)

SMA – Smooth muscle myosin heavy chain isoform A

SMB – Smooth muscle myosin heavy chain isoform B

SMTN – Smoothelin

SR – Sarcoplasmic reticulum

$T_{1/2}$ – Time to half of maximal shortening

TAGLN – Transgelin

TB – Tidal breathing

TBP – TATA-binding protein

TGF-β - Transforming growth factor beta

TLC – Total lung capacity

μM – Micromolar

ZYX - Zyxin

Acknowledgements

The road to accomplishing a PhD is not a journey that is taken alone and therefore I have many people I would like to thank for help along the way. I will start off by thanking my supervisors Dr. Peter Paré and Dr. Chun Seow who have provided me guidance and taught me almost everything I know and for giving me the opportunity to attend conferences both locally and internationally; these chances taught me more than any course ever could. I would like to thank Dr. Paré for taking a chance on an undergraduate from a relatively unknown University out in the Fraser Valley. He has been an exceptional mentor to me and helped nurture my scientific curiosity. His ever calming presence has helped me remain calm and focused during my studies. To Dr. Seow I would like to say thank you for teaching me much about biophysics, a topic I knew nothing about when I first entered the lab. He has also been an important mentor for me and has always been willing to answer any questions about mechanics I could come up with. Both of my supervisors have been key to my success and productivity in the lab.

I would also like to thank Dr. Bossé who was a post doctoral fellow in the lab when I began and took on the task of teaching me the techniques necessary for a lot of what is in this thesis. He helped me publish two first author manuscripts under his supervision and has been vital in making me the successful scientist I am. Dr. Bossé helped me get comfortable with my training as a scientist and I owe him a huge amount of gratitude.

To the other members of my lab, thank you for providing years of friendship, camaraderie, and great memories. There have been many that have come and gone over the years but they have all had an impact on me, so thank you Dr. Chin, Dr. Syyong, Dr. Raqeeb, Mr. Norris, Mr. Liu, Mr. Lan, Mr. Swyngedouw, Mrs. Banaem, Dr. Zhang, and Mr. Solomon.

To the various members of the Center for Heart Lung Innovation for everything you have done. You've been supporters, friends, colleagues and collaborators who have enabled me to reach my goals. To Mr. Elliott and Mrs. Samra for your help with all the help sectioning, staining and troubleshooting. You were always willing to help me whenever I came asking. Mr. English, thank you for scanning countless number of slides over the course of my training.

Finally I would like to acknowledge all the people I have met and had stimulating conversations or beers with at the variety of conferences I have been privileged to attend. I have made many friendships and connections that no doubt will prove valuable in achieving my future career goals.

Dedication

This thesis is dedicated to my parents, Paula and Peter Kast, and Doug and Heather Pascoe, without whom none of my education would have been possible. Thank you for trying your hardest to understand all of my research and always supporting me; it has been a long haul but you have helped me make it. I would also like to dedicate it to my fiancée Amanda Hargreaves who stood by my side throughout all the classes, experiments, funding applications and long days of writing it took me to get to this point. You have been perfectly supportive and offered me a break from the constant intellectual wear and tear. Finally David Vandenberg, thank you for being my best friend, constant supporter and an ear that is always willing to listen.

Chapter 1 Introduction[1]

1.1 Asthma Overview

In 2012 it was estimated asthma affected the lives of over 2 million Canadians (1) and this number has been on the rise for a number of years. Asthma deaths are rare but the cost of treating asthma is over $40 million annually in British Columbia alone (2). The World Health Organization defines Asthma as a chronic inflammatory condition characterized by chronic, recurring episodes of wheezing and breathlessness (3) caused primarily by airway constriction and airway inflammation. Asthma is also hallmarked by the structural remodeling that occurs in the airways. These changes include: increase in the mass of the airway smooth muscle (ASM) surrounding the airways (4), epithelial damage and hyperplasia (5), goblet cell metaplasia (6), mucus hyper-secretion and basement membrane thickening (7), and are collectively termed airway remodeling (8) (Figure 1.1). Asthma is typically diagnosed by a physician using a spirometric test to measure forced expiratory volume in 1 second (FEV_1) with or without a bronchodilator to determine the level of airway constriction. Healthy patients generally have an FEV_1/FVC (FVC – Forced vital capacity) ratio of above 70%, meaning they can expire 70% of their lungs volume in 1 second. A history and physical examination can also be used but when the diagnosis is in doubt a test for airway hyperresponsiveness can be preformed. In this test the subject is challenged with an aerosol of histamine or methacholine and measures of airway narrowing are made, most frequently by spirometry and the determination of FEV_1. Asthmatic subjects show an exaggerated responsiveness to the stimuli which is termed airway hyperresponsiveness (AHR) or bronchial hyperresponsiveness (BHR). Most commonly the test involves the generation of dose response curve on which a PC_{20} or dose response slope (DRS) can be measured to help quantify the degree of AHR (9, 10). PC_{20} is the dose of an agonist that elicits a 20% fall in FEV_1.

To help treat the main symptom of asthma, which is breathlessness, bronchodilators (β2-agonists) are prescribed and act to relax the ASM that actively narrows the airway during an asthma attack. Bronchodilators achieve this by increasing cAMP levels in the cell through the β2-adrenergic receptor (11, 12). cAMP is a second messenger that increases calcium efflux and decreases the activity of myosin light chain kinase (MLCK) (see figure 1.2). The other staple of asthma treatment is the use of

[1] Parts of this chapter have been published. Pascoe CD, Wang L, Syyong HT, Pare PD. A Brief History of Airway Smooth Muscle's Role in Airway Hyperresponsiveness. *J Allergy* 2012.

glucocorticoids to control inflammation in the airways that likely causes most of the structural changes within the asthmatic airway (13). Even with these normally effective therapies, a subset of patients (around 5-10%) are known to be steroid resistant and represent one of the most difficult challenges in asthma management (14). In these patients, antileukotrienes such as montelukast and zileuton may be of some use (15–17).

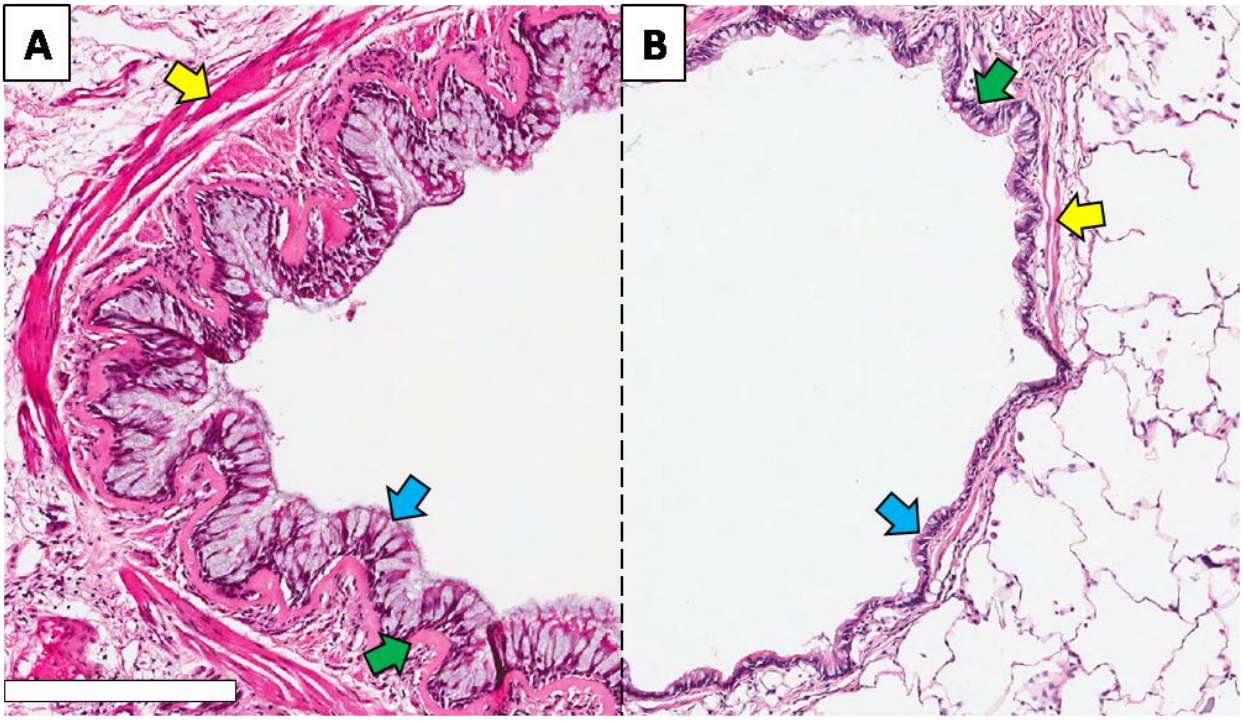

Figure 1.1 Comparison between asthmatic airway on left (A) and non-asthmatic airway on right (B). Airways are stained using hematoxylin and eosin (H&E). Blue arrows identifiy the epithelial layer. Green arrows identifies the basement membrane. Yellow arrows identify the ASM layer. Remodeling changes including ASM hypertrophy and hyperplasia are clearly visible in the asthmatic airway. Scale bar is 300µm.

1.2 Airway Hyperresponsiveness

The term AHR has become synonymous with asthma and it is one of its hallmark features. AHR is defined as an increased sensitivity to normally non-noxious stimuli and was first reported by Alexander and Paddock in 1921 (18) when they noted that an attack of asthma could be precipitated by subcutaneous injections of pilocarpine, a muscarinic receptor agonist. Similarly Weiss et al. in 1932 (19) found that asthmatics became more breathless and had a greater fall in FVC in response to intravenous

histamine than did non-asthmatic subjects. A wide variety of stimuli can trigger AHR in asthmatics including: acetyl-beta-methylcholine (20), carbachol (21), histamine (22), leukotrienes (23), prostaglandin F2α (24), propranolol (25), cold air (26), sulphur dioxide (27), dust (28), and exercise (29). Most of these act directly on smooth muscle but others act to cause secondary release of contractile agonists (e.g. cold air) or inhibition of bronchodilating factors (e.g. propanolol). These studies illustrate a key feature of AHR, that it is non-specific. If a subject is hyperresponsive to one stimulus they are hyperresponsive to all agents that act by stimulating smooth muscle contraction. This observation is important since it suggests that the phenomenon is primarily postjunctional (i.e., on the muscle side of the neuromuscular junction) and not related to specific abnormalities of any specific agonist receptors on smooth muscle cells.

These data support the hypothesis that a change in ASM phenotype is responsible for the phenomenon of AHR in asthma but an additional important early observation was that AHR is not limited to asthmatics. Patients with a variety of diseases characterized by airway obstruction show AHR and the degree of airway responsiveness is related to the degree of baseline airway obstruction (30–32). These results suggest that the responsiveness may be a consequence of the airway narrowing rather than a predisposing factor. However in asthma, AHR is relatively independent of baseline lung function (33) suggesting that the underlying mechanisms may be distinct from the AHR seen in COPD and other airway diseases. Interestingly, normal healthy individuals show a range of responsiveness to methacholine (34) suggesting that airway reactivity may be genetically determined.

A pivotal study by Woolcock et al. (9) published in 1984 shows that an important feature of AHR in asthma is an increase in the maximal achievable airway narrowing in response to histamine; most non-asthmatic subjects can inhale high concentrations of histamine leading to little airway narrowing. They show that asthmatics not only responds at a much lower dose or concentration (around 1mg/ml vs. 100mg/ml) than non-asthmatics (increased sensitivity) but that the amount of airway narrowing measured by the decline in forced expiratory flow is much greater. This was attributed to a lack of a normal mechanism in asthmatics that inhibits severe airway narrowing in non-asthmatics and hints at a link to maximal ASM contraction.

A seminal observation by De Vries et al. in 1962 showed that there is diurnal variation in responsiveness (35) with the greatest responsiveness occurring at night when the baseline airway narrowing tends to be greatest. Kerrebijin in 1970, showed AHR increases after an acute spontaneous attack of asthma and then improves over time as the attack subsides (36), again suggesting that AHR is a

consequence of asthma, or at least that a portion of AHR is variable. Parker et al. in 1965 show that AHR occurs during or after a respiratory tract infection in normal subjects supporting the concept of acquired, reversible AHR (31). Additional important observations by various studies were that AHR increases after the late, but not the early, response by asthmatics (37) to inhaled allergen and that AHR could be attenuated by prolonged anti-inflammatory therapy (38). Together, these data show that ASM can contribute to AHR but is unlikely to be the only contributing factor. Inflammation and viral infection are two other factors that may be important contributors to AHR.

1.3 Airway Smooth Muscle and AHR

It has long been recognized that muscular constriction of the bronchi contributes to airway narrowing in asthma. In his 1698 treatise on asthma Floyer wrote, "the Bronchia are contracted … and that produces the Wheezing noise in Expiration, and that this Symptom does not depend on Phlegm is plain, because the Hysteric, who have no Phlegm, Wheeze very much" (39). In mid-nineteenth century, Salter (40) wished that it could be "shown beyond cavil that spasmodic stricture of the bronchial tubes is the only possible cause of asthma, that it is adequate to the production of all the phenomena." He was referring to the "spastic contraction of the fiber-cells of organic muscle," which we now refer to as the ASM.

In a landmark study of the pathology of asthma Huber and Koessler (41) described and quantified the increased mass of ASM compared to controls. The evidence for an increase in muscle mass and the relative contributions of hypertrophy and hyperplasia to this process has been recently analyzed in a study by James et al. in 2012 (4); Thus there is little doubt that ASM is increased in asthma. The questions that remain are whether this increase is the cause of airway hyperresponsiveness (AHR) or whether there are additional fundamental changes in the phenotype of the ASM which contribute to AHR.

Despite the increasing interest in AHR during the 60s and 70s, there were few attempts to study the mechanism. As early as 1951, Schild et al. (42) found that lung tissue and bronchial muscle obtained from an asthmatic patient's release more histamine and the airways responds with contraction to challenge with house dust mite or pollen compared to a non-asthmatic tissue. It was not until the early 1980s that there was speculation that AHR was caused by an intrinsic alterations in ASM structure or function. The prevalent theories prior to that were related to pre-existing airway narrowing (43, 44), increased sensitivity of airway irritant receptors (45) or a relative deficiency of beta adrenergic

bronchodilation (46). Freedman (47) and Benson (43) were among the first to systematically consider the potential link between the structural and functional changes in the airways and AHR. They pointed out that airway wall thickening and/or baseline airway smooth muscle tone could amplify the airway narrowing caused by a subsequent stimulus supporting the concept that AHR was a manifestation of airway disease and not a root cause.

Studies of excised human airway smooth muscle began in the 1980s and for the most part failed to incriminate ASM, although most of the initial studies examined only isometric force. Although some studies suggest that ASM from asthmatics is stronger (48, 49) the bulk of the data (50–54) show that the maximal force that ASM can generate does not differ in asthmatic and non-asthmatic individuals. These studies spawned a number of different avenues of investigation in an attempt to explain AHR. Generally these studies focus on additional properties of ASM that could be important in generating AHR or on additional explanations for AHR that do not involve a fundamental change in ASM phenotype. In 1986, Moreno et al. (55) presented an extensive theoretical analysis of the geometric factors which could link ASM activation to excessive airway narrowing without the need for excessive ASM force production, amplifying the earlier work of Freedman (47). Additionally, James et al. (56) and Wiggs et al. (57) had quantified the potential contribution of airway wall remodeling to increased maximal airway narrowing. Further work by Lambert et al. (58) concluded that the increase in ASM mass was potentially the most important structural change to explain AHR (provided that the increased ASM mass retained its contractile phenotype). This conclusion has been supported by recent work from Oliver et al. (59) who added cyclical stress to the model to simulate breathing. Their analyses confirmed the importance of increased ASM mass and also suggested that increased ASM could explain the failure of asthmatics to respond to deep inspirations (DIs).

The other mechanical properties of ASM that have been explored as potential contributors to AHR include an increased maximal amount of shortening, increased velocity of shortening, reduced relaxation, and a reduced effect of strain on the reduction of force that occurs with breathing and deep inspiration. Ma et al. (60) examined the maximal shortening and the shortening velocity of primary isolated ASM cells from asthmatic and normal subjects and found both greater maximal shortening and faster shortening associated with an increased expression of myosin light chain kinase. Léguillette et al. (61) studied the relative expression of two isoforms of human myosin in the ASM of asthmatic and non-asthmatic subjects. They found that there was increased mRNA for the SM-B isoform in asthmatic tissue which is associated with an increased rate of propulsion of actin. However, studies on asthmatic tracheal

ASM show no difference in maximal shortening or shortening velocity (53). It is possible that the inflammation occurring around the intraparenchymal airways does not involve the trachea and that this may be the reason why no differences in mechanical properties are seen. However, this then questions whether there are intrinsic differences within the ASM in asthmatics or whether the differences only manifest themselves in an allergic inflammatory environment. It has also been suggested that the intrinsic plasticity of ASM could play a role in the development of AHR through adaptation to shorter lengths (62–64) and adaptation to basal tone induced by inflammatory mediators and other agonists (65, 66). This will be discussed in more detail in subchapter 1.5. Further studies on better characterized asthmatics are needed.

1.4 Smooth Muscle Physiology

Smooth muscle cells are important in the function of hollow organs and vessels throughout the body including the bladder and digestive tract and function to narrow the lumen of these hollow organs to either propel or regulate the flow of their contents (67). Smooth muscle cells lack the characteristic banding pattern of skeletal muscle sarcomeres and are not under conscious control (67). Within the airways, ASM plays an important role in moving liquid through the lung during development and may assits in fetal lung development (68), however in the adult lung ASM appears to sereve no known function and is often referred to the appendix of the lung (69). ASM does, however, have a well characterized role in exacerbations of asthma. ASM is arranged helically around the airways (70) and acts to narrow the airways and increase resistance to flow in response to a variety of contractile agonists including: acetylcholine (ACh) (71), histamine (72) , leukotrienes (73), prostaglandins (74) and serotonin (74). Contraction is primarily initiated by agonists binding to their G-coupled protein receptors to liberate the second messenger inositol triphosphate (IP_3). IP_3 acts on IP_3 receptors within the sarcoplasmic reticulum to release Ca^{2+}. Like skeletal muscle, Ca^{2+} is necessary for contraction in smooth muscle whereby myosin light chain kinase (MLCK) is activated by the Ca^{2+}-CAM complex and then phosphorylates the 20-kDa light chain of myosin (MLC_{20}), allowing for the myosin head to interact with actin and undergo cross-bridge cycling (75). To relax the cell, cyclic AMP (cAMP) acts to remove Ca^{2+} and increase myosin light chain phosphatase (MLCP) activity thereby de-phosphorylating MLC_{20} and causing the myosin head to detach from actin. In addition to the classical contractile pathway, there are proteins which act to sensitize the cell to Ca^{2+} by inhibiting MLCP or activating MLCK. These proteins include the kinase ROCK (76) and CPI-17 (77). The ‘classical’ contractile pathway is summarized in Figure 1.2.

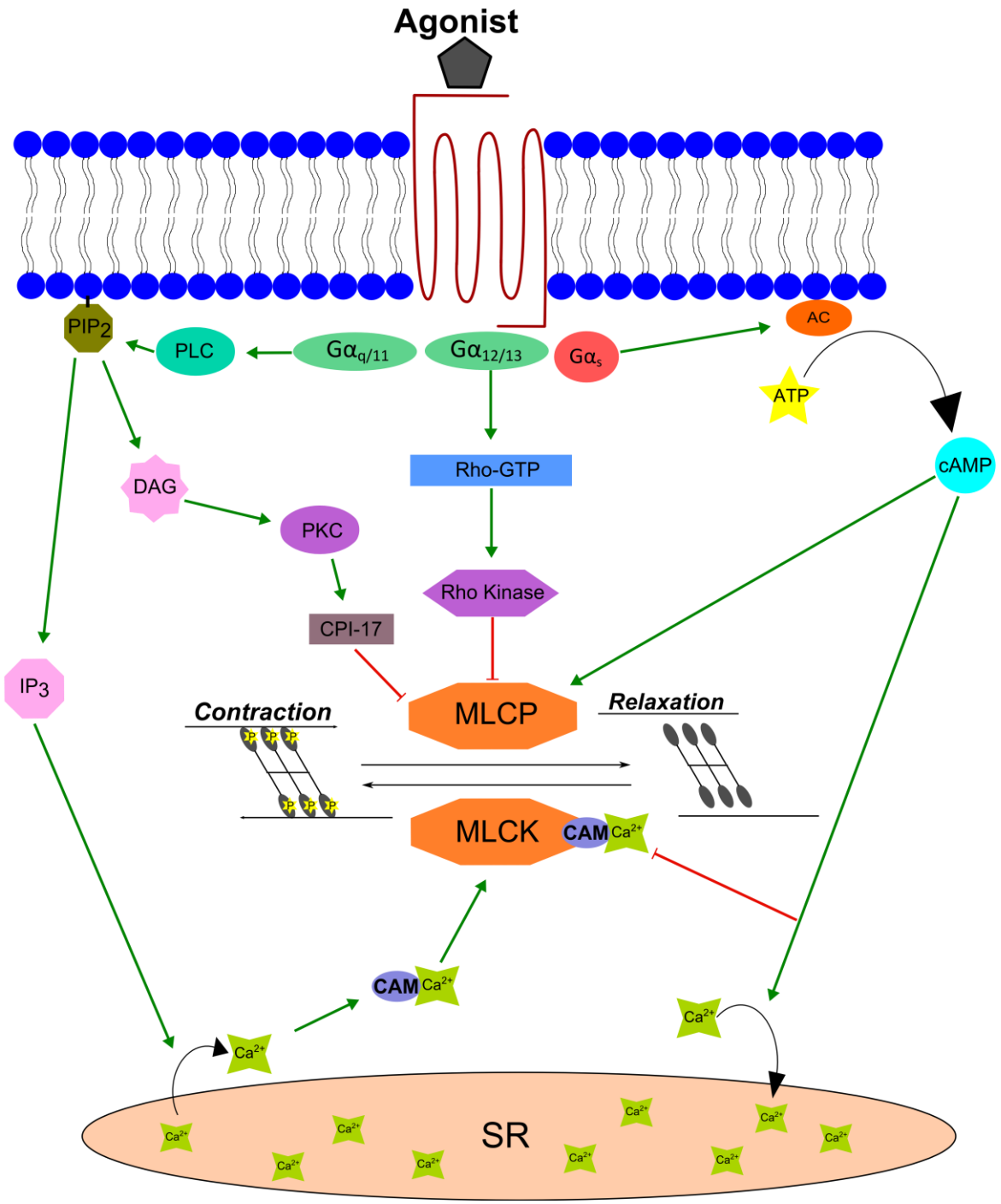
Agonist
PIP2
PLC
Gαq/11
Gα12/13
Gαs
AC
ATP
cAMP
DAG
PKC
Rho-GTP
Rho Kinase
CPI-17
IP3
Contraction
MLCP
Relaxation
MLCK
CAM
Ca2+
SR

Figure 1.2 Schematic of ASM contraction and relaxation pathways. Binding of agoinsts to membrane receptors activates phopholipase C (PLC) through a G-protein ($G\alpha_{q/11}$). PLC hyrdolyzes phosphatidylinositol 4,5-bisphosphate (PIP_2) into two second messengers: diacylglycerol (DAG) and inositol 1,4,5-triphosphate (IP_3). IP_3 works to the sarcoplasmic reticulum (SR) to release calcium (Ca^{2+}) which then binds to calmodulin (CAM) and activates myosin light chain kinase (MLCK). Actiavated MLCK phosphorylates the light chain of the myosin and initiates cross bridge cycling. DAG activates protein kinase C (PKC) which in turn activates C-kinase potentiated protein phosphatase-1 inhibitor (CPI-17). CPI-17 is an inhibitor of myosin light chain phosphatase (MLCP). In parallel to this pathway, $G\alpha_{12/13}$ activates the GTP binding protein RHOA which activates Rho Kinase. Rho kinase can inhibit MLCP. Removal of the agonist or binding of a relaxing compound activates the inhibitor G protein $G\alpha_S$ to relax the muscle. $G\alpha_S$ activates adenylate cylcase (AC) which produces the second messenger cyclic AMP (cAMP). cAMP relaxes the muscle by: 1) activating MLCP, 2) increasing the re-uptake of Ca^{2+} into the SR and 3) inhibiting MLCK activity.

There are qualitative similarities between the contraction of skeletal and smooth muscle. Both show length dependence of force and shortening as characterized in the length-tension relationship and load-dependence of shortening velocity as characterized in the force-velocity relationship. The length tension relationship of smooth muscle, like skeletal muscle, has an optimal operating length (l_0) for producing force (78) but this length is not a unique length and is instead able to change by the process of length adaptation. Unlike skeletal muscle, the smooth muscle length tension relationship is broad and the maximal active force is relatively independent of muscle length (79). This is again also the result of length adaptation occurring as the muscle length is changed. The ability of smooth muscle to produce force over large ranges in length may be due to the lack of a rigid sarcomeric structure like the one present in skeletal muscle (80, 81). The velocity of shortening for smooth muscle follows a hyperbolic curve that can be fitted by the Hill equation (79) indicating that the sliding-filament and cross-bridge mechanism of contraction observed in striated muscle is also operative in smooth muscle. It also indicates that increasing loads, such as occur during airway narrowing, decrease the velocity of shortening. Interestingly, smooth muscle that has shortened to a given length produces less force at that length than when the muscle contracts isometrically from the same length, another indication of plasticity (82). This may be because during contraction, the attachment of actin to the cell membrane adhesion complexes is more rigid and the actin cytoskeleton cannot remodel to adapt to the shorter

length (83). However, when the muscle is passively shortened first, the actin is not rigidly attached to the membrane complexes and the process of actin and myosin filament remodeling and subsequent length adaptation can occur allowing the muscle to produce more force (63, 80, 81, 83). It has been shown in a recent manuscript that myosin filaments in smooth muscle are not confined to a single unique length and therefore could contribute to the process of length adaptation by allowing the addition or subtraction of short fragments of myosin filaments to contractile units (84). Other noticeable differences between skeletal and smooth muscles are the differences in velocities of shortening and maximal unloaded shortening. Smooth muscle shortens up to 8 times slower than skeletal muscle (79) but it is able to shorten substantially, up to 80% of the muscles original length compared to 40% in skeletal muscle (79). This difference in shortening between smooth and skeletal muscle is likely due to the lack of z-bands which limit the shortening as of skeletal muscles. The intrinsic plasticity of smooth muscle that allows it to adapt to different lengths or to different levels of activation may play an important role in the development of AHR in a diseased state.

1.5 ASM Plasticity: Length and Force Adaptation

The term length adaptation (also called plasticity) refers to the ability of the muscle to adapt its contractile capacity to length changes. Pratusevich et al. (64) showed that ASM is able to rapidly adapt to different lengths and maintain optimal force generation over a large length range. They observed that the adaptive process consists of two stages, an immediate reduction in force generation following the length change followed by a gradual recovery of the force toward that which was achieved before the length change. When length oscillation (to simulate DIs) was applied to un-stimulated ASM, a similar two-staged adaptive process was observed (85). A reduction in active force in response to stimulation was observed immediately after the oscillation and the magnitude of active force reduction was linearly related to the amplitude of the oscillation. After this initial reduction, the muscle underwent the adaptation process by which active force increases gradually with each stimulation until stabilizing at the level that was present prior to length oscillation. The adaptation process takes about 30 to 40 min to complete depending on the species of animal and how frequently the muscle is stimulated. McParland et al. (86) showed that ASM from pigs can adapt to a shortened state induced by carbachol within 30 min, resulting in increased force, shortening and shortening velocity.

The effects of subacute and chronic (hours to days) length changes on contractile and structural features have been examined in various skeletal muscle preparations. In the diaphragm, as an example,

chronic shortening is clinically relevant in emphysema because the hyperinflation caused by emphysema results in persistent shortening of the muscle (87). When emphysema is induced in experimental animals by lung elastolysis, the muscle recovers its ability to generate force at short lengths because sarcomeres are subtracted in series over a period of days to weeks (88, 89). Addition of sarcomeres in series occurs during chronic muscle lengthening (90). In smooth muscle however, there is no defined sarcomeric structure and therefore length adaptation must occur by a different mechanism (81). It has been shown that length adaptation in smooth muscle may occur by the rearrangement of the contractile apparatus and actin skeleton (80, 81). Changes in the number of contractile elements (myosin and actin) in series and parallel (80, 81) could account for the ability of ASM to adapt to different lengths and the addition or subtraction of myosin units to or from the filaments could also play a role in adaptation (84).

Structural remodeling in asthmatic airways includes increased mucus secretion, excessive deposition of extracellular matrix, thickening of the airway wall, smooth muscle cell hypertrophy/hyperplasia and angiogenesis. These structural alterations could act to narrow the airway and influence airway function by allowing ASM to operate and adapt to short lengths. ASM adaptation to prolonged length changes is much faster than skeletal muscle. It was observed that when ASM strips are passively lengthened or shortened in vitro over a period of 24 hr, length-tension (L-T) curves shifted compared to the control curve, allowing maintenance of maximal isometric force at the new length (63). The result is that ASM adapted to a shorter length is able to generate the same maximal force at longer lengths. Compounding this effect there is a shift of the passive length tension curve to the left, indicating stiffening of the ASM and making reversal of the shortened state by DIs more difficult. Naghshin et al. (91) showed that adaptation to passive shortening is reversible after 3 days but not after 7 days. These results suggest that ASM adaptation to shortening can not only occur quickly but that more permanent changes can occur if the shortened conditions persist.

Another form of ASM plasticity which could contribute to AHR is the effect of tone on smooth muscle contractility. This is an old idea (42) but has received recent attention due to the studies of Bossé and associates (65, 66, 92) who used sheep trachealis to model the effect of basal tone on ASM's ability to contract (66). They have shown that tone induced with cholinergic agonists, prostanoids or histamine results in a more than additive effect on subsequent force production in response to electric field stimulation. They have termed this phenomenon force adaptation and have modeled the increased airway narrowing that could come about because of force adaptation (65). For example, they calculate

that force adaptation occurring in an airway of the 9th generation could increase airway narrowing by 48% and airway resistance by 274%. Force adaption is a very plausible contributor to exaggerated airway narrowing in asthmatics given the abundance of inflammatory mediators and spasmogens that the ASM of asthmatics is exposed to. In addition the loss of this tone when the ASM is examined *in vitro* may be one explanation for the failure of excised asthmatic ASM to show altered contractile function in most studies. It is unlikely that force adaptation or length adaptation is the sole cause of AHR but instead is one of a number of components that leads to AHR in asthmatic subjects.

1.6 Deep Inspirations: Bronchodilation and Bronchoprotection

Important papers by Fish in the late 1970's (93)(94) and Skloot et al. (95)in 1995, showed that in asthmatics DI fails to prevent airway narrowing, suggested a whole new paradigm for AHR and asthma, the possibility that there might be a fundamental difference in the ASM's response to stress or strain in asthma. A large number of *in vitro* and *in vivo* studies designed to establish the mechanism of this difference followed these publications. Although the physiological processes responsible for the beneficial effects of DI are unknown, they are thought to involve mechanical stretch of the ASM during lung inflation (96). However other factors may also be involved including neural and humoral pathways (97).

In vitro studies showed that the contractile capability of an isolated ASM strip is attenuated by subjecting it to length oscillations (98)(85). Fredberg et al. (99) developed a model to demonstrate that mechanical strains in ASM caused by tidal breathing or DI causes detachment of myosin heads from actin sooner than it would during static contraction, leading to a steady-state equilibrium. They suggested that in asthma, disruption of this equilibrium leads to the "frozen" contractile state where the muscle is not stretched enough to allow enough mechanical perturbation to disrupt the cross-bridges.

DI is an inhalation that expands the lung volume toward total lung capacity. There are considerable data showing that DIs are effective in reversing bronchoconstriction in healthy subjects using measurements of resistance (Raw) and forced expiratory volume in one second (FEV_1). By contrast, DI is not effective or even further exaggerates existing bronchoconstriction in some asthmatic subjects, especially when the airway narrowing occurs during spontaneous or antigen-induced acute asthma attacks (100). This paradoxical response to DI was recognized as early as the 1960s and 70s (45, 101). There is a spectrum between the normal response (DI-induced bronchodilation) and severe asthma (DI-induced bronchoconstriction); mild and well controlled asthmatics behave more like non-

asthmatics. However it was the observation that DI taken prior to a bronchoconstricting stimulus attenuates the subsequent airway narrowing that has rekindled major interest in this phenomenon (95, 102–108) which has been termed DI-induced bronchoprotection as opposed to bronchodilation. It has been suggested that asthmatics uniquely lack the bronchoprotective effect of DIs (107). It has long been accepted that stretching contracted ASM by DI reduces bronchospasm by disrupting actin-myosin cross-bridges (99)(89). However, when a DI is taken prior to stimulation, there should be few or no cross-bridges. Hence bronchoprotection could not be explained by a physical detachment of cross-bridges. Wang et al. postulated that the bronchoprotective effect of DIs can be explained by the adaptive behavior of ASM in response to DI (85, 96).

The two-stage phenomenon in ASM strips after length oscillation (described in sub chapter 1.5) resembles the sequence of events during DI-induced bronchoprotection in normal subjects. When DIs are immediately followed by administration of a stimulant, airway luminal narrowing is less than it would be without a DI (109) and the decline in FEV_1 is reduced (110). DI protects the airways from excessive bronchospasm. This is similar to the initial reduced contraction observed in ASM when a length oscillation is applied. However, bronchoprotection by DI is temporary. The stimulant-induced bronchospasm gradually returns to what it would be without a DI (102). This recovery process is paralleled by the *in vitro* finding that the active force generated by ASM gradually returns to the same level as prior to length oscillation (53, 85, 111). These similarities between the bronchoprotection of DI in vivo and ASM adaptation in vitro suggest that the dynamics of ASM length tension behavior and pathologic alterations in this behavior have the potential to play an important role in airway hyperresponsiveness.

1.7 Length Adaptation's Role in Deep Inspirations

The first evidence for a relationship between length adaptation in ASM and AHR was obtained in guinea pig model of maturation. The recovery of active force in adult guinea pig ASM is gradual, complete, and follows a time course similar to that observed in the ASM from adults of other species. On the other hand, when length oscillations are applied to ASM obtained from airways of 1-wk old guinea pigs, the subsequent active force increased to about 110% of the stable maximal active force generated before mechanical oscillation and was maintained throughout the adaptation process (112). This increase of force after the initial reduction is termed force potentiation. These data suggest there is a lack of ASM adaptation in response to mechanical perturbations in immature ASM and is consistent

with the clinical observation that AHR is greater in infants and that DI is ineffective in attenuating airway narrowing in infants as it is in asthmatics (113).

More recently Raqeeb et al. (114) studied ASM *in vitro* using dynamic scenarios which more closely resemble *in vivo* airway mechanics where ASM is constantly subjected to low level length oscillations due to tidal breathing interspersed with occasional DI. In their study design they tested the effect of "tidal breathing" with or without "DI" on force development as well as length oscillation in between stimulations during force recovery. They found that adaptation is interrupted by length oscillations, which suggests that in healthy normal lung where ASM is constantly stretched by breathing motions the force could not reach its maximal level, that is, the second stage of adaptation could not be completed. This would be beneficial to maintain airway patency.

Most recently, Chin et al. (53) directly compared the effect of length oscillation on tracheal ASM strips from non-asthmatic and asthmatic subjects. Immediately after length oscillation ASM from asthmatics showed less force reduction (~half of that in non-asthmatic ASM) and during subsequent recovery the ASM from asthmatics recovered more rapidly and completely. These results suggest that there is a fundamental difference in ASM response to strain: a reduced response in asthmatics to length oscillations; the difference is intrinsic and not because the strain is reduced by stiffer airways. A reduced initial force reduction is consistent with loss of bronchoprotection in asthmatics.

Despite the general concordance between *in vitro* and *in vivo* studies and computational models recent work suggests that solely mechanical explanations for the effects of DI may be simplistic. Transmural pressure changes comparable to those produced by tidal breathing do not affect the response of airway segments to a contractile agonist and with amplitudes greater than 10 cm H_2O the airways only respond with a transient dilation (115–118). Noble and colleagues (116) using isolated airway segments also demonstrate that the capacity of simulated DIs to reduce bronchoconstriction is markedly restricted by stiffening of the airway wall with contractile stimuli. Furthermore, the transient airway dilation observed in airway segments is smaller, compared to the relatively larger effect seen in intact airways in vivo (119, 120).

Some *in vivo* studies are however, not completely concordant with simple mechanical explanations. Although prior DI has reproducibly been shown to differentially modify the methacholine-induced decline in FEV_1 in asthmatics and non-asthmatics, other studies have shown that there is no differential effect on the changes in FEV_1/FVC ratio (121), partial expiratory flow (122) or airway resistance assessed using the forced oscillation technique (FOT) (123). One interpretation of this

discrepancy is that a prior DI may not alter the initial airway narrowing produced by a constrictor but instead make the ASM more responsive to subsequent strain during the DI required to perform an FEV_1 maneuver. This potential mechanism is supported by a recent study of the effect of DI in mice (124).

Together, these data support the idea that the reduced airway response following a DI is likely more complicated than a simple stretch of ASM. One plausible explanation for the ASM response to length oscillation is a corresponding reduction in myosin filament density which has been demonstrated in swine ASM (125). A similar change in ASM ultrastructure following a DI may explain its bronchoprotective effect. Alterations in myosin filament density in the ASM of asthmatic subjects may make it less prone to disruption following strain, although this has yet to be demonstrated in humans.

1.8 Molecular Alterations in ASM in Asthma

An understanding of the molecular mechanisms behind the potential changes in ASM that could lead to AHR have been few and conflicting. Studies using freshly isolated ASM cells from bronchial biopsies have focused on the expression of a small number of genes involved in smooth muscle contraction. In 2002, Ma et. al. showed that ASM cells from asthmatic subjects had an increased capacity to shorten and do so faster than non-asthmatic subjects (60). In agreement with this result, they saw that cells from asthmatic subjects expressed a greater amount of MLCK than did non-asthmatics. As discussed earlier, MLCK is responsible for phosphorylating the regulatory chain of myosin to allow for cross bridge cycling. The greater the level of phosphorylation the greater the velocity of shortening (126), therefore it stands to reason that increased MLCK would lead to a greater velocity of shortening in asthmatic subjects. The increased expression of MLCK was confirmed in a more recent study using RNA from bronchial biopsies (61) however in a study using laser captured ASM from bronchial biopsies Woodruff et. al. showed there was no increase in the expression of MLCK (127). Adding to the confusion over MLCK is a study in 2012 showing no increase in the shortening velocity of tracheal ASM from asthmatics (53). The study by Léguillette et. al. also showed increased expression of mRNA for myosin heavy chain and its isoforms (61). The smooth muscle myosin heavy chain gene (MYH11) can undergo differential splicing to result in 4 distinct isoforms named: SM1, SM2, SMA and SMB, which can pair together to form four distinct proteins: SM1A, SM2A, SM1B, SM2B (128, 129). It has been shown that the SMB variant, containing a 7 amino acid insert, can propel actin filaments at a great velocity than the other variants (130) and thus is a very attractive target for explaining increased ASM

velocity in asthmatics. These data suggest that a change in the relative proportion of the two myosin isoforms could increase ASM shorting velocity and could contribute to AHR in asthmatics. They saw increased expression of the mRNA for the SMA, SMB and SM2 isoform with the SMB isoform being the most greatly changed. They did not measure the relative abundance of the protein for the two isoforms. The earlier study by Ma et. al. could not detect the SMB variant in their samples (60) and the study by Woodruff saw no difference in the expression of smooth muscle myosin but did not look at different isoforms (127). It still remains to be seen whether an intrinsic change in the expression of MLCK or myosin in asthmatic ASM is responsible for AHR. There is a need for more studies with greater number of subjects using new gene expression quantification techniques.

Other gene expression studies on ASM have focused on exposing ASM cells to various inflammatory mediators under the assumption that it is inflammation that induces changes in the ASM and that the ASM itself is not intrinsically different (65). These studies have used IL-13 (131–133), IL-1β (131) and TGF-β (131) and measured gene expression changes using microarray. They found that a variety of genes were induced by exposure to the cytokines of which histamine receptor H1 (131, 133), IL-13 receptors (132, 133) and tenascin C (131, 133) were commonly changed. While these studies show that cultured ASM can respond to and produce (134, 135) inflammatory cytokines it is uncertain whether these effects contribute significantly *in vivo* (136). This is because cultured ASM cells can take on a synthetic phenotype that is not entirely contractile (137). A study by Halayko et al. in 1996 showed that after 5 days in culture with serum, the expression of contractile proteins smooth muscle myosin heavy chain (sm-MHC), MLCK, calponin and α-smooth muscle actin was reduced by over 75% (137). These proteins gradually returned following confluence in the ASM cells but the levels of non-muscle myosin, which rose with culturing, did not return to pre-culturing levels. Cultured ASM take on a phenotype that has been termed synthetic-proliferative and do not shorten in response to contractile agonists and do not look like typical ASM cells (137, 138). In canine ASM cells it has been shown that serum starvation (removal of serum for extended periods) can induce a sort of hypercontractile phenotype which is marked by an increase in MLCK expression (138, 139) however the same has not been shown in human ASM cells. Studies identifying the influence of inflammatory cytokines on intact ASM tissue would be valuable for supporting the synthetic roles of ASM in asthma.

The majority of large genetic studies in asthma have focused on using GWAS to look for contributors to AHR and asthma. Most of the results from these studies point to changes in genes important in epithelial function and or immune cell function and have been reviewed in other papers (140). One GWAS study found an association between a polymorphism in the ADAM33 gene and asthma

in Caucasians (141). ADAM33 is expressed in ASM and mesenchyme (142) and is thought to play an important role in tissue remodeling in asthma. It remains to be seen whether similar GWAS or large scale studies will detect a difference in proteins that could alter the contractile phenotype of the ASM in asthma.

1.9 Experimental Summary

The research that I conducted during my PhD was designed to advance our understanding of the potential role that ASM has in the generation of AHR. In the following chapters I will examine how ASM could play a role in AHR with or without intrinsic phenotypic changes within the ASM. The first three chapters will focus on physiological muscle phenomena while the last chapter focuses on identifying potential intrinsic phenotypic differences within the ASM and how all these features of ASM can contribute to AHR.

Chapter two examines whether the phenomenon known as force adaptation can occur under conditions that more closely mimic the *in vivo* setting. To test this, we applied oscillations that mimicked tidal breathing (TB) with or without periodic DIs that mimic sighs occurring *in vivo* to a muscle undergoing force adaptation in response to the contractile agonist carbachol.The rationale is that if force adaptation occurs under dynamic conditions it would lend more credibility to the idea that it could be important in AHR. We hypothesize that agonist induced force adaptation is resistant to applied oscillations. The aim of this chapter was to show that: 1) carbachol can induce force adaptation in tracheal ASM; 2) that applied oscillations would not strain the activated muscle enough to inhibit force adaptation; and 3) that tension oscillations are a more physiologic means of applying oscillations to activated ASM. This work was published in the American Journal of Respiratory Cell and Molecular Biology (92).

Chapter three examines the interplay between stress, strain and ASM activation and how they work to limit the effectiveness of breathing oscillations on the attenuation of ASM force. The ASM was contracted using increasing concentrations of ACh with or without oscillations mimicking breathing maneuvers of different amplitude to generate dose response curves. We hypothesized that even at low levels of activation, strain induced by the oscillating stresses are too low to cause a significant decrease in the contractility of the muscle. The aim of these experiments were to show: 1) increasing muscle activation stiffens the muscle; and 2)a history of oscillations will increase the effectiveness of these

small strains and may be related to the bronchoprotective effect of DIs. The results of this study were published in the Journal of Applied Physiology (143).

In chapter four, we test whether the ASM plays a role in the bronchoprotective effect afforded by DIs and how phenomenon such as length and force adaptation may attenuate this phenomenon. We simulate two DIs prior to ASM shortening to determine how they affect the ASM compliance to a third FEV_1-like DI. It is hypothesized that the prior DIs will increase the compliance of the ASM to the third stretch and that this increase in compliance can explain the bronchoprotective effect observed in vivo. Using a computational model, we aim to show that although the change in compliance is small, it is effective at opening closed airways and increasing the measured FEV_1. We also aim to show that adaptation of the muscle to a shorter length or to basal tone will abolish this increased compliance. This manuscript is published in the Journal of Applied Physiology.

These first 3 chapters focus on physiological muscle phenomenon and their potential role in AHR or asthma. The final chapter focuses on determining if there are intrinsic phenotypic changes that play a role in AHR or accentuate the effects of the prior mentioned ASM phenomenon. Using the Nanostring nCounter system we quantified the expression of 100 genes thought to be important in ASM function and examined their relationship to airway remodeling and asthma. Immunohistochemistry was used to analyze the expression of the most significantly different mRNA expression results. We hypothesize that there will be differences in the expression of genes and proteins related to contraction and contractile regulation, cytoskeletal organization and its regulation and calcium handling that could help explain the ASMs role in AHR. We aim to show that: 1) expression of the mRNA and protein correlate with remodeling changes in the airway and; 2) can help explain mechanical measurements done in a previous study on the same subjects (53). The work presented in this thesis will help explain the interactions between ASM activation, breathing oscillations and potential molecular alterations in cytoskeletal proteins in asthmatic ASM that could stiffen that airway and contribute AHR.

Chapter 2 Force Oscillations Simulating Breathing Maneuvers Do Not Prevent Force Adaptation[2]

2.1 Introduction

Airway smooth muscle (ASM) is innervated by the vagus nerve, which provides a constant level of baseline tone (144). However, in patients with asthma, the ASM is exposed to a wide variety of inflammation-derived spasmogens, including histamine (145), leukotrienes (146), endothelin (147), and prostaglandins (148), that can induce a greater degree of tone. Induction of tone by the addition of a spasmogen was shown to enhance the force-generating capacity of the ASM through a process known as "force adaptation" (66). In those experiments, ASM was exposed to the spasmogen acetylcholine (ACh), and the force-generating capacity of the muscle was assessed periodically before and after ACh administration by stimulating the ASM with electrical field stimulation (EFS). The results demonstrated that ACh exposure increases the force generated by the ASM in response to the same two stimuli (ACh + EFS) in a time-dependent fashion (i.e., force adaptation). Therefore, in addition to an increase in force due to a greater level of ASM activation achieved by adding a second contractile stimulus (ACh), a synergistic interaction occurred between the tone and the activated ASM that rendered the muscle stronger over time. In static conditions, this increase in force was shown to occur at different ASM lengths and was shown to be preserved after a length change (elongation or length reduction) (149). These results have prompted the suggestion that the gain in force caused by force adaptation may contribute to airway hyperresponsiveness (AHR) in patients with asthma, particularly in individuals who have increased airway tone. Although this phenomenon could be present in healthy individuals due to vagal tone, the increased tone experienced by ASM in asthma could cause an exaggerated effect.

Previous studies of force adaptation were performed under static conditions. However, to simulate more adequately the dynamic conditions that prevail in vivo, the length of the ASM would not be static. The ASM encircling the airways is stretched and released constantly due to changes in transpulmonary pressure and lung volumes that are required for breathing. This dynamic environment is thought to attenuate ASM force and protect against AHR. For example, small length oscillations (0.25–1.0% strain) at a physiological breathing frequency have been shown to decrease the total force produced by ACh (10^{-7} M) by as much as 25% (111). Stretches up to 8% in the same study showed a

[2] A version of this chapter has been published. C Pascoe, Y Jiao, CY Seow, PD Paré, Y Bossé. Force Oscillations Simulating Breathing Maneuvers do not Prevent Force Adaptation. *American Journal of Respiratory Cell and Molecular Biology.* Vol. 47, No. 1 (2012), pp. 44-49

decrease of almost 70% in force generated in response to ACh. In another study, length oscillations (ranging from 5 to 35% strain) caused a decrease in isometric force produced by EFS, ranging from approximately 5% with the smallest oscillations to approximately 40% with the largest oscillations (85).

Length oscillations (i.e., swings in ASM length) have been shown to not only reduce ASM-force (85, 111, 150, 151) but also to reduce force adaptation (114). However, in that previous study (114), the authors applied fixed-length oscillations and did not take into account the fact that ASM length oscillations are attenuated in the presence of tone. In vivo, the fluctuation in pressure required for breathing imposes force oscillations, not length oscillations, on the airway wall. Therefore, the ASM is subjected to swings in tensile stress that are not linearly related to changes in muscle length. In the presence of tone, the force oscillations required to achieve these length oscillations are unphysiological (i.e., magnitude greater than the ones achieved due to the swings in transpulmonary pressure required for breathing).

In the present study, we aimed to test whether force adaptation occurs under oscillating conditions using force oscillations instead of length oscillations. This better simulates what occurs in vivo when a pressure change (force per unit area) induces a length change in the ASM layer as opposed to a length change inducing a force change (as in length oscillations). The force oscillations used simulated the changes in airway wall tension that would prevail in vivo in an airway of the fourth generation during breathing maneuvers (tidal breathing alone or tidal breathing + deep inspiration (DI)). The objective of these experiments was to compare the degree of force adaptation under static and oscillating conditions to determine whether normal breathing patterns can inhibit force adaptation. We hypothesized that force adaptation will occur under conditions that more accurately mimic the cyclical strains experienced by the ASM in vivo.

2.2 Materials and Methods

2.2.1 Tissue Preparation

Sheep tracheas used in these experiments were obtained from a local abattoir. The use of the tissue was approved by the Committees on Animal Care and Biosafety of the University of British Columbia. Tracheas were removed soon after the animals were sacrificed and put in Krebs solution (pH 7.4; 118 mM NaCl, 4 mM KCl, 1.2 mM NaH_2PO_4, 22.5 mM $NaHCO_3$, 2 mM $MgSO_4$, 2 mM $CaCl_2$ and 2g/L dextrose). Upon arrival at the laboratory, tracheas were cleaned of blood and stored in Krebs solution at

4°C until further processing. ASM strips for experiments were dissected from ~2 cm-long tracheal segments. While the tracheal segment was still intact, two incisions were made on the epithelial layer and the distance between them was measured. The tracheal segments were then cut open and pinned, epithelial side down, in a waxed-floor dissecting bath filled with Krebs solution. The adventitial connective tissue covering the ASM layer was then removed. The tissue was flipped over and pinned down again making sure that the two epithelial incisions made previously were at the same distance as measured in situ. The epithelial layer was then removed from the muscle layer. ASM strips 5-6 mm in length and ~ 1.5 mm in width were dissected out leaving both extremities attached to the cartilage. Two aluminum foil clips were then wrapped around the ASM strips at either extremities while the ASM was maintained at its in situ length. The distance between the two clips was measured before the ASM strips were cut away from the rest of the tracheal segment. The ASM strips flanked by foil clips were then mounted vertically in a muscle bath. The bottom clip was attached on a stationary hook and the upper clip was attached on a hook connected to the lever arm of a servo-controlled force-length transducer by a surgical thread (size 6). The distance between the clips during the dissection was used to adjust the length of the ASM strips once installed in the muscle bath. This length is hereafter called $L_{in\ situ}$. The organ bath was filled with Krebs solution that had been pre-heated to 37°C and aerated with a gas mixture of 95% O2 and 5% CO2. The temperature of the bath was also maintained by circulating 37°C water through a jacket that surrounded the organ bath.

2.2.2 Equilibration Period

ASM strips were subjected to an equilibration period before the start of the experimental protocol. During equilibration, the ASM strips were activated every 5 minutes with a 9- second electrical field stimulation (EFS, 60 Hz, 12 volts). Krebs solution was replaced every 5 minutes following EFS with warmed (37°C), aerated Krebs solution. Equilibration was completed when a plateau in isometric force was reached (i.e., after which there was no further increase in force in response to subsequent EFS). The force produced by EFS at that time was called F_{max}. Therefore, F_{max} is the force generated by the ASM in response to EFS at in situ length after a stable plateau was achieved but prior to the introduction of tone. The equilibration period took ~1 hour.

2.2.3 Protocol to Assess Force Adaptation in Dynamic Conditions

Two independent sets of experiments were performed to determine the effect of tidal breathing or tidal breathing + DI on force adaptation. The sequence of interventions is illustrated in Figure 2.1 A. The first step reproduced force adaptation under static conditions as previously described (6). Briefly, The ASM was exposed to the continuous presence of carbachol (CCh) to induce tone. The concentrations of CCh used ranged between 5 nM and 25 nM (average 20 nM). The force generated by CCh (F_{CCh} or tone) was monitored over time and the force-generating capacity of the ASM was assessed at 5-min intervals using EFS. The first EFS in the presence of tone was at 3 min following the administration of CCh and then at 5-min intervals onward. The ASM was subjected to this 5-min cycle until a plateau in total force (EFS-induced force + CCh-induced tone) was reached (~25 min). After force adaptation was completed, tone was removed, and the ASM recovered for 30 minutes while the 5-minute cycle of EFS was maintained.

The subsequent step assessed the effect of force oscillations mimicking tidal breathing on muscle force in the absence of carbachol (CCh). Details on force oscillation calculations are included in the next section. The oscillations were maintained until the EFS-induced force reached a new plateau (the new F_{max} under force oscillating conditions). The final step assessed force adaptation under force oscillating conditions. Tone was then reintroduced and maintained for 23 minutes as described for static conditions using the same concentration of CCh. Force oscillations were applied on top of the tone and were kept at the same magnitude as in absence of CCh.

The second set of experiments was identical to the first set described above except that the DI was included and the first step of the protocol (static conditions) was omitted. Representative traces of a complete 5-minute cycle without and with the tone are shown in Figures 2.1 B and 2.1 C, respectively. In the first set of experiments DI was omitted. The oscillations were present throughout the 5-minute cycle except during the measurement of isometric EFS-induced force where the oscillations were stopped for 40 seconds (10s before, 9s during, and 21s after EFS). The DI occurred once per cycle at 2 minutes before EFS. The values for CCh-induced tone were recorded immediately before every EFS, and the values for total force were recorded at the force peak during EFS as illustrated in Figure 2.1 C. The force produced by EFS is the total force minus either the resting tension (in the absence of CCh) or the tone (in the presence of CCh). Fresh Krebs (with or without CCh) was replaced after every EFS.

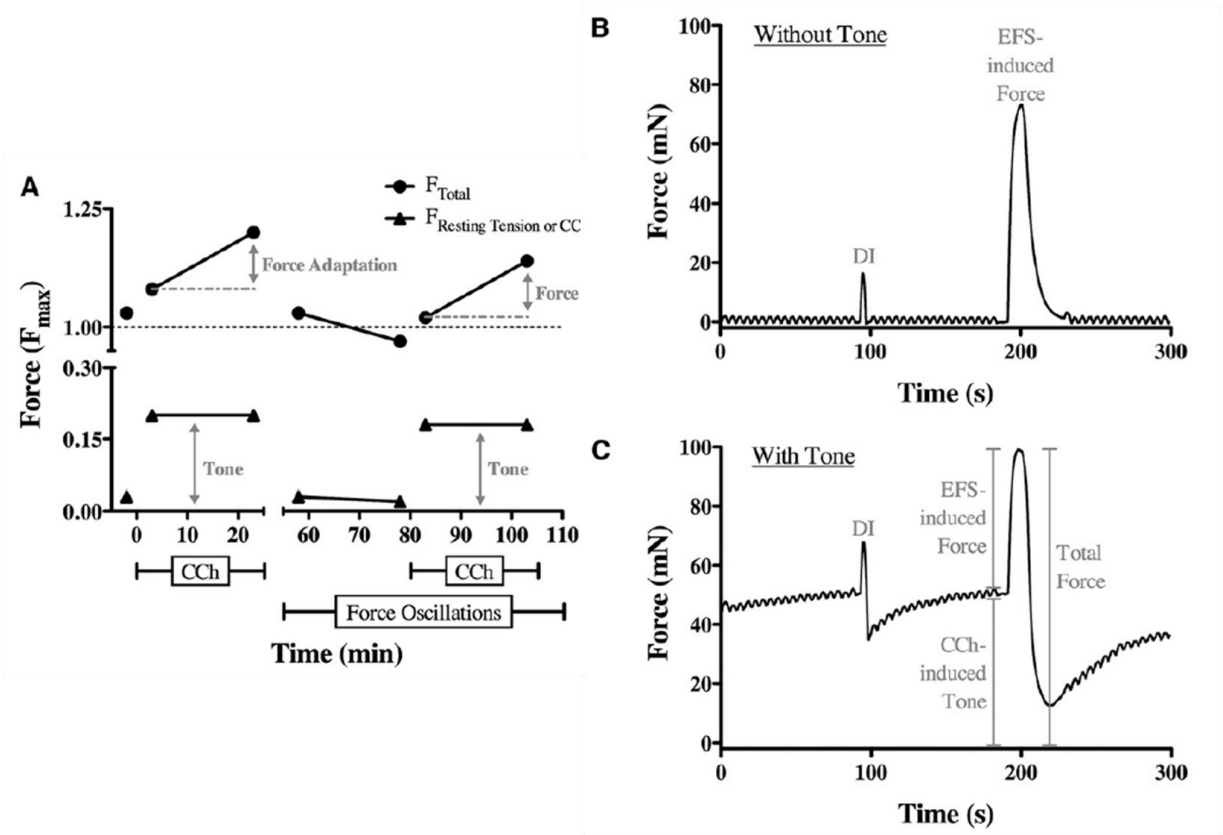

Figure 2.1 Schematic and sample traces for protocol. (A) Protocol to illustrate the sequence of interventions and hypotheses. (B and C) Representative force traces of a 5-minute cycle without (B) and with (C) tone in force-oscillating conditions simulating tidal breathing and deep inspirations (DI). CCh=carbachol; EFS=electrical field stimulations.

2.2.4 Force Oscillations

Force oscillations were performed at breathing frequency (0.2 Hz) with truncated sine waves (without trough), which was designed to mimic tidal breathing patterns (i.e., a full breathing cycle every 5 seconds). The DI occurred once every 5 min at the same frequency as tidal breathing (1 semi-sine wave in 5 sec). The magnitude of the force oscillations was simulating the oscillations in tension experienced by the wall of an airway of the 4th generation (which has an average radius of 2.22 mm at the middle of the ASM layer when the lung volume is at functional residual capacity (152, 153)) during 3-cmH_2O excursions of transpulmonary pressure from 5 to 8 cmH_2O for tidal breathing and during a 25-cmH_2O excursion of transpulmonary pressure from 5 to 30 cmH_2O for the DI. The changes in the wall tension caused by such excursions were calculated based on Laplace relationship (tension = pressure x radius), assuming that the airways resemble a thin-walled cylinder (this seems a reasonable assumption

since the ratio of wall thickness/airway luminal diameter is ~1/22 in a non-asthmatic airways of the 4th generation).

Since the airway wall is also strained during these swings in transpulmonary pressure, the calculated change in wall tension also has to take into account the change in radius (at the middle of the ASM layer). Equations developed by Lambert and coworkers (153) and morphological data for a 4th generation airway taken from James (56), Kuwano (154) and Wiggs (152) and their respective coworkers were used to make this adjustment. The magnitude of the tension oscillations was the same for every ASM strip (0.74 mN/mm for tidal breathing and 6.24 mN/mm for the DI) but the magnitude of the force oscillations depended on the size of the ASM strip. This is because the force required to apply a given tension within the wall of an airway depends on the length of the airway segment that is being studied. Since the ASM is arranged circumferentially around the airways, this width represents the portion of the airway length that would be studied in vivo. It was thus possible to calculate the force oscillations required to obtain a given tension oscillations based on the width of the ASM strips studied.

To estimate the width of the ASM strips, we assumed that the ASM generates a stress (force/cross-sectional area) of 100 KPa in response to EFS following the equilibration period (so F_{max} = 100 KPa or 100 mN/mm2) and that the thickness of the ASM strips was 0.3 mm. The value of F_{max} (in mN) was thus used to calculate the width of the ASM strips. Knowing the length of the airway wall that would be covered in situ by this estimated width of the ASM strip and the changes in wall tension occurring during tidal breathing, we were then able to calculate the force oscillations (in mN) to which an ASM strip of that particular width would be subjected to in vivo. Another assumption made for this calculation was that the changes in wall tension caused by breathing are borne exclusively by the ASM layer and not by the other parallel elastic elements of the airway wall. This assumption is likely to be correct when the ASM is active (in the presence of tone) but is more likely to be inaccurate when the ASM is fully relaxed. However, the strain experienced by the ASM in our experiments in response to these force oscillations in the absence of tone was 6.5 ± 2.6% for tidal breathing and 24.2 ± 2.6% for DI. These values are similar to the ASM length oscillations that were predicted to occur in fully relaxed airways during the changes in lung volume caused by these breathing maneuvers (4% for tidal breathing and 25% for DI) (111). These results suggest that this last assumption is reasonable.

2.2.5 Calculation of Force Adaptation

Force adaptation is a gain in ASM force-generating capacity caused by the introduction of tone (tone is a sustained contraction) triggered by a spasmogen. To assess force adaptation, one needs to measure the time-dependent increase in total force generated in response to a given stimulus (in our experiments a spasmogen + electrical field stimulation (EFS)).

It is important to mention that the force produced in response to EFS is not the maximal force that ASM is capable of generating. Adding a spasmogen to the muscle bath increases ASM activation beyond that achieved by EFS and consequently generates more force. Therefore, to quantify force adaptation, one first needs to distinguish the effect of force adaptation from the additive effect that occurs simply by adding a spasmogen. Figure 2.2 addresses this issue. These data are taken from the experiments undertaken to first describe force adaptation (66). The tone induced by ACh is not shown in Figure 2.2, but the tone was relatively consistent over time. This represents an ideal scenario. In these circumstances, force adaptation can be defined simply as the time-dependent increase in total force caused by exposure of ASM to a spasmogen. This is also the scenario that we drew in Figure 2.1 to explain the experimental protocol, as well as our hypotheses.

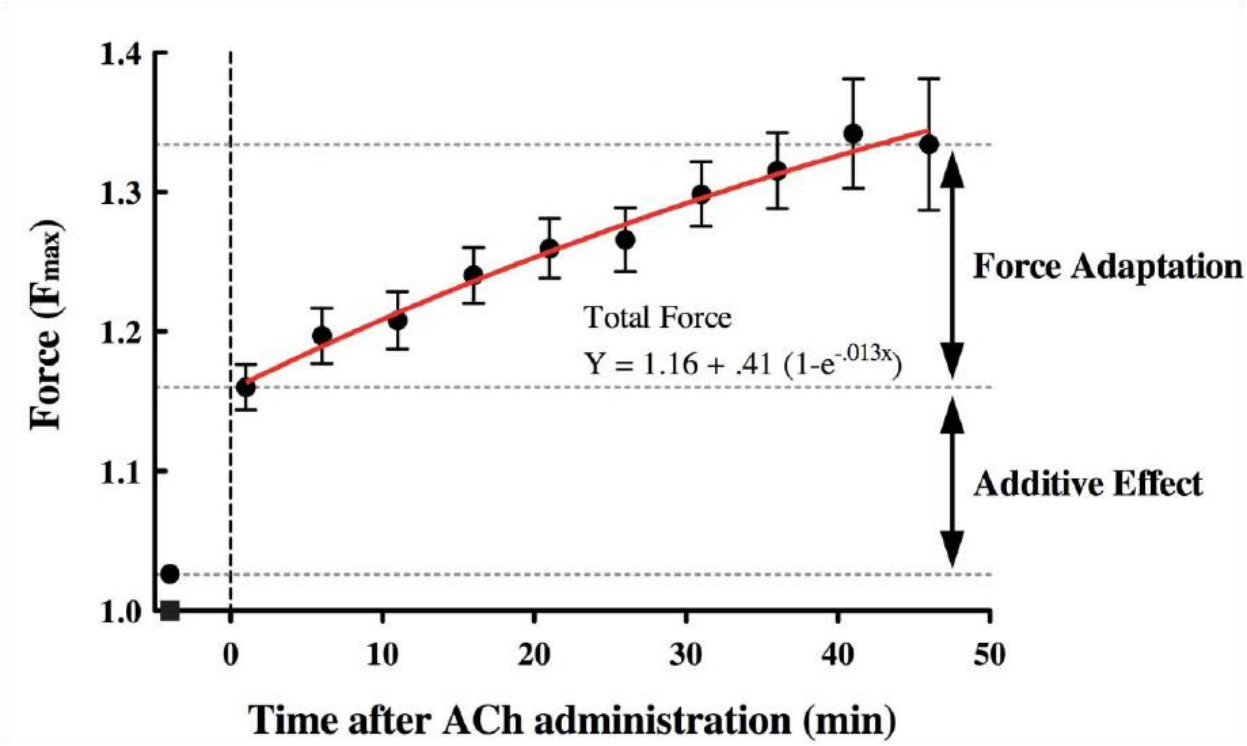

Figure 2.2 Time course of change in total force (circles: EFS-induced force + tone-induced by ACh) before and after administration of ACh (10-7 M). The square and circle at time -4 min are EFS-induced force and total force, respectively. In absence of tone (i.e., without ACh), the total force is EFS-induced force plus resting tension. All the force data were normalized to F_{max}, which is the EFS-induced force produced by any ASM strips prior the administration of ACh. The difference in total force between -4 min (last EFS prior ACh administration) and 1 min (first EFS following ACh administration) is called the additive effect. The time-dependent increase in total force after the 1 min time-point is called force adaptation. The data points after time zero were fitted with an exponential equation (red line) of the form: $y = y^o + a(1-e-Kx)$ that is shown below the curve: where: y^0 is the y value when x (time) is zero; a is the span, defined by the difference between the plateau and y^0; and K is the time constant. The increase in total force after time zero is statistically significant (one-way ANOVA, $p<0.05$). n = 14.

However, the magnitude of tone is a dependent variable. One can control the concentration of the spasmogen in the muscle bath, but not the force produced by the muscle in response to that concentration. The fact that ACh maintained a consistent tone over time in our previous experiments was convenient, but it is not the case for the tone induced by other spamogens. As mentioned above,

we know that the increase in total force induced by a spasmogen is due to 2 things: 1) an additive effect; and 2) force adaptation. While we know that force adaptation occurred at any level of tone (66), the effect of changing tone on total force is unknown. To isolate the effect of force adaptation, one needs to understand the interplay that exists between tone and its additive effect on total force. Figures 2.3 and 2.4 address this issue.

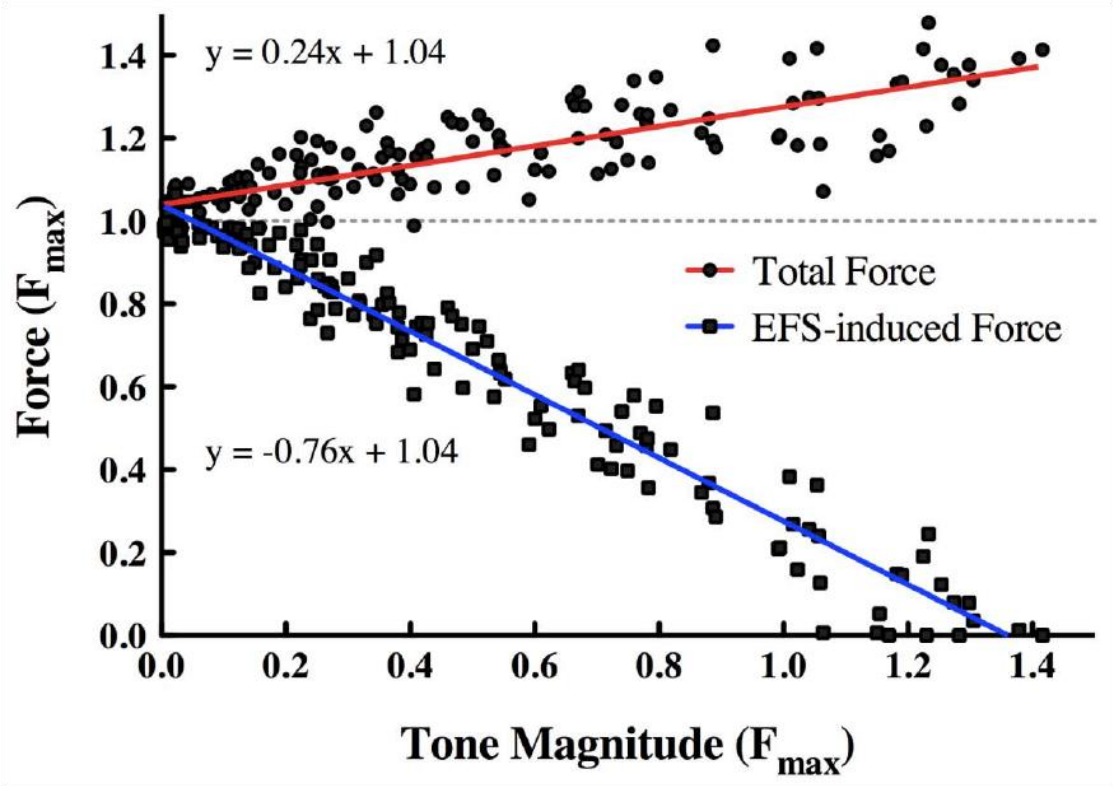

Figure 2.3 Relationship between the magnitude of tone, EFS-induced force and total force. Every circle (total force) and its vertically aligned square (EFS-induced force) are from an independent experiment (most of the time a different ASM tissue, but sometimes several points are from the same tissue but with different ACh concentrations as shown in Figure 2.4). ACh-induced tone was recorded immediately before EFS and the total force was recorded at the force peak during EFS. The force produced by EFS is the total force minus the tone. Total force (circles) and EFS-induced force (squares) are plotted against the magnitude of tone. Linear regressions were used to fit the data (EFS-induced force in bleu and total force in red, $r = 0.98$ and 0.82, respectively: $p \leq 0.0001$). A reciprocal relationship can be seen between EFS-induced force and tone magnitude, so when tone is greater EFS-induced force is lower. However, the total force increased as the magnitude of tone increased. That means that the additive effect of tone on total force is greater when the tone is greater, and vice versa (i.e., the additive effect of tone on total force is lower when the tone is lower). It also implies that, independently of force adaptation, a change in muscle tone changes the total force. So when tone changes over the time-course of an experiment, one needs to correct for this changing additive effect of tone on total force to quantify the effect of force adaptation. $n = 152$.

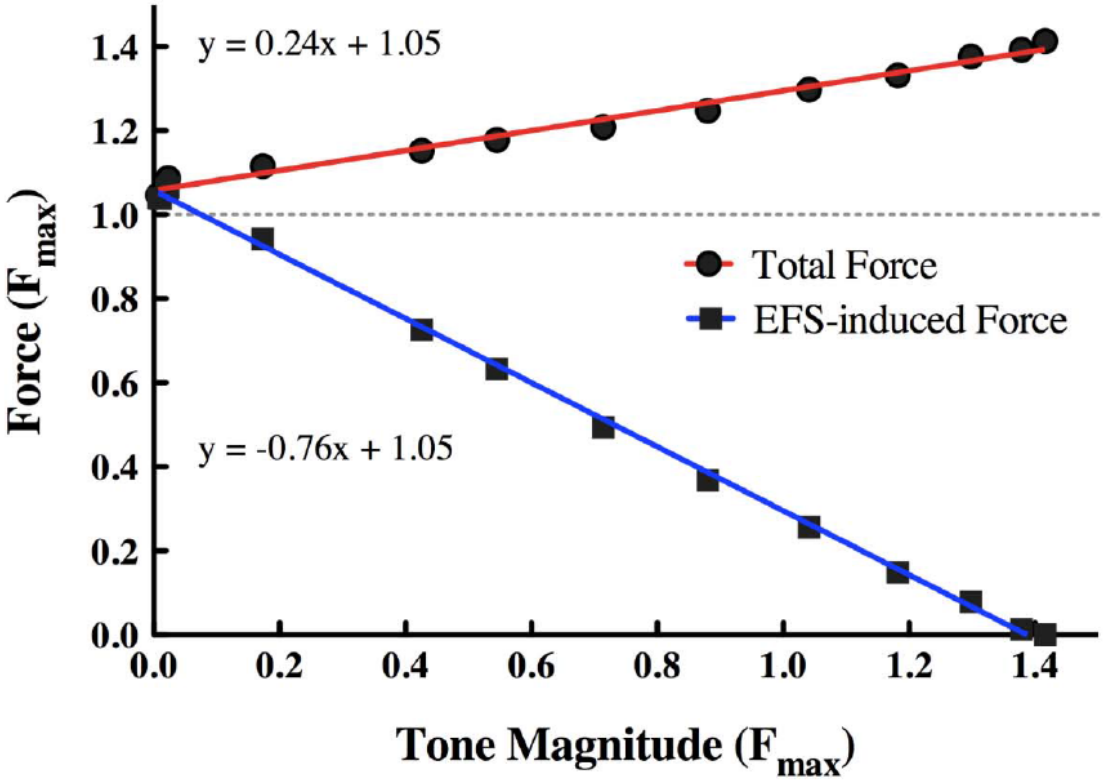

Figure 2.4 Relationship between the magnitude of tone, EFS-induced force and total force on same ASM strip was stimulated with 14 different concentrations of ACh (10-9 to 3 x 10-3 M). The muscle was allowed to fully recover from the previous stimulation before a new concentration was tested. One representative experiment is shown, but this experiment was repeated 3 times with similar results. The correlation coefficients (r) for the linear regressions are 0.99 and 1 for total force and EFS-induced force, respectively ($p \leq 0.0001$).

As shown in those figures, there is a reciprocal relationship between EFS-induced force and tone, so that the greater the tone the lower the EFS-induced force. This makes sense since there is just so much force the muscle can produce. When more force is produced by the tone-inducing agonist, less is available for EFS-induced force. However, the relationship between EFS-induced force and tone is not perfectly reciprocal. Otherwise, the total force would always equal 1 (the gain in force caused by tone would be exactly compensated for by the loss in EFS-induced force caused by the same tone). Figures 2.3 and 2.4 show that it is not the case. The total force increased as the tone increased. This means that the gain in total force caused by an increased tone is always greater than the decline in EFS-induced force caused by the same increase in tone.

In other words, the effect of tone on total force is proportional to the magnitude of tone. Therefore, during a time-course of 25 min (as in our experimental design), changes in muscle tone over time affect the total force by changing the magnitude of this additive effect independently of force adaptation. One thus needs to correct for this effect to isolate the effect of force adaptation. Figure 2.5 addresses this issue.

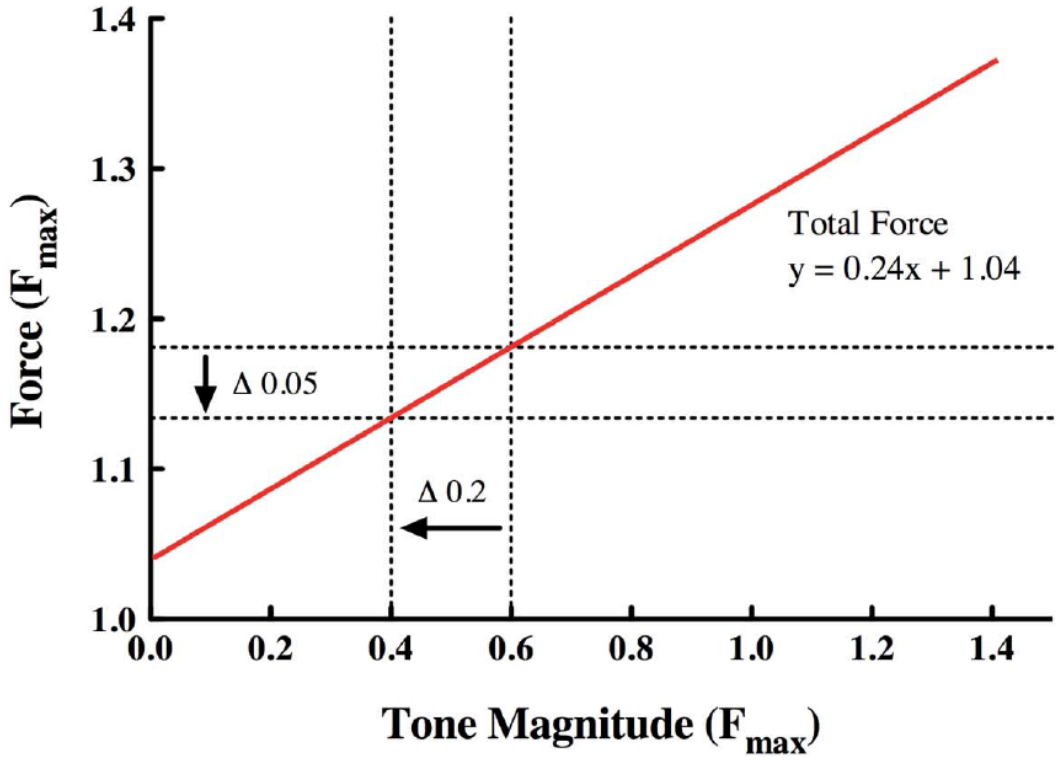

Figure 2.5 Example showing force adaptation correction for the change in the additive effect caused by a change in the magnitude of tone. The linear regression in red is taken from Figure 2.3. In this example, a decline in tone of 0.2 F_{max} reduces the additive effect of tone on total force by 0.05 F_{max}. This correction was made at every time points (5-min intervals) along the time-course of spasmogen exposure using the first EFS (at 3 min) after the introduction of tone as the reference point. This correction has to be made to the change in total force occurring between the same two time-points to quantify force adaptation.

We made that correction in the present study because the time taken by CCh to reach its peak force (between 8 and 13 min) is longer than ACh, and also because the tone produced by CCh slowly declined after reaching its peak. Without this correction (i.e., quantifying force adaptation just by

measuring the change in total force over time) force adaptation would be overestimated at the early time points following CCh administration (as the tone was rising) and underestimated at the later time points (as the tone was dropping). Having said that, the changes in CCh-induced tone over time were rather small. The effect of this correction (explained in Figure 2.5) on force adaptation is thus also small. In the present study, one can roughly calculate the effect of force adaptation by measuring the change in total force over time. Since there is no way to quantify the contribution of force adaptation on total force in the first 3 min following the addition of CCh, we assumed that the effect up to 3 min is only additive. Force adaptation was thus quantified starting at the first EFS following the administration of CCh. We are aware that this slightly underestimates the effect of force adaptation.

2.2.6 Statistical Analyses

Resting tension, CCh-induced tone, EFS-induced force, and total force obtained for each muscle strip were normalized to F_{max} before averaging. Data shown are means ± SEM. For the changes in forces occurring over time, a repeated–measures, one-way ANOVA and a Tukey's multiple comparison posttest were used. For comparison of the values of force adaptation, resting tension, EFS-induced force, and tone induced by CCh under static versus dynamic conditions and for comparison of strains with or without tone, a t test was used. All statistical analyses were performed using Prism 4 (GraphPad Software, San Diego, CA), and $p<0.05$ was considered statistically significant.

2.3 Results

The effect of CCh on total force over time under static conditions is shown in Figure 2.6. CCh-induced tone rose to a maximum of 0.64 ± 0.10 F_{max} at 13 minutes. At 3 minutes after CCh administration, the total force (EFS-induced force + CCh-induced tone) rose to 1.21 ± 0.04 F_{max} from an initial value of 1.038 ± 0.009 F_{max} (EFS-induced force + resting tension) ($P < 0.005$). Despite a slight decline in CCh-induced tone over time, total force continued to rise over time to a value of 1.35 ± 0.05 F_{max} at 23 minutes after CCh administration, which was significantly higher than the initial values at time −2 and 3 minutes ($P < 0.005$). The gain in force caused by force adaptation at time 23 minutes under static conditions was 0.11 ± 0.02 F_{max}.

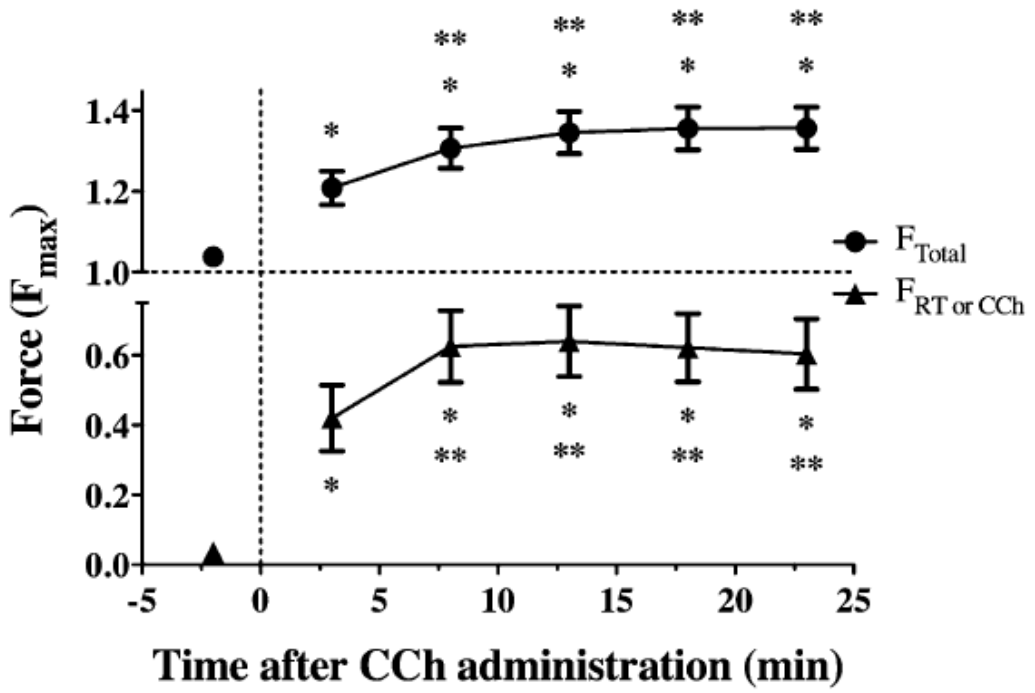

Figure 2.6 Static Force Adaptation. Time course of changes in airway smooth muscle (ASM) tone (*triangles*) and total force (*circles*) after administration of CCh (at time 0) in static conditions. Values at every time point are from force traces similar to the ones shown in Figure 2.1 A and B. * significant difference ($p<0.05$) comparing the points before (-2 min) with those after CCh administration. ** significant difference ($p<0.05$) comparing the first (3 min) with the subsequent points after CCh administration (n=15).

The effects of force oscillations that mimicked tidal breathing on resting tension and total force over time are shown in Figure 2.7 A. None of these forces declined significantly over time (from 0.045 ± 0.01 to 0.03 ± 0.01 and from 1.05 ± 0.02 to 1.00 ± 0.01 F_{max} for resting tension and total force, respectively; $p > 0.05$). The effect of adding CCh on total force over time under oscillating conditions simulating tidal breathing is shown in Figure 2.7 B. CCh-induced tone rose to a maximum value of 0.46 ± 0.07 F_{max} after 13 minutes. Total force rose over the course of 23 minutes from 1.03 ± 0.01 F_{max} to 1.25 ± 0.04 F_{max} ($p < 0.005$). The initial rise in total force 3 minutes after CCh administration (1.08 ± 0.03 F_{max}) was not significant. The gain in force caused by force adaptation at 23 minutes in force oscillation conditions simulating tidal breathing was 0.14 ± 0.02 F_{max}. Comparisons of resting tension, EFS-induced force, the magnitude of tone induced by CCh, and force adaptation between static conditions versus force oscillation conditions mimicking tidal breathing are shown in Figure 2.8.

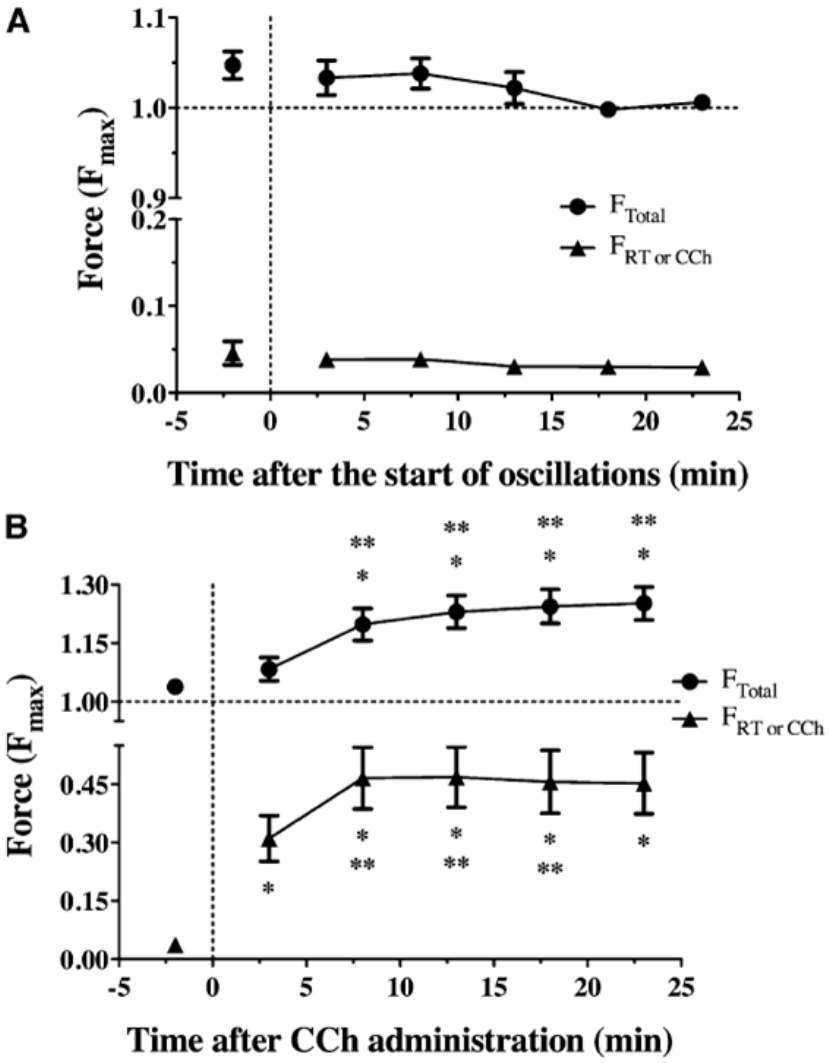

Figure 2.7 Tidal breathing oscillations on relaxed or force adapted tissue. (A) Time course of changes in ASM resting tension (*triangles*) and total force (*circles*) after the introduction of tidal breathing simulations (at time 0) in relaxed ASM strips (n=4–15, depending at which time the plateau in EFS-induced force was reached). (B) Time course of changes in ASM tone (*triangles*) and total force (*circles*) after the administration of CCh (at time 0) during tidal breathing simulations. *Significant differences ($p<0.05$) comparing the points before (−2 min) with those after CCh administration. **Significant differences ($p<0.05$) comparing the first (3 min) with the subsequent points after CCh administration (n=15).

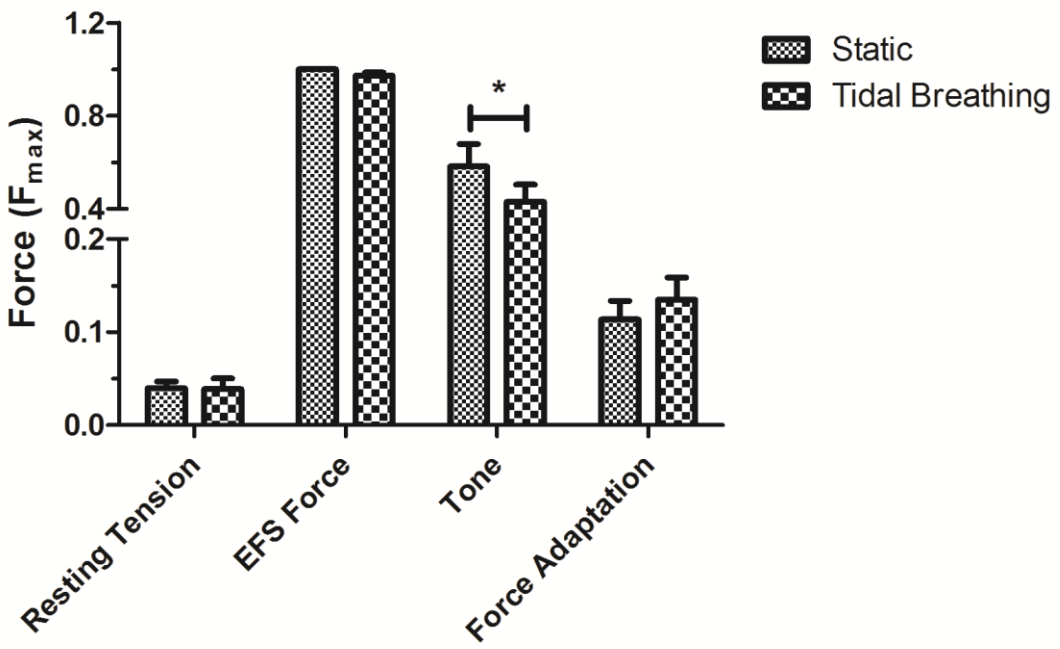

Figure 2.8 Effect of tidal breathing simulations on resting tension, EFS-induced force, tone induced by CCh, and force adaptation. Bars represent the average values ± SEM normalized to EFS force in static condition. *Significant differences between static versus simulated tidal breathing conditions ($p<0.05$) (n=15).

The effects of force oscillations that mimicked tidal breathing and DI on resting tension and total force over time are shown in Figure 2.9 A. Resting tension did not decline significantly over time (from 0.03 ± 0.01 to 0.025 ± 0.00 F_{max}). However, total force decreased significantly ($p < 0.05$) over time (from 1.03 ± 0.01 to 0.96 ± 0.03 F_{max}). The effect of adding CCh on total force over time under force oscillating conditions mimicking tidal breathing + DI is shown in Figure 2.9 B. CCh-induced tone rose to a maximum value of 0.35 ± 0.09 after 13 minutes. Total force rose over the course of 23 minutes from 1.03 ± 0.01 F_{max} to 1.26 ± 0.06 F_{max} ($p < 0.005$). The gain in force caused by force adaptation at 23 minutes under force oscillating conditions mimicking tidal breathing and DI was 0.11 ± 0.03 F_{max}. Comparisons of resting tension and EFS-induced force between static conditions and force oscillating conditions mimicking tidal breathing + DI are shown in Figure 2.10. The results of both sets of experiments (tidal breathing and tidal breathing + DI) are summarized in Table 2.1.

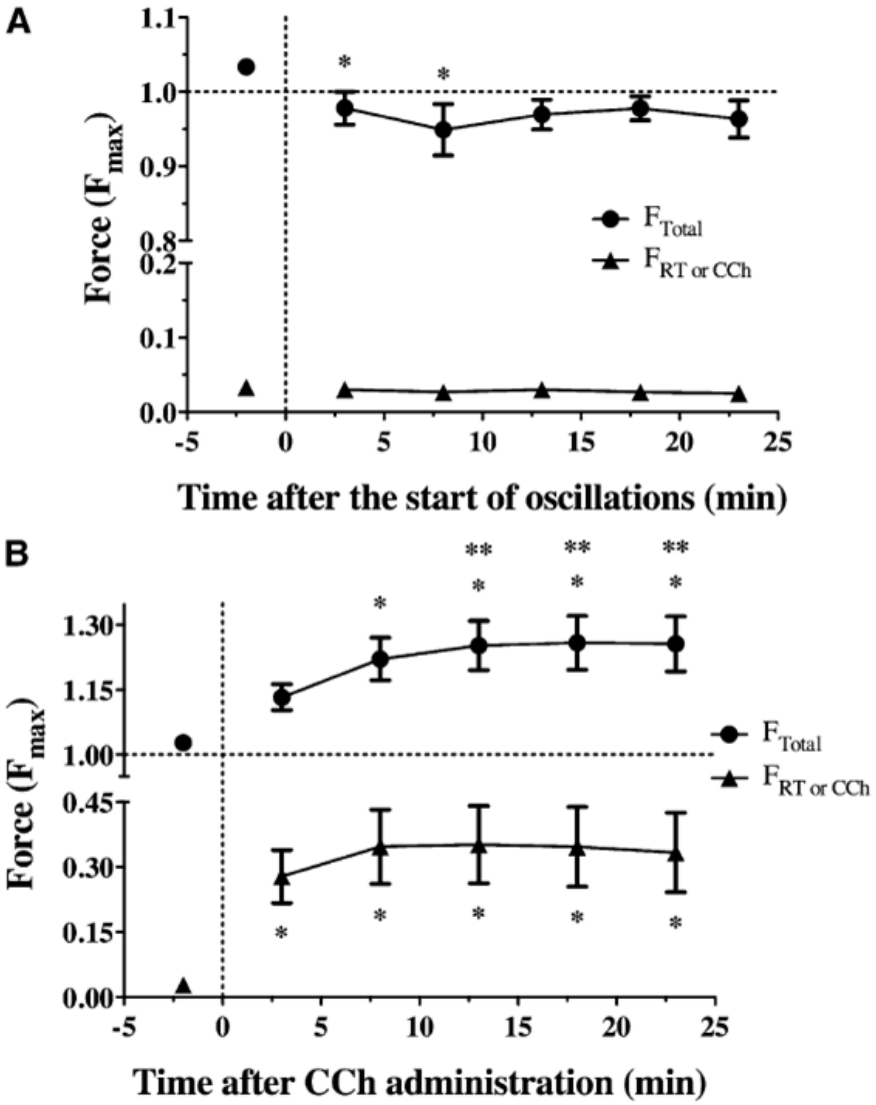

Figure 2.9 Tidal breathing oscillations plus DI on relaxed or force adapted tissue. (A) Time course of changes in ASM resting tension (*triangles*) and total force (*circles*) after the introduction of force oscillations mimicking tidal breathing and DI (at time 0) in relaxed tissue. *Significant differences ($p<0.05$) when comparing the points before (−2 min) with those after the start of oscillations (n=9). (B) Time course of changes in ASM tone (*triangles*) and total force (*circles*) after the administration of CCh (at time 0) in simulated tidal breathing + DI conditions. *Significant difference ($p<0.05$) comparing the points before (−2 min) with those after CCh administration. **Significant differences ($p<0.05$) comparing the first (3 min) with the subsequent points after CCh administration (n=9).

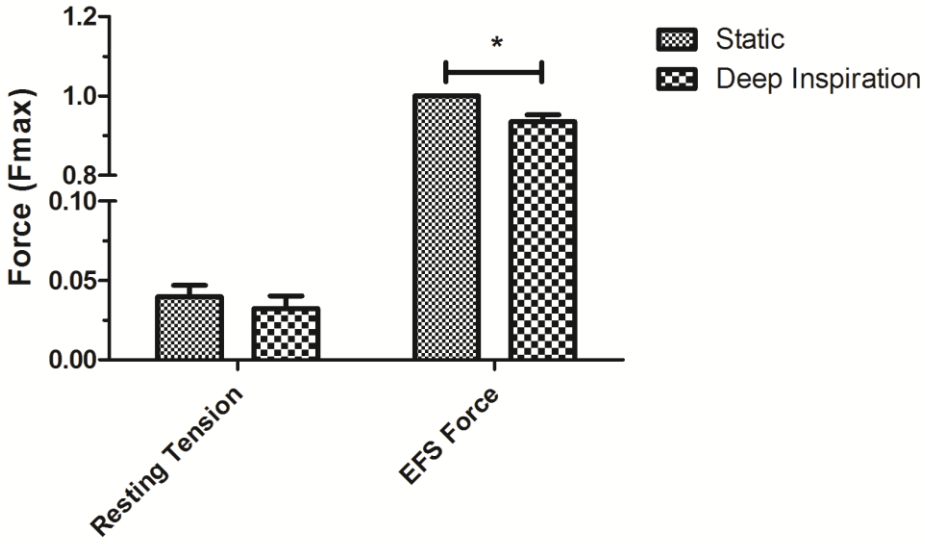

Figure 2.10 Effect of breathing maneuver simulations (tidal breathing + DI) on resting tension and EFS-induced force. Bars represent the average values ± SEM normalized to EFS force in static condition. *Significant differences between static versus simulated tidal breathing + DI conditions ($p<0.05$) ($n=9$).

Forces	Static	Tidal Breathing	Tidal Breathing + DI
Resting tension	4.0 ± 0.7%*	3.9 ± 1.2%	3.2 ± 0.8%
EFS-induced force	100 ± 0%	96.8 ± 1.1%	93.5 ± 1.8%
Tone	58.2 ± 9.7%	43.1 ± 7.4%	
Force adaptation	11.4 ± 2.0%	13.5 ± 2.4%	11.3 ± 3.0%

Table 2.1 Summary of force adaptation results. *All values are expressed as percentage of Fmax (i.e., the force produced by EFS in static conditions after the equilibration period and before the administration of carbachol [CCh]). The value of tone in the protocol that included DI was omitted to avoid bias comparisons. This is because a different set of experiments (with different ASM tissues) was used to obtain these data. Even if the concentrations of CCh were approximately the same (23 nM for static and tidal breathing versus 16 nM for tidal breathing + DI), the tone induced by CCh is variable from one tissue to the other. The average tone in that set of experiments was 33.2 ± 8.3%.

The effect of tone on the strains (length oscillations) experienced by the ASM during these breathing maneuver simulations was also investigated. Strains induced by simulated tidal breathing and DI under relaxed (without tone) and activated (with tone) conditions are shown in Figure 2.11. In

activated ASM, force oscillations mimicking tidal breathing caused strains of 0.4 ± 0.1%, which were significantly lower than the 6.5 ± 2.6% strains induced by the same maneuvers in relaxed ASM ($p < 0.05$). In response to DI simulations, the strain experienced by the muscle in the presence of tone was 9.3 ± 2.3%. This value was significantly less than the 24.0 ± 2.6% strain experienced by the relaxed muscle during simulated DI.

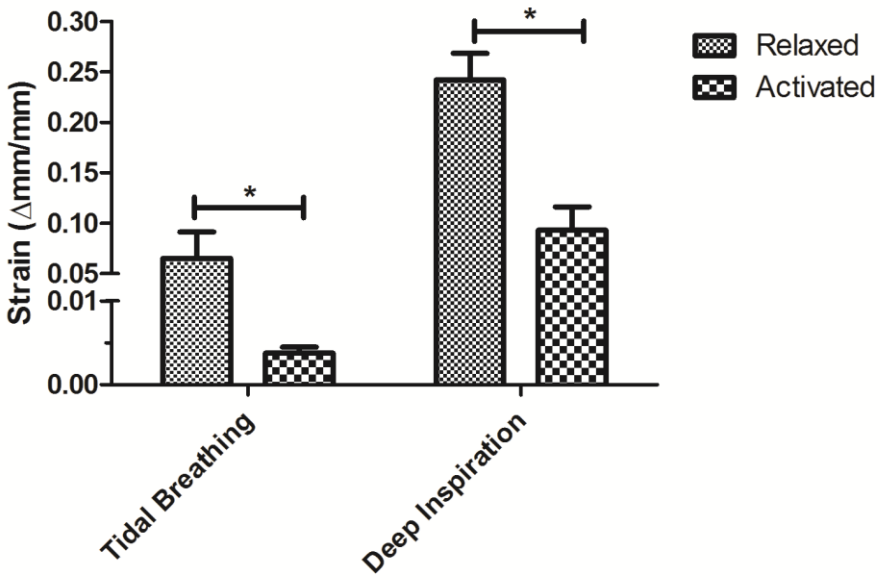

Figure 2.11 Strain experienced by the ASM during tidal breathing and DI simulations. Strain was measured as the fraction of change in length (mm) caused by the force oscillations over the initial length of the muscle. *Significant differences comparing relaxed and activated ASM ($p<0.05$). n=24 for tidal breathing simulations and n=9 for tidal breathing + DI simulations.

2.4 Discussion

Previous studies on isolated ASM strips have used length oscillations to mimic breathing patterns (111, 114, 150). *In vivo*, relatively constant changes in force caused by breathing maneuvers result in different length changes of the ASM depending on whether the muscle is activated or not. A non-active muscle experiences a greater degree of strain (length change) when a force is applied to it than occurs in its activated counterpart. This concept was illustrated recently in an *in vivo* study in which the lungs of dogs were subjected to progressive increases in insufflation pressure before and after the establishment of a baseline tone induced by histamine inhalation (155). It was shown that the caliber of the airways was always greater in the absence of tone at any insufflation pressure tested. Therefore,

using length oscillations to mimic breathing without taking into account the amount of ASM activation may result in greater force oscillations than experienced in vivo. In the present study, force oscillations were used to better represent the strain that would be experienced by activated and non-activated ASM in vivo.

The main goal of this study was to investigate whether force adaptation occurs under force oscillating conditions that mimic tidal breathing with or without periodic DI. The results show that simulated breathing maneuvers do not affect the level of force adaptation. Under static conditions, tone induced by CCh resulted in an 11.4 ± 2.0% increase in ASM force-generating capacity. This increase was similar to that reported in previous studies done in our laboratory, which showed that ACh-induced tone causes a rise in ASM force-generating capacity of 13% under static conditions (66). In conditions simulating tidal breathing and tidal breathing + DI, the gain in force caused by force adaptation was 13.5 ± 2.4% and 11.3 ± 3.0%, respectively. These results are in contrast to the findings of a recent study using length oscillations to mimic breathing patterns, which showed that the length oscillations applied (8 and 25% strain for tidal breathing and DI, respectively) were enough to almost completely abolish force adaptation in muscle activated with ACh (114). The problem with using length oscillations in activated muscle is evident; the pressure swings that would be necessary to induce 25% strain in an airway wall with activated muscle are unphysiologic. It has been shown that the decline in ASM force caused by breathing maneuver simulations is proportional to the strain (116). In the present study, we show that adding ASM tone greatly attenuated the strain (length change) induced by force oscillations (Figure 2.7). Consequently, the decline in ASM contractility that would normally prevail in relaxed airways due to the straining forces of breathing maneuvers can be lost when the ASM is activated. Taken together, these results suggest that normal force oscillations experienced during breathing may not strain the ASM enough to disrupt the force adaptation process in the presence of tone.

An additional difference in the present protocol as compared with the previous study assessing force adaptation under length oscillating conditions (114) is the timing of the oscillations. In the study of Raqeeb and coworkers (114), the length oscillations were initiated at the same time as the tone. Because breathing maneuvers are known to decrease ASM contractility (reviewed in Reference (156)), the decline in force caused by these maneuvers likely masked the increase in force caused by force adaptation. More appropriate experiments would need to be done to assess whether force adaptation occurs in length-oscillating conditions.

It is unknown how much narrowing an increase in total force of approximately 11% would cause in an airway. A mathematical model predicted that introducing tone by adding a spasmogen, together with the resulting force adaptation that ensues, can increase ASM shortening by approximately 10%, airway narrowing by approximately 50%, and resistance to airflow by approximately 275% in an airway of the ninth generation (65). Force adaptation may thus contribute significantly to AHR. The results of the present study extend this conclusion by showing that the force oscillations that act on the airway wall in vivo during breathing maneuvers cannot prevent force adaptation. These results reinforce the possibility that force adaptation may contribute to AHR in patients with asthma who have increased airway tone. Whether force adaptation occurs in vivo and to what extent it can influence the degree of airway responsiveness remain to be tested.

Using trachealis muscle as a model to study ASM has shortcomings compared with using intact airway or bronchial smooth muscle strip, such as the lack of mechanical coupling between the ASM and other airway wall structures (157) or the relative quantity of smooth muscle in a tracheal strip compared with a bronchial ASM strip (158). In an airway in situ, it is possible that the full-force oscillations imposed by breathing would not “reach” the ASM layer. Considering that the airways are composed of numerous other cell types and extracellular matrix, it is likely that some of the force applied by pressure changes against the airway wall would be absorbed or dissipated by the other airway constituents rather than being applied to the ASM layer. Similarly, if the ASM were to become uncoupled from the other wall structures (157) or if the airway wall was uncoupled from the parenchyma (159, 160), the strain experienced by the muscle would be lessened even further. In our experiments, we applied the highest force oscillations likely to be experienced in vivo to the isolated trachealis muscle strip. Because we did not see any attenuation in force adaptation under these conditions, it is reasonable to assume that our results would stand in an intact airway. Hence, for the purposes of this study we believe that the trachealis muscle and our experimental protocol constitute a suitable model.

We also simulated tension oscillations that prevail in normal (i.e., nonasthmatic) airways. This is because data on the relationship that exists between transpulmonary pressure and the cross-sectional area of the airways of a given generation are required to precisely calculate wall tension oscillations that would be caused by breathing maneuvers within that generation of airways (change in tension = change in pressure × change in radius). These data are available for normal human lungs (153) but not for human asthmatic lungs. However, because asthmatic airways are thicker (56, 154) and uncoupled from the parenchyma (159, 160), the strain experienced by the asthmatic ASM during breathing is probably

less than in normal airways. If we had tried to model tension oscillations in asthmatic airways, the muscle would have been operating in a more static environment in which force adaptation would have been more likely to occur.

Based on our results, it would be incorrect to conclude that force oscillations are unlikely to affect airway narrowing in vivo. The tone generated by the ASM in response to CCh was significantly lower during simulation of tidal breathing. Therefore, there is the possibility that breathing maneuvers are able to attenuate the effect of spasmogens on the ASM. Taken together, our study results suggest that force oscillations simulating breathing maneuvers reduce ASM force and may thus protect against excessive airway narrowing in vivo. However, the phenomenon of force adaptation occurs independently of whether the force oscillations are present and may thus contribute to AHR.

Future experiments should aim to determine the relationship between the magnitude of strain and force adaptation. The force oscillations required to achieve the strain needed to attenuate ASM contractility or affect force adaptation are likely to increase as the amount of tone increases. Therefore, it would also be necessary to determine at what level of tone the force oscillations imposed by normal breathing patterns cease to induce sufficient strain to affect ASM contractility or force adaptation. It will also be necessary for future studies to tease out the intracellular components that play a role in force adaptation. These components could be cytoskeletal or contractile apparatus in origin or they could originate at the cells' adhesion junctions. Because force adaptation occurs quickly (within five minutes), it is unlikely that the phenomenon is due to transcriptional changes; it is more likely due to a rearrangement or restructuring of cellular components. Experiments inhibiting protein translation should be done to answer this question.

2.5 Conclusion

In a situation that more closely simulates *in vivo* conditions where the ASM is subjected to force but not length oscillations, force adaptation occurs. These results suggest that force adaptation may take place in airways where there is increased ASM tone due to the presence of inflammation-derived spasmogens. The gain in force caused by force adaptation may contribute to AHR and to asthmatic symptoms by increasing the narrowing of the airways that occurs in asthmatic lungs.

Chapter 3 Decrease of Airway Smooth Muscle Contractility Induced by Simulated Breathing Maneuvers Is Not Simply Proportional to Strain[3]

3.1 Introduction

The movement of air in and out of the lung is caused by changes in pressure generated by cyclical expansion of the thoracic cavity. The airways, like any structure inside the thoracic cage, are stressed to change shape by these oscillating pressures. The strain (i.e., changes in shape) of the airway wall implies that all of its constituents, including the airway smooth muscle (ASM), are continuously subjected to length changes during breathing. There is considerable interest in the effect of these length oscillations on ASM contractility and the bulk of the evidence suggests that the effects of oscillating strain on ASM mechanics are not small; that is, they decrease ASM contractility considerably (59, 85, 111, 150, 151, 161). Because it is the strain experienced by the ASM rather than the applied stress that seems to be better correlated with the decline of ASM force (116, 162), an important variable related to the effect of breathing on ASM contractility is airway wall stiffness.

One of the most important factors that modifies airway wall stiffness is ASM tone (i.e., ASM activation). In lung disorders such as asthma, the overexpression of many inflammation- derived spasmogens such as leukotrienes, histamine, and others, can contribute to ASM tone (163). Even changes in pH were recently shown to affect ASM tone (164). No matter its origin, increasing tone stiffens the airway wall, which would be expected to decrease the amount of strain and possibly attenuate the decline of ASM contractility induced by breathing maneuvers. The effect of increasing tone on the strain and decline of force caused by simulated breathing maneuvers has never been systematically investigated. However, previous studies have shown that ASM pre-shortened with high concentrations of ACh re-lengthens when subjected to force oscillations simulating breathing maneuvers (59, 165–168). This phenomenon was dubbed force fluctuation-induced re-lengthening (165, 167, 168). These studies confirmed the results of earlier studies showing that length oscillations decrease ASM contractility (59, 85, 111, 150, 151, 161). The concordance of these studies using either force or length oscillations is counterintuitive, because with high tone, the strain induced by force oscillations would be expected to be very low. It raises the possibility that the stress itself in the absence

[3] A version of this chapter has been published. Pascoe CD, Seow CY, Paré PD, Bossé Y. Decrease of airway smooth muscle contractility induced by simulated breathing maneuvers is not simply proportional to strain. *J Appl Physiol* 114: 335–343, 2013

of strain (or in the presence of very small strain) may be sufficient to decrease ASM contractility. These later studies did not assess strain induced by force oscillations in a relaxed ASM and compare them with the strain obtained at different levels of activation (only one concentration of ACh was used). Thus, these studies were not designed to determine whether preventing the strain by increasing tone would attenuate the decline of ASM contractility induced by the oscillating stress of breathing.

The present experiments were undertaken to determine the influence of increasing tone on the strain caused by stress oscillations that simulate breathing maneuvers and to determine the relative effects of strain and stress on ASM force. Our results demonstrate that decreasing strain by increasing tone was slightly but significantly associated with an attenuated decline of ASM contractility induced by simulated breathing maneuvers. This finding is pertinent to individuals who have greater ASM tone, such as asthmatics. The ASM of such individuals may not be strained as much by the stress imposed by breathing maneuvers. Consequently, they may not fully benefit from the decrease in ASM contractility caused by breathing, rendering them more likely to be hyperresponsive due to ASM hypercontractility. However, our results also show that preventing the strain almost entirely by high tone was not sufficient to completely block the decline of contractility induced by these physiological levels of stress.

3.2 Methods

3.2.1 Tissue Preparation

Sheep tracheas used in these experiments were obtained from a local abattoir. The use of the tissue was approved by the Committees on Animal Care and Biosafety of the University of British Columbia. Tracheas were removed soon after the animals were killed and put in Krebs solution (118 mM NaCl, 4 mM KCl, 1.2 mM NaH_2PO_4, 22.5 mM $NaHCO_3$, 2 mM $MgSO_4$, 2 mM $CaCl_2$, and 2 g/liter dextrose; pH 7.4). Upon arrival at the laboratory, tracheas were cleaned of blood, fat, and loose connective tissue, and stored in Krebs solution at 4°C until further processed. ASM strips for experiments were dissected from ~2-cm-long tracheal segments. The in situ length of a relaxed tracheal smooth muscle bundle connecting the C shaped cartilage ring was measured. The tracheal rings were then cut open. Adventitial connective tissue and the epithelial and subepithelial layers were dissected away from the tracheal smooth muscle layer, and muscle strips (~6 mm long, 1 mm wide, and 0.3 mm thick) were isolated. The muscle strips were attached on both ends with aluminum foil clips. The ASM strips flanked by foil clips were then mounted vertically in a muscle bath. The bottom clip was attached to a stationary hook and the upper clip was attached to a hook connected to the lever arm of a servo-controlled force-length

transducer by a surgical thread (size 6). The distance between the clips during the dissection was used to adjust the length of the ASM strips once installed in the muscle bath to the length that it was in situ. This length is hereafter called Lin situ. The organ bath was filled with Krebs solution that had been preheated to 37°C and aerated with a gas mixture containing 95% O_2 and 5% CO_2. The temperature of the bath was also maintained by circulating 37°C water through a jacket that surrounded the organ bath.

3.2.2 Equilibration Period

ASM strips were subjected to a conditioning period before the start of the experiments. During the conditioning, the ASM strips were activated every 5 min with a 9-s electrical field stimulation (EFS) (60 Hz, 12 volts). Krebs solution was replaced every 5 min following EFS with warmed (37°C), aerated Krebs solution. The conditioning was completed when a plateau in isometric force was reached (i.e., after which there was no further increase in force in response to subsequent EFS). The force produced by EFS at that time was called F_{max}. Therefore, F_{max} is the force generated by the ASM in response to EFS at in situ length after a stable plateau was achieved minus the resting tension. The conditioning period took ~1 h.

3.2.3 Protocol 1

In protocol 1, we set out to determine the level of oscillating stress that was required not only to strain the relaxed ASM (i.e., not activated with exogenous ACh) but also to decrease its force-generating capacity sufficiently so that the effect of adding increasing levels of tone could be investigated. A physiological range of stress oscillations that simulated transpulmonary pressure excursions of 3, 5, 10, 15, 20, and 25 cm H_2O was tested. The methodology employed for these simulations is explained below. ASM length changes (i.e., strain) induced by the simulated pressure swings were recorded and ASM force-generating capacity was assessed periodically in response to either EFS or ACh. For EFS, the oscillations were present throughout the 5-min cycle except during the measurement of isometric force, when the oscillations were stopped for 40 s (10 s prior, 9 s during, and 21 s after EFS). A representative trace showing simulated normal breathing prior, during, and after EFS-induced force has been previously published (92). The 5-min cycles of oscillations were continued until no further decrease in ASM force was observed (i.e., when the force in response to EFS had reached a new plateau in oscillating conditions). The same procedure was performed for force measurement in response to ACh at 10^{-5} M, except that a 2-min period without oscillations was used after every ACh administration, which was the time needed for ASM to reach its near maximal force in response to this concentration of ACh. The concentration of ACh was chosen because it generates a consistently large response. The

decline of force caused by oscillations was calculated by subtracting the force generated by either EFS or ACh under static conditions from the force generated by the same stimulus when the oscillations were momentarily stopped following the start of the oscillations.

3.2.4 Protocol 2

In protocol 2, ACh concentration-response curves from 10^{-9} to 10^{-4} M were performed in a cumulative fashion with or without stress oscillations that simulated either repetitive pressure excursions of 20 cm H_2O or the pressure excursions occurring during normal breathing pattern (i.e., tidal breathing + a deep inspiration (DI) every 5 min). Hence, three ACh concentration-response curves were performed in each tissue strip. The ASM was allowed to recover completely between every concentration-response curve. ACh was washed away repeatedly with Krebs solution and the muscle strip was allowed to sit for 30 min while stimulated to contract at 5-min intervals with EFS before the next concentration-response curve. The purpose of the repeated EFS was to gauge tissue recovery over time. The order of the oscillating conditions (none, 20 cm H_2O, and breathing pattern) was randomized. The oscillations were initiated just before adding the first concentration of ACh. The force values were taken at the maximal force obtained in the first 5 min for every ACh concentration. During breathing pattern simulation that included a DI, the force values were taken 2 to 2.5 min after the simulated DI. In the presence of oscillations, the force values were taken at the trough when the ASM strip was at $L_{in\ situ}$ [functional residual capacity (FRC) for the simulation of breathing]. The strain at every ACh concentration was the average strain of three oscillations taken at the maximal force obtained during the 5-min stimulation. The decline of force caused by oscillations was calculated by subtracting the force generated by ACh under static conditions from the force generated by the same concentration of ACh under oscillating conditions.

3.2.5 Protocol 3

In protocol 3, the maximal force that can be achieved in response to a given concentration of ACh was attained under static conditions prior to the instigation of stress oscillations. The force value at 100 s after ACh administration was always chosen because it allowed time for the muscle to reach its near maximal force in response to any of the ACh concentrations used (10^{-7}, 10^{-6}, 10^{-5}, or 10^{-4} M). This force was the reference value for calculating the changes of force over time that occurred either spontaneously or in response to the oscillations. The stress oscillations simulated transpulmonary pressure excursions of 10 cm H_2O from FRC, 20 cm H_2O from FRC, or those occurring during normal breathing (tidal breathing + intercalated DI). Each tissue was exposed to these three oscillating

conditions and also stimulated once for the same amount of time in the absence of oscillations in a randomized fashion. Therefore, each muscle was stimulated to contract four times in response to the same concentration of ACh. Every tissue was exposed to the four conditions, but was exposed to only one concentration of ACh. Different sets of tissues were used for different concentrations. The ASM was allowed to recover completely between ACh stimulations (ACh was washed away repeatedly with Krebs solution and the tissue was al- lowed to sit for 30 min while stimulated to contract at 5-min intervals with EFS, before the next ACh stimulation). The ACh stimulation in the absence of oscillations was a time-control to measure the time- dependent changes of ACh induced tone. These changes were taken into account to calculate the effect of the oscillations on ASM force. This was to distinguish changes in ACh-induced tone that sometimes occur over time from the effect of the oscillations. The force values in the oscillating state were taken 5 min after the beginning of the stress oscillations, which allowed sufficient time to reach a new dynamic plateau. During breathing pattern simulation that included a DI, the force value was taken 2.5 min after the simulated DI. These values were taken at the trough of the oscillations when the muscle was back to its length under static conditions (back to simulated FRC).

3.2.6 Simulations of Breathing Maneuvers

The stress oscillations imposed on ASM strips simulated the tension oscillations experienced by the wall of a fourth-generation airway during transpulmonary pressure excursions of different magnitude (e.g., 3 cm H_2O from 5 to 8 cm H_2O to mimic tidal breathing, and 25 cm H_2O from 5 to 30 cm H_2O to mimic a DI from FRC to total lung capacity (TLC)). We chose airway generation 4 because the thickness of the wall is approximately equal to the thickness of the trachealis (~0.3 mm) (56, 154). Therefore, assuming that the tension is transmitted homogenously across the entire thickness of the wall, the stress experienced by our tracheal strips would be the same as the stress experienced by the ASM of an airway of the fourth generation in vivo. Representative force (upper) and length (lower) traces are shown in Figure 3.1 in the absence (A) and presence (B) of tone elicited by ACh. The stress oscillations at any chosen magnitude were performed at breathing frequency (0.2 Hz) with half sine waves (without a trough) to mimic maneuvers from, and back to, FRC (i.e., one semi-sine wave every 5 sec).

The changes in wall tension caused by such excursions were calculated on the basis of the Laplace relationship (tension = pressure x radius), assuming that the airways resemble a thin-walled cylinder (a reasonable assumption because the ratio of wall thickness/airway luminal diameter is ~1/22 in a non-asthmatic airways of the fourth generation (56, 154)). Because the airway wall is also strained

during these swings in transpulmonary pressure, the calculated change in wall tension also has to take into account the change in radius (at the middle of the ASM layer). Equations developed by Lambert and coworkers (153) and morphological data for a fourth generation airway taken from James et al. (56), Kuwano et al. (154), and Wiggs et al. (152) were used to make this adjustment. The magnitude of the tension oscillations was the same for every ASM strip (e.g., 0.74 mN/mm for tidal breathing and 6.24 mN/mm for the DI) but the magnitude of the force oscillations depended on the width of the ASM strip. This is because the force required to apply a given tension within the wall of an airway depends on the length of the airway segment that is being studied. Because the ASM is arranged circumferentially around the airways, this width represents the portion of the airway length that would be studied in vivo. To estimate the width of the ASM strips, we assumed that the ASM generates a stress (force/cross-sectional area) of 100 kPa (169) in response to EFS following the conditioning period (so F_{max} = 100 kPa or 100 mN/mm^2) and that the thickness of the ASM strips was 0.3 mm. The value of F_{max} (in mN) was thus used to calculate the width of the ASM strips. Knowing the length of the airway wall that would be covered in situ by this estimated width of the ASM strip and the changes in wall tension occurring during breathing maneuvers, we were then able to calculate the force oscillations (in mN) that had to be imposed on tracheal strips to simulate the amount of stress to which the ASM is subjected in vivo. This approach is an efficient way to calculate the force oscillation required to obtain a given stress oscillation without the need for measuring the cross-sectional area of ASM strips by histology, which would only be possible a posteriori (i.e., after the mechanical measurements).

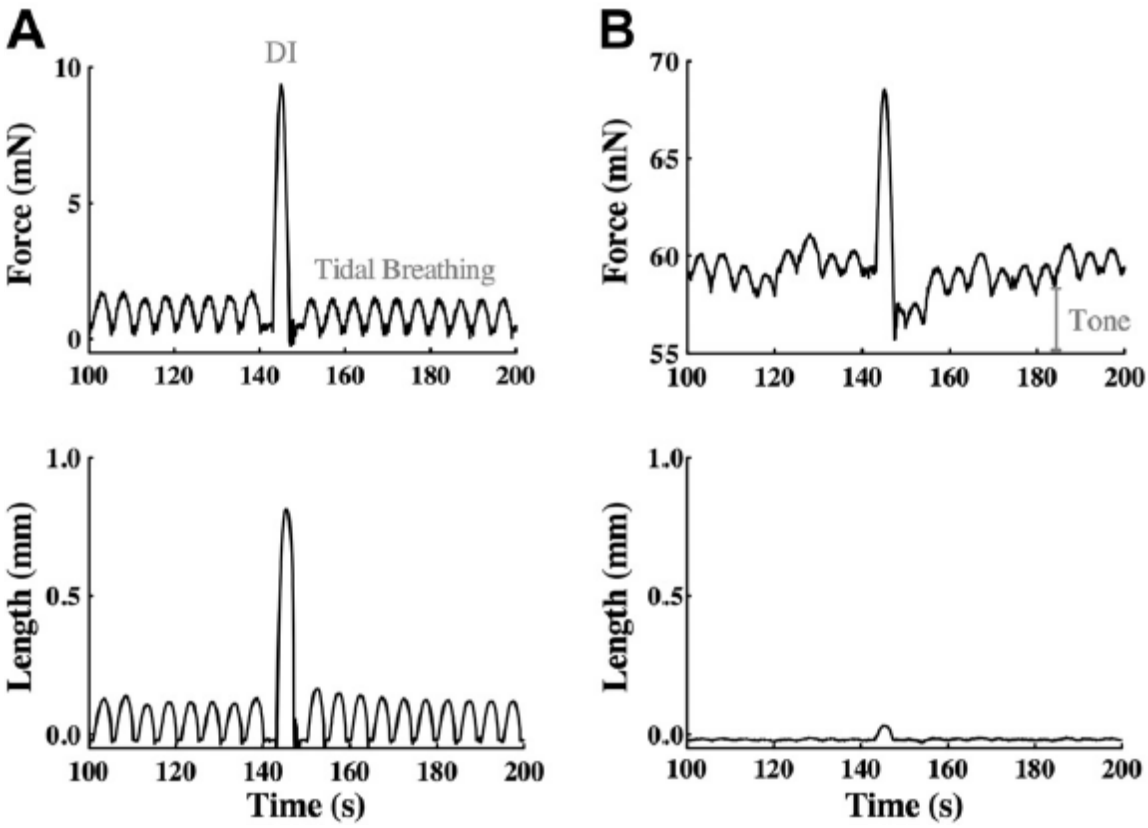

Figure 3.1 Representative traces of force (upper) and length (lower) during simulated breathing maneuvers in the absence (A) or in the presence of tone (B). The tone in this example was induced by ACh at 10^{-5}M. Notice that the y-axis for the force trace in B does not start at 0. The tone markedly attenuated the changes in length (i.e. strain) caused by the stress oscillations. There is a small, transient decrease in force and a small lengthening following the simulated deep inspiration (DI).

3.2.7 Statistical Analyses

Resting tension, EFS-induced force, and ACh- induced tone obtained for each muscle strip were normalized to Fmax before averaging. Data shown are means ± SD. Linear regression analysis of individual tissue and the mean of their slope were used to measure the relationship between stress vs. strain, stress vs. decline of force, and strain vs. decline of force. Two-way ANOVAs were used to compare the effect of different oscillating conditions and different ACh concentrations on strain and the decline of force, as well as their interactions. Repeated measures for one or two factors were performed whenever appropriate. Two-way repeated measures ANOVA for both factors were conducted in R (version 2.15.1) using the ANOVA function from the car package. All the other statistical analyses were

performed using Prism 5 (GraphPad Software, San Diego, CA). A value of $p<0.05$ was considered significant.

3.3 Results

3.3.1 Stress Oscillations on Relaxed ASM (Protocol 1)

In protocol 1, the oscillations were always performed when the ASM was relaxed (i.e., not activated with ACh). ASM force generation was assessed by measuring the response to both EFS and ACh (Fig. 3.2, left and right, respectively) while the oscillations were interrupted. In Fig.3.2A, the strain is plotted against the magnitude of stress. Linear regression analyses show that the strain was related to the magnitude of the stress oscillations. Tidal breathing and simulated repetitive DI strained the relaxed ASM strips by 5.7% ± 1.2% and 21.2% ± 2.0%, respectively, in the set of experiments using EFS to measure force and by 4.5% ± 1.35 and 23.2% ± 4.2%, respectively, in the set of experiments using ACh to measure force. In Figure 3.2B, the decline of force is plotted against the magnitude of stress. The decline of force was calculated as the force generated by the muscle in response to either EFS or ACh prior to oscillations minus the force generated by the same tissue after a new plateau of force was reached following the start of the oscillations (see Protocol 1 in Materials and Methods). The linear fit of these relationships indicates that the decline of EFS-induced force was related to the magnitude of the stress oscillations. However, this was not always the case for ACh-induced force. Two linear regressions were not significant (from the triangle symbols pointing up, $Y = 0.50X + -3.38$, $r^2 = 0.58$, $p = 0.07$; and from the hexagon symbols, $Y = 0.12X + 5.06$, $r^2 = 0.11$, $p = 0.53$). Tidal breathing and repetitive simulated DI in relaxed ASM strips decreased force by 1.2% ± 0.5% and 18.2% ± 1.2%, respectively, in the set of experiments using EFS to measure force and by 3.4% ± 1.7% and 17.6% ± 5.2%, respectively, in the set of experiments using ACh to measure force. In Fig. 3.2C, the strain and the decline of force induced by the oscillating stress are plotted together. The fit of these linear regressions indicates that they were related when EFS was used as the contractile stimulus. Again, this was not always the case when ACh was used as the contractile stimulus. Two linear regressions were not significant (from the square symbols, $Y = 13.08X + 5.20$, $r^2 = 0.06$, $p = 0.63$; and from the diamond symbols, $Y = 49.60X + -6.75$, $r^2 = 0.50$, $p = 0.11$). From this study, it was concluded that simulations of 20 cm H2O-transpulmonary pressure excursions were required to cause sufficient strain (21.4% ± 1.5% and 20.1% ± 3.5%) and decline of force (19.3% ± 2.8% and 14.8% ± 4.0%) so that the effect of tone on both strain and decline of force induced by the oscillating stress can be measured. Simulations of 20 cm H_2O-transpulmonary pressure excursions were

therefore performed in the following experiments. A normal breathing pattern (i.e., tidal breathing + a DI every 5 min) was also investigated due to its in vivo relevance.

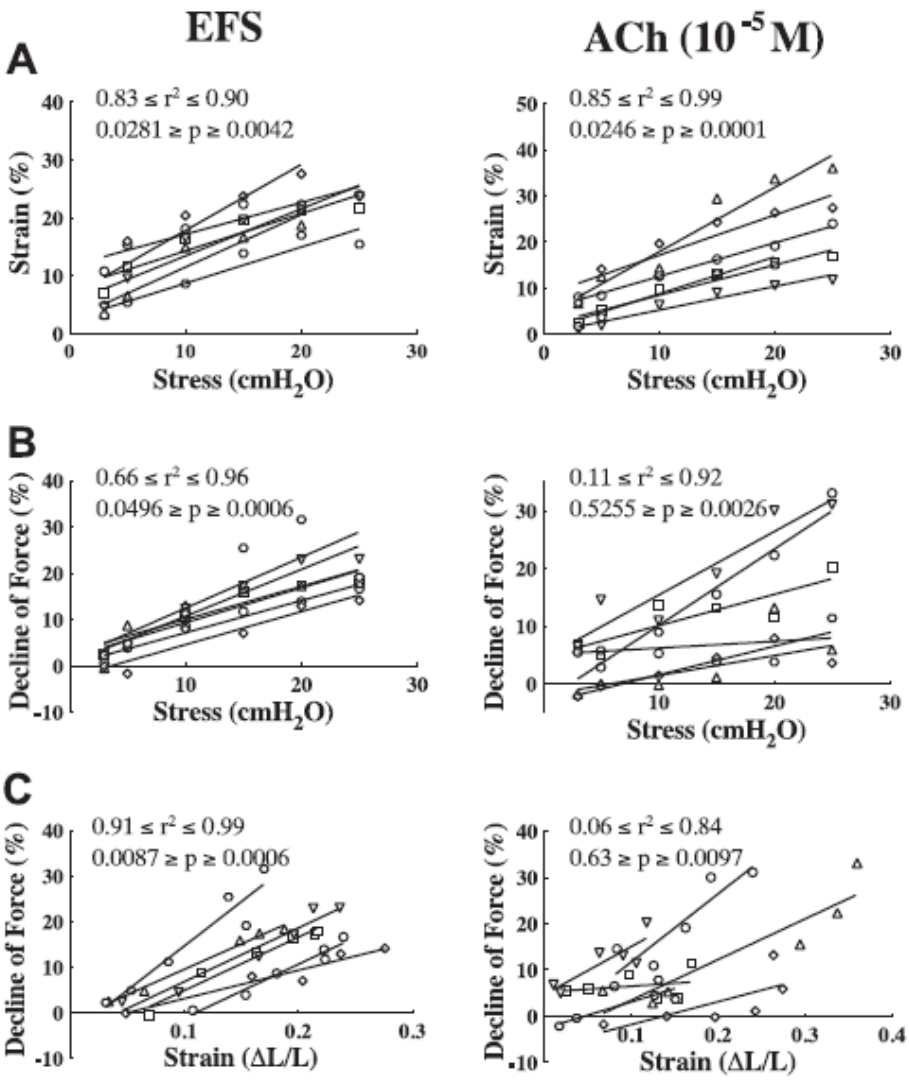

Figure 3.2 The relationships between strain, stress, and decline of force induced by breathing simulations. The force generated by ASM was measured in response to either electrical field stimulation (EFS) (left) or ACh (right). The ASM was subjected to stress oscillations as described in Fig. 1 that simulated the tension oscillations experienced by the wall of a fourth-generation airway during excursions of transpulmonary pressure from functional residual capacity (5 cm H_2O) of a magnitude indicated on the x-axis (in A and B). In this set of experiments, ASM strips were oscillated in a relaxed condition (i.e., prior to EFS or ACh stimulation) and the oscillations were interrupted during force measurement (see Materials and Methods). Linear regressions from individual tissues are shown, together with their range of r^2 (goodness of fit) and p values. The means of the slopes were significantly different from 0 ($p \leq 0.0003$); n = 6.

3.3.2 Stress Oscillations during Force Development (Protocol 2)

Figure 3.3 shows representative force (left) and length (right) traces illustrating the sequence of interventions used in protocol 2. The force oscillations were consistent throughout and the force generated by ACh was concentration-dependent. The length oscillations (strain) caused by the stress oscillations decreased as the concentration of ACh increased (Fig. 3.3, right).

Figure 3.4 shows the concentration-response curves under oscillating conditions that simulate either breathing pattern (tidal breathing with periodic DI; A) or 20 cm H_2O-transpulmonary pressure excursions from FRC (B). They are compared with the concentration-response curves obtained under static conditions (same tissues in A and B). Interestingly, the simulated breathing pattern (tidal breathing + periodic DI) had a weak but significant effect on ASM force (A). The significant effect due to condition (oscillating vs. static), together with the lack of significant interaction, suggests that the oscillations reduced the ASM capacity to generate force by the same amount at all concentrations of ACh. The effect of simulated 20 cm H_2O-transpulmonary pressure excursions was more pronounced (B). The oscillations reduced the ASM response to exogenous ACh, and this effect was significantly increased with increasing ACh concentrations (the interaction was significant). It should also be noted that the two curves did not converge at the higher doses of ACh, where the strain was lowest.

The effect of stepwise increases of ACh concentration on ASM strain induced by different stress oscillations is shown in Fig. 3.5. As observed under relaxed conditions (Fig. 3.2), the strain was related to the magnitude of the stress oscillations. Increasing ACh concentrations decreased ASM strain to an extent at which the strain was almost abolished irrespective of the magnitude of the stress oscillations (at 10^{-4} M, the strain induced by simulated 3, 20, and 25 cm H_2O-transpulmonary pressure excursions were 0.09% ± 0.02%, 0.64% ± 0.05%, and 0.90% ± 0.05%, respectively). The significant interaction ($p \leq 0.0001$) indicates that the strain induced by oscillating stress was greatly affected by the concentration of ACh.

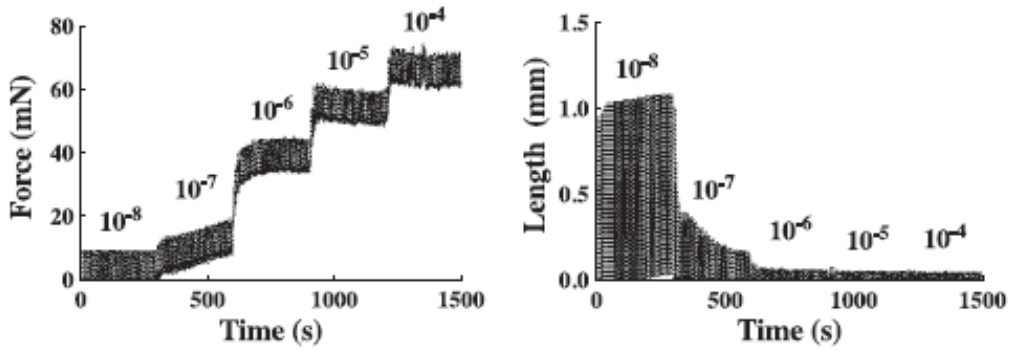

Figure 3.3 Representative traces of force (left) and length (right) showing the sequence of interventions used in protocol 2. The simulated breathing maneuvers were started just before the stepwise increases of ACh concentration. ACh concentration was changed every 5 min. In this example, the magnitude of the stress oscillations simulated transpulmonary pressure excursions of 20 cm H_2O from functional residual capacity. The effect at 10^{-9} M is not shown because even at 10^{-8} M (first concentration shown) no measurable force was generated. Notice that as the tone increased, the strain induced by the stress oscillations decreased.

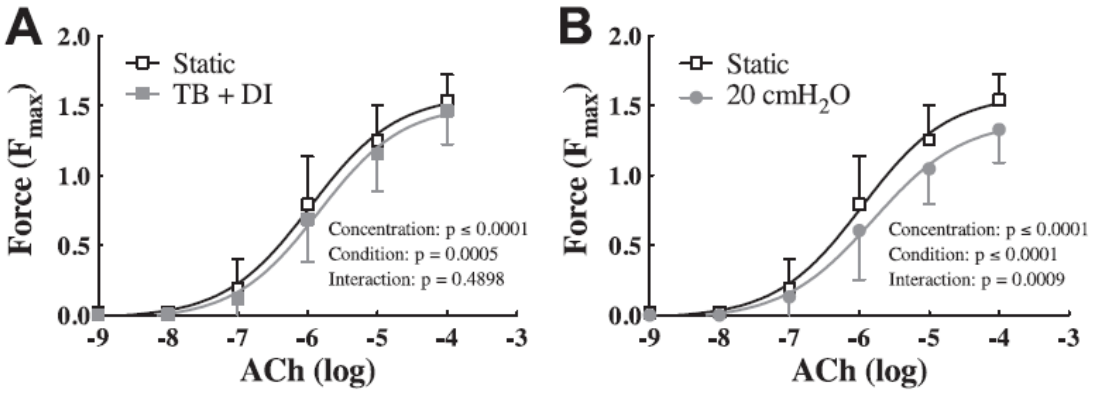

Figure 3.4 The effect of stress oscillations on ACh concentration-response curves. Breathing pattern (tidal breathing (TB) with intermittent deep inspiration (DI)) (A) or 20 cm H_2O-transpulmonary pressure excursions from functional residual capacity (B). These results are from force traces such as the one shown in Fig. 3. The forces are the maximal force obtained during the first 5 min following every concentration of ACh. The forces are normalized to Fmax, which is the force generated in response to electrical field stimulation minus the resting tension after the conditioning period and prior the administration of ACh (see Materials and Methods). The results of the two-way ANOVA are shown in the inset; n = 9.

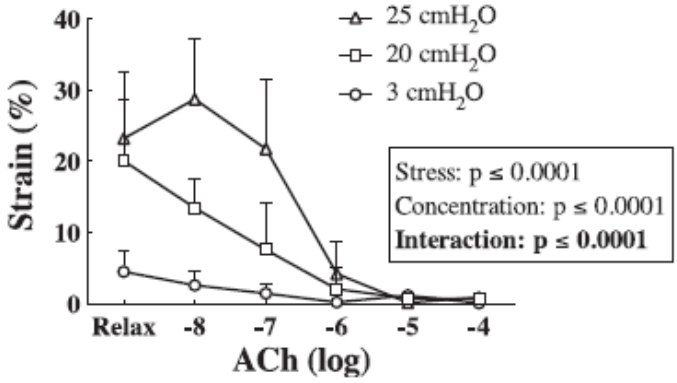

Figure 3.5 The effect of stepwise increases of ACh concentration on ASM strain induced by stress oscillations that simulate either 3 (tidal breathing), 20, or 25 (deep inspiration) cm H_2O-transpulmonary pressure excursions from functional residual capacity. These results are from length traces such as the one shown in Fig. 3. The results of the two-way ANOVA are shown in the inset; n = 9.

3.3.3 Stress Oscillations after Force Development (Protocol 3)

Figure 3.6 shows a representative force trace showing the sequence of interventions used in protocol 3. The stress oscillations were initiated 100 s after the administration of ACh. The effect of increasing stress on the strain of ASM stimulated to contract with different concentrations of ACh is shown in Fig. 3.7. The stress-strain relationship found in relaxed muscle is also shown as a reference. These later results are from Fig. 3.2A (right). As observed in Figs. 3.2 and 3.5, the strain was proportional to the magnitude of the stress oscillations. Also observed in Fig. 3.7 is the attenuating effect of increasing concentrations of ACh on strain. The effect was especially evident beyond 10^{-6} M, when even high stress became ineffective for straining ASM. The bottom of the y-axis has been magnified to better visualize the concentration-dependent decrease of ASM strain. The significant interaction ($p \leq 0.0001$) indicates that the stress-dependent ASM strain was greatly affected by ACh concentration. The data showing the decline of force induced by simulating breathing maneuvers in both protocol 2 and protocol 3 are presented in Fig. 3.8. The word “history” in the figure legend refers to the results of protocol 2, when oscillating history was present before taking force measurements at different ACh concentrations. The words “no history” refer to the results of protocol 3, when the oscillations were instigated after ACh had reached its maximal contractile effect. Only the results obtained with the simulated 20 cm H_2O-transpulmonary pressure excursions are shown, because neither breathing pattern nor 10 cm H_2O-transpulmonary pressure excursions affected force significantly. The strain obtained at every ACh

concentration in the two protocols is also shown. The strain obtained in both protocols is almost overlapping. The strain was reduced by more than half with 10^{-7} M of ACh compared with the strain experienced by ASM strips exposed to the same oscillating stress in a relaxed condition (compare the upper horizontal dashed line, taken from results shown in Fig. 2 (right) when ASM was exposed to simulated 20 cm H_2O pressure excursions without ACh, with the strain obtained in the presence of 10^{-7} M of ACh in Fig. 3.8). A further increase of ACh to 10^{-6} M almost completely abolished ASM strain. In contrast to strain, the decline of force induced by the oscillating stress was very different between the two protocols. With a prior history of oscillations (protocol 2), the decline of force was similar to the decline produced by oscillations in relaxed ASM (protocol 1); and this was true no matter the concentration of ACh. To visualize this effect, compare the lower horizontal dashed bar in Fig. 3.8, which was taken from results shown in Fig. 3.2 (right) (obtained by using protocol 1 in which the muscle was oscillated in a relaxed condition and stimulated to contract with 10^{-5} M ACh when the oscillations were momentarily stopped), with the decline of force obtained by the same stress at every ACh concentration (black bars). The larger SD at 10^{-7} M is due to the lack of response of some ASM strips to respond to that concentration of ACh under oscillating conditions (and if there was no force, there was no decline of force). Without oscillating history (protocol 3), 10^{-7} M of ACh attenuated the decline of force by 35.3% (compare the lower horizontal dashed bar, taken from results shown in Fig. 3.2 (right), with the decline of force obtained at 10^{-7} M in Fig. 3.8). However, further stepwise increases of ACh only slightly attenuated, in a concentration-dependent manner, the decline of ASM force. This was different from the results obtained with protocol 2 (with oscillating history), when no reduction in the decline of force was observed with increasing concentrations of ACh. The results obtained with both protocols demonstrate a striking difference between the effect of tone on strain vs. its effect on the decline of force.

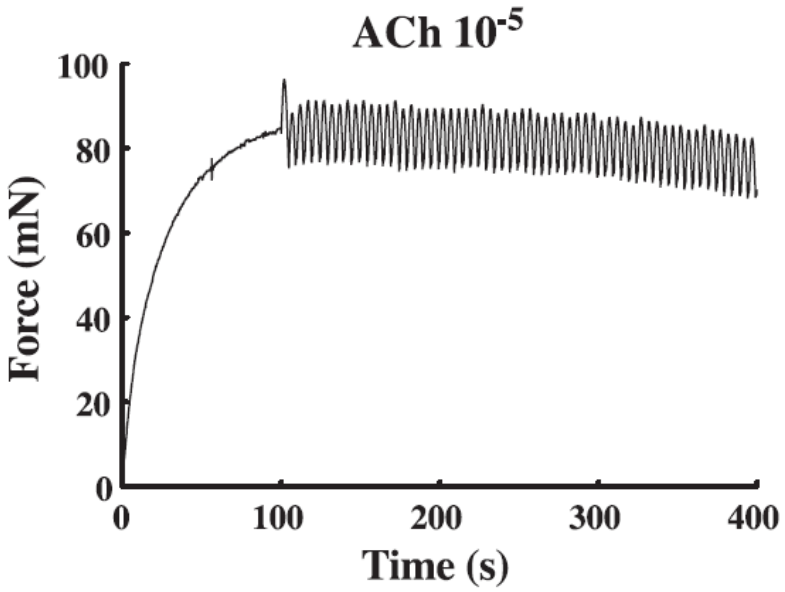

Figure 3.6 Representative force trace showing the sequence of interventions used in protocol 3. The stress oscillations were initiated 100 s after ACh administration. In this example, 10^{-5} M ACh was used and the magnitude of the stress oscillations simulated transpulmonary pressure excursions of 20 cm H_2O from functional residual capacity.

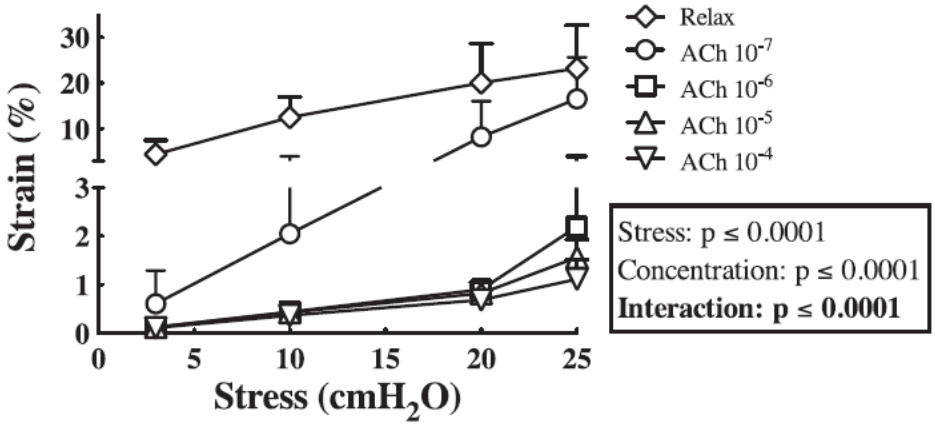

Figure 3.7 The effect of different ACh concentrations on ASM strain induced by stress oscillations that simulate either 3 (tidal breathing), 10, 20, or 25 (deep inspiration) cm H_2O-transpulmonary pressure excursions from functional residual capacity. The deep inspiration excursions were intermittent (once per 5 min), while all other oscillation were ongoing. These results are from force traces such as the one shown in Fig. 6. Notice that two different scales are used on the y-axis. The results of the two-way ANOVA are shown in the inset; n = 8.

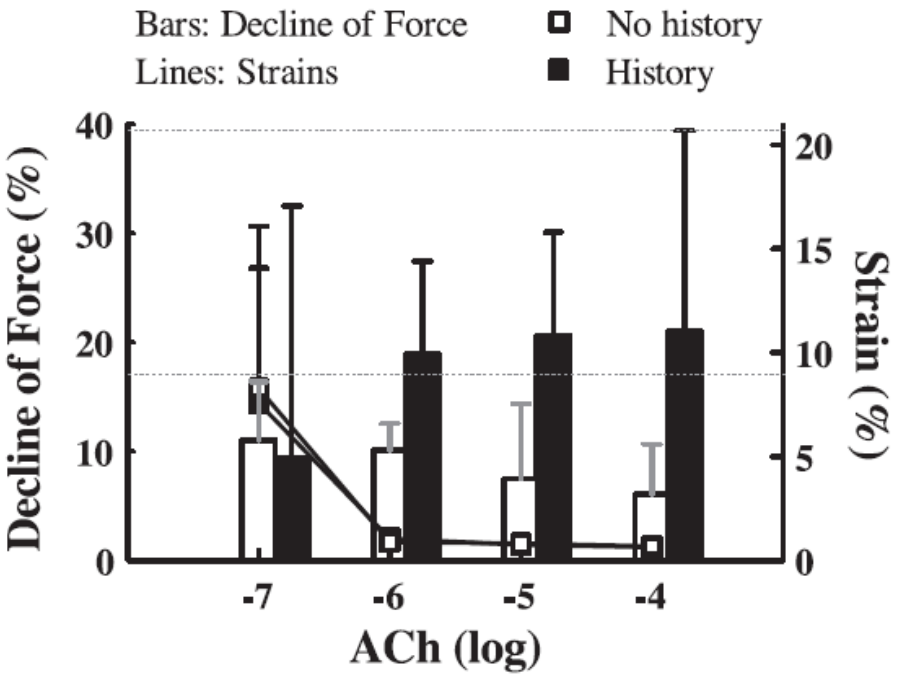

Figure 3.8 The effect of stepwise increases of ACh concentration on both ASM strain (lines) and the decline of force (bars) induced by oscillating stress that simulates 20 cm H_2O-transpulmonary pressure excursions in both protocol 2 (n = 9) (black), where there was an history of oscillations, and in protocol 3 (n = 8) (white), where there was no history of oscillations. The horizontal dashed lines are to compare with the strain (upper line) and the decline of force (lower line) induced by these stress oscillations in protocol 1 when the ASM was relaxed (i.e., not stimulated with ACh) during the oscillations.

3.4 Discussion

In the present study, we sought to determine whether it is the stress or the attendant strain that is responsible for the decline of ASM force associated with breathing maneuvers and whether tone can prevent the decline of force by attenuating the strain. Other investigators have examined the effects of simulated breathing oscillations on ASM force generation but have done so using a different protocol involving ASM shortening and subsequent relengthening in response to oscillations (59, 165–168). Our study examined the strain and the decline of force triggered by different oscillating conditions at different levels of ASM activation elicited by different ACh concentrations. Our results demonstrated that the decline of force caused by oscillating stress is related to the strain, especially when the oscillations were performed when the ASM was relaxed. However, when the stress oscillations were

applied during force development, decreasing the strain by increasing tone had much less or no effect, on the decline of force. This suggested that the oscillating history may be sufficient to decrease ASM force, or that the decline of force is disproportional to the magnitude of strain under some circumstances. This lack of proportionality is further supported by the finding that a significant decline of force was still observed at high ACh concentrations when the strain was very small (protocol 3), indicating that there is sometimes a clear mismatch between the pronounced effect of tone on strain and its more modest effect on the decline of force.

3.4.1 Strain Induced by Simulations of Breathing Maneuvers

It is important to determine whether and to what extent the ASM is strained by the oscillating stress acting on the airway wall during breathing maneuvers. In this study, a physiological range of stress was applied to ASM to measure its effect on strain. In relaxed ASM, our results showed that stress excursions of 2.5 and 20.8 kPa, which simulate tidal breathing and DI, respectively, strained the ASM strips by 4.5% ± 1.3% and 23.2% ± 4.2%, respectively. These values are also similar to the strain obtained in a previous study using the same experimental setting (6.5% ± 2.6% for tidal breathing and 24.2% ± 2.6% for DI) (92). These values are also very close to the ones predicted on the basis of changes in lung volume during these breathing maneuvers (4% and 25% for tidal breathing and DI, respectively), which were based on the assumption that the airway perimeter changes in proportion to the cube root of the changes in lung volume (111).

3.4.2 Effect of Tone on Strain

Recent *ex vivo* and *in vivo* studies have demonstrated that the decline of contractility or the relief from bronchoconstriction is better correlated with strain than with stress (116, 162). These findings have urged the search for factors affecting airway wall stiffness. One of the more obvious factors affecting airway wall stiffness in vivo is ASM tone (i.e., muscle activation). In the presence of tone, the amount of stress imposed by breathing maneuvers presumably remains the same, but the level of strain is likely to be negatively affected. In the present study, we measured the impact of tone on the stress-strain relationship. The results suggested that concentrations of ACh that are sufficient to trigger a measurable amount of force are very effective in preventing ASM strain. When the stress generated by ASM was approximately equal to the oscillating stress (e.g., the stress generated by ASM in response to ACh at 10^{-7} M was 16.4 kPa ± 2.8 and the stress imposed by simulation of 20 cm H_2O-transpulmonary pressure excursions was 16.7 kPa), the strain was reduced by more than half (20.7% ± 3.5 vs. 7.92% ± 1.7%). A critical point was also observed at 10^{-6} M, when the strain almost disappeared

even at the highest stress tested. This was not surprising because 10^{-6} M of ACh generated 72.6 kPa ± 5.3, which represents almost four times the stress caused by a simulated DI (20.8 kPa). Together, these results suggest that very little tone (i.e., small percentage of the maximal force-generating capacity of the ASM) can almost abrogate the strain caused by any physiological level of stress.

3.4.3 Lack of Decline of Force with Tidal Breathing

Ultimately, our experiments were designed to determine whether a physiological range of stress before or during ASM stimulation could affect ASM force and whether the changes of force are correlated with the level of strain. At a level of stress that simulates tidal breathing, the declines of force were very small, irrespective of whether the oscillations were finished before stimulations (protocol 1) or were initiated during (protocol 2) or after (protocol 3) force development. It was previously demonstrated using ex vivo airway preparations that simulated tidal breathing has very little effect on contractility (117, 118). However, the real strain experienced by the ASM in those ex vivo airway preparations is difficult to determine. It was argued that the smaller effect (or the lack of effect) of tidal breathing simulations on isolated airways compared with ASM subjected to length oscillations may be due to a failure to transmit the changes in airway wall tension to the ASM cells (so that the changes in tension may be dissipated by other structures in the airway wall). Our isolated ASM strip was ideal to answer this unresolved question. It allowed complete control over the stress acting on the ASM strips and its concomitant effect on strain and on force. Our results suggest that the lack of bronchodilating effect of tidal breathing may not be due to the failure to transmit the swings in tension to the ASM, because tidal breathing simulations had no effect in our ASM preparations. The controversial issues concerning the bronchodilating effect of tidal breathing have been discussed previously (170).

3.4.4 Decline of Force Induced By Strain at Higher Oscillating Stress

At higher levels of oscillating stress, the decline of force became significant. The decline of force in conditions simulating 20 cm H_2O-transpulmonary pressure excursions was about 20%. This was true when the oscillations were performed in a relaxed muscle prior to stimulation (protocol 1), as well as when the oscillations were initiated prior to stimulation, irrespective of the concentration of ACh (protocol 2). This later observation suggests that strain is not the only contributing factor affecting ASM force. It raises the possibility that strain history may be sufficient to attenuate ASM force. However, the decline of force in protocol 3 was slightly but significantly attenuated as the concentration of ACh increased (Fig. 8). So in the absence of strain history, the magnitude of strain is related (although not proportionally) to the decline of force, suggesting that preventing strain by increasing tone does

attenuate the decline of force induced by oscillating stress. This is consistent with a very recent study discussed next (171).

As we were writing this manuscript, Lavoie and coworkers reported a similar relationship between the diminution of strain induced by tone vs. the alteration of ASM contractility in precision-cut lung slices (PCLS) from human lungs that were subjected to oscillating conditions simulating breathing (171). The sequence of the intervention they used resembled protocol 3 of the present study, in which muscle stimulation was initiated and the maximal level of contraction achieved before instigating stress oscillations. Not only did they show that tidal breathing was inefficient to bronchodilate stimulated airways no matter the initial amount of bronchoconstriction, but they found that increasing the severity of bronchoconstriction attenuated the strain and the level of bronchodilation induced by higher magnitudes of stress. Lavoie and coworkers measured airway narrowing (ASM shortening), which is more relevant to in vivo physiology than our approach of measuring ASM force. On the other hand, our approach offers a better control over the load. It is difficult to estimate the amount of stress that is actually transmitted to the muscle during breathing maneuver simulations in PCLS. The authors used the stress that was necessary to strain the airways by a physiological amount in the relaxed airway smooth muscle and exposed the activated airways to the same stress. However, they cannot quantify this stress. It is also difficult to set the preload in PCLS. Our experimental setup allowed precise control of the stress acting on the muscle and its effect on changes in ASM length (strain) at any given level of tone. Nevertheless, despite using two different approaches, tissues from different locations within the lung (trachea vs. intraparenchymal airways) and different species (sheep vs. humans), the conclusions drawn are similar. Collectively, these studies suggested that limiting strain by increasing tone attenuates the decline of force caused by oscillating stress. This suggests that the results of Lavoie and coworkers (171) may be explained at least partially by the effect of strain on ASM force.

3.4.5 Decline of Force Not Induced By Strain at Higher Oscillating Stress

In addition to the Lavoie et al. study, our results also demonstrated that tone results in a change in the slope of the relationship between strain and the decline of force compared with the relaxed ASM (protocol 1). In both protocol 2 and protocol 3 a decline of force was still present at high levels of tone despite the quasi absence of strain. In protocol 3, for example, ACh at 10^{-4} M reduced the strain to 0.7% during simulated 20 cm H_2O-transpulmonary pressure excursions while the decline of force was still 6.1%. It is also important to notice that the declines of force are expressed in percentages, not in absolute values. In absolute values, a 6.1% decline of force at 10^{-4} M when the ASM generated 141.2

kPa ± 4.0 is greater than the decline of 11.1% that occurred at 10^{-7} M when the ASM generated 16.4 kPa ± 2.8 (8.6 vs. 1.8 kPa). This implies that very little strain is sufficient to substantially affect ASM force. However, this was only true when the oscillating stress was high. At the same level of strain induced at lower oscillating stress (such as the one occurring during tidal breathing simulations), no decline of force was observed. If only very little strain is sufficient, one would predict that even simulated tidal breathing would substantially decrease ASM force at low tone. Together, the results suggested that several factors may govern the decline of force induced by breathing maneuvers. One factor may be the magnitude of strain, as previously suggested (116, 171). This is easy to conceive. Greater levels of strain would lead to greater levels of disturbance in myosin cross-bridge cycling (172), as well as in the interconnectivity between the contractile apparatus and the surrounding tissue (173). However, in our hands, strain did not explain everything (in terms of force decline). Another factor that seemed to contribute to the decline of force induced by breathing maneuvers is the magnitude of stress itself. The ASM may be endowed with the ability to sense changes in stress even when the strain induced by the stress is minimal due to the presence of tone. Small strain could cause signaling through such a hypothesized stress sensor. Although we are not aware of any such sensing mechanism, it could explain the results of the present study. It would also reconcile the consistent finding that force oscillations cause relengthening of highly activated ASM even when the strain is expected to be very limited (59, 165–168).

3.4.6 Relevance of These Findings *in vivo*

Translating our findings to *in vivo* observations such as bronchodilation and bronchoprotection (i.e., attenuated airway responsiveness due to a DI, or a series of DIs, taken prior the induced constriction) offered by DIs is not an easy task. *In vivo* studies have suggested that the magnitude of the airway wall strain is an important determinant of the respiratory relief obtained by the oscillatory stress of breathing maneuvers. For example, airway distensibility was demonstrated to correlate positively with the bronchodilator effect of DIs (162). In that study though, the distensibility was not measured during the bronchoconstrictive challenge. More convincingly, the size of lung volume expansion attained during repeated DI maneuvers was positively related to the bronchodilator effect (174). Increasing the depth of breathing, and presumably the strain on the airway wall, during exercise was also associated with a bronchodilator effect, similar in magnitude to high doses of a β2-agonist (175). Even in severe cases of bronchoconstriction such as during a late asthmatic reaction or a spontaneous asthmatic episode, increasing the depth of breathing by exercise has been shown to have a potent bronchodilator

effect (176). This may be relevant to the findings of the present study. In inflamed airways, a larger amount of spasmogens are present (65). These spasmogens increase the level of ASM activation and likely limit the strain experienced by the airway wall during breathing; similar to the effect of increasing concentrations of ACh on the strain induced by simulated breathing maneuvers reported in the present study. Despite presumably smaller airway wall strain in inflamed conditions, increasing the depth of breathing still has of powerful dilating effect (176). This supports our conclusion stating that high stress with only little strains may be sufficient to decrease ASM contractility and perhaps bronchodilate the airways in vivo.

We do not want to pretend that airway physiology can simply be explained by ASM mechanics. Even comparisons between *ex vivo* measurements of ASM strips with whole airway segments can be tricky. Whereas oscillations of ASM strips were shown to decrease subsequent isometric force development, equivalent pressure oscillations of whole airway segments prior to ASM stimulation were shown to increase isovolumetric contraction (177). This was also confirmed *in vivo*. DIs taken prior to bronchoconstriction were shown to increase airway responsiveness when the measure of airway narrowing (therein conductance) did not require a DI maneuver (122). In this later study, the bronchoprotective effect of DIs was confirmed when the measure of narrowing did require a DI (therein, forced expiratory volume in 1 s − FEV_1). The authors concluded that DIs prior to bronchoconstriction increase airway responsiveness but facilitate bronchodilation during a subsequent DI (the later only in healthy subjects) (5). This finding is consistent with the fact that bronchoprotection (measured using FEV_1) is impaired only in asthmatics (reviewed in Ref. (178)). To test this observation in our experimental settings, we will need to measure the tension required to relengthen a contracted strip that has been subjected, or not, to previous force oscillations. The ultimate answers to those complicated issues will certainly come from the concerted input of findings obtained by experiments performed at different scales (molecule, cell, tissue, organ, and whole organism).

3.5 Conclusion

In conclusion, the results of this study suggest that tone can greatly attenuate the strain and, to a lesser extent, the decline of force experienced by ASM during simulated breathing maneuvers. An additional benefit from therapeutic strategies aimed at decreasing tone may thus be an increase in the efficacy of breathing maneuvers to stretch the ASM and, by doing so, decrease its force-generating capacity. However, the results also suggest that the decline of force induced by oscillating stress cannot

be precisely predicted by measuring the magnitude of strain, because the decline of force and the strain were related but their proportionality varies with oscillatory history. Altogether, and to the extent to which the force generated by ASM is involved, the results suggest that a significant part of the bronchodilator effect of DIs should persist with large or small strain that arises at low or high tone, respectively.

Chapter 4 Bronchoprotective Effect of Simulated Deep Inspirations in Tracheal Smooth Muscle[4]

4.1 Introduction

Two of the cardinal features of asthma are the failure of deep inspirations (DIs) to dilate a constricted airway (101, 179) and the inability of DIs taken prior to methacholine challenge to attenuate subsequent airway responsiveness (108). The former of these two phenomena is known as DI-induced bronchodilation and the latter is known as DI-induced bronchoprotection. Malmberg et al. first showed the bronchoprotective effect of DIs in non-asthmatics whereby two DIs taken up to 10 minutes before the administration of methacholine attenuated the decrease in forced expiratory volume in one second (FEV_1)(102). This phenomenon later became known as the bronchoprotective effect of DIs (108) and was shown to be absent in asthmatic subjects (95). It has also been shown that bronchoprotection has a larger effect than does the bronchodilation effect of DIs (106) and that the former is more likely to be associated with airway hyperresponsiveness (AHR) (107). Yet the bronchoprotective effect of DIs is only seen when airway narrowing is assessed after challenge using a test that requires a DI (such as an FEV_1) (121, 122). When airway narrowing was assessed using airway conductance or maximal flows on partial flow volume curves (111) there was no beneficial effect of prior DIs and no differences between asthmatic and normal subjects. These results imply that the prior DIs act to make the airways more responsive to the beneficial effect of subsequent DIs.

Airway smooth muscle (ASM) displays remarkable plasticity and can adapt to a wide range of lengths while maintaining its ability to develop force and shorten (62–64). This is known as length adaptation and has been postulated to be a mechanism contributing to AHR in asthma (180). ASM can also adapt to basal tone induced by contractile agonists in a phenomenon known as force adaptation (66, 92). Force adaptation could stiffen the ASM and the airway wall and act to prevent stretching of the ASM layer, thereby limiting bronchoprotection. Length adaptation is also known to stiffen ASM (63, 91, 181) and could act alone or in concert with force adaptation to inhibit the beneficial effects of DIs.

We hypothesized that simulated DIs taken prior to ASM shortening would increase the compliance of ASM to a subsequent DI and that adaptation to shorter lengths or induction of force adaptation would lead to inhibition of this bronchoprotective effect. Our data indicates that prior DIs do

[4] A version of this chapter has been published. Pascoe CD, Donovan GM, Bossé Y, Seow CY, Paré PD. Bronchoprotective Effect of Simulated Deep Inspirations in Tracheal Smooth Muscle. *J Appl Physiol* (EPub 2014).

not affect the amount of shortening induced by acetylcholine (ACh) but do modestly increase the compliance of ASM to a subsequent DI. We also show that length adaptation and force adaptation can inhibit the increased compliance caused by prior DIs. Together our data suggest that increased ASM compliance due to prior DIs contributes to the bronchoprotective effect of DIs in non-asthmatic airways.

4.2 Materials and Methods

4.2.1 Tissue Preparation

Sheep tracheas used in these experiments were obtained from a local abattoir. The use of the tissue was approved by the Committees on Animal Care and Biosafety of the University of British Columbia. Tracheas were removed soon after the animals were sacrificed and put into Krebs solution (pH 7.4; 118 mM NaCl, 4 mM KCl, 1.2 mM NaH_2PO_4, 22.5 mM $NaHCO_3$, 2 mM $MgSO_4$, 2 mM $CaCl_2$ and 2 g/L dextrose). Upon arrival at the laboratory, tracheas were cleaned of blood, fat and loose connective tissue, and stored in Krebs solution at 4°C until further processed. ASM strips for experiments were dissected from ~2 cm-long tracheal segments. Two small incisions were made in the epithelium when the relaxed tracheal smooth muscle bundles were still connecting the C-shaped cartilage rings and the distance between the incisions was measured. These were used as landmarks to preserve the *in situ* length of ASM during the dissection. The tracheal rings were then cut open, unfolded and secured at a length adjusted so that the distance between the two epithelial incisions was the same as measured in the closed rings. Cartilage, adventitial connective tissue and the epithelial layer were dissected away from the tracheal smooth muscle layer and muscle strips (~7mm long, 1mm wide and 0.3mm thick) were isolated without cutting the anchoring points on the cartilage at both ends. An aluminum foil clip was then attached on both ends of the muscle strips and the distance between the clips was measured. The strips were then mounted vertically in an organ bath. The bottom clip was attached to a stationary hook while the upper clip was attached to a hook connected to the lever arm of a servo-controlled force-length transducer by surgical thread (size 6). The distance between the clips measured during the dissection was used to adjust the length of the ASM strip to the length that it was *in situ.* This length is hereafter called L_{ref}. The organ bath was filled with Krebs solution that had been pre-heated to 37°C and aerated with a gas mixture containing 95% O_2 and 5% CO_2. The temperature of the bath was also maintained by circulating 37°C water through a jacket that surrounded the organ bath.

4.2.2 Equilibration Period

ASM strips were subjected to an equilibration period before the start of the experiments. During equilibration, the baseline tone of the ASM strips was monitored. Once the baseline tone decreased to approximately 2-3mN the strips were activated every 5 minutes with a 9-second electrical field stimulation (EFS) (60 Hz, 12 volts). Krebs solution was replaced every 5 minutes following EFS with warmed (37°C), aerated Krebs solution. The equilibration was completed when a plateau in isometric force was reached (i.e., after which there was no further increase in force in response to subsequent EFS). The force produced by EFS at that time was called F_{max}. Therefore, F_{max} was the force generated by the ASM in response to EFS at L_{ref} length after a stable plateau was achieved. The equilibration period took ~1 hour.

4.2.3 Calculation of Force Oscillations (Adapted from Pascoe et al. 2013 (143))

The stress oscillations imposed on the ASM strips in this study simulated the tension oscillations experienced by the wall of a 4th-generation airway during transpulmonary pressure excursions of different magnitude; e.g., 3 cmH_2O to mimic tidal breathing and 25 cmH_2O to mimic a DI from functional residual capacity (FRC) to total lung capacity (TLC). The changes in wall tension caused by pressure oscillation excursions were calculated based on the Laplace relationship (tension = pressure x radius), assuming that the airways resemble a thin-walled cylinder (an appropriate assumption since the wall thickness/airway luminal diameter ratio is about 1/22 in a non-asthmatic airways of the 4th generation) (56, 154). Since the airway wall is also strained during these swings in transpulmonary pressure, the calculated change in wall tension also has to take into account the change in radius (at the middle of the ASM layer). Equations developed by Lambert and coworkers (153) and morphological data for a 4th generation airway (56, 152, 154) were used to make this adjustment. The magnitude of the tension oscillations was the same for every ASM strip but the magnitude of the force oscillations depended on the width of the ASM strip. Since the ASM is arranged circumferentially around the airways, this width represented the portion of the airway length that would be studied. We estimated the width of the ASM strips by assuming the ASM generates a stress of 100 kPa in response to EFS following the equilibration period and that the thickness of the ASM strips was about 0.3 mm. The value of force (in mN) was then used to calculate the width of the ASM strips. Knowing the length of the airway wall that would be covered *in situ* by this estimated width and the changes in wall tension occurring during breathing maneuvers, we were then able to calculate the force oscillations (in mN) that needed to be imposed on the tracheal strips to simulate the stress to which the ASM is subjected to *in vivo*. This approach has

been used in our two previous studies and provides force oscillations that result in physiologic strains in relaxed conditions (92, 143). A similar approach for calculating load on ASM during a DI has been previously used by others in ovine tracheal strips (59)

4.2.4 Bronchoprotection Protocol

Following equilibration of the tissue, we examined the effect of prior length perturbations that mimic deep inspirations (DI) on subsequent shortening of the muscle and its response to a third force-controlled DI-like maneuver. Specifically, the interventions began with two stretches of 25% L_{ref} which were applied to mimic two DIs to total lung capacity (TLC). The stretches were applied over 5 seconds each. The control protocol was identical except that no simulated DIs were applied. The order of the control or experimental protocols was randomly assigned. Ten seconds after the DIs (or at the same time without DIs), the lever was switched to force control and the tissue was shortened with acetylcholine (ACh – 1μM) against an isotonic load equivalent to 15% of F_{max}. The muscle was allowed to shorten to a plateau value for 60 seconds after which a third quick (over 0.5 seconds) DI-like stretch was applied (see figure 4.1). This third DI stretch was achieved by applying a force perturbation calculated to be equivalent to a DI achieved with an inspiratory pressure of 25 or 50 cm H_2O. Calculations of the amplitude of the stress perturbation needed to mimic *in vivo* pressure changes of 25 and 50 cm H_2O were done in the same manner as described earlier. Following 100 seconds of recording, the ASM was washed three times with Krebs solution to remove the ACh and allowed to return to L_{ref} by itself. The tissue was left to recover for 30 minutes. During this recovery time, there was no EFS stimulation and the tissue was washed with Krebs every 5 minutes. Following the recovery period, the tissue was stimulated once again with EFS until a stable plateau was reached. Following re-equilibration, the tissue was subjected to the alternate protocol. For both control and experimental protocols we measured the amount of maximal shortening before the third DI stretch was applied, the peak re-lengthening (strain) in response to the third DI stretch and the rate of re-shortening ($T_{1/2}$ or time taken to re-shorten to half of the maximal re-shortening) following the stretch.

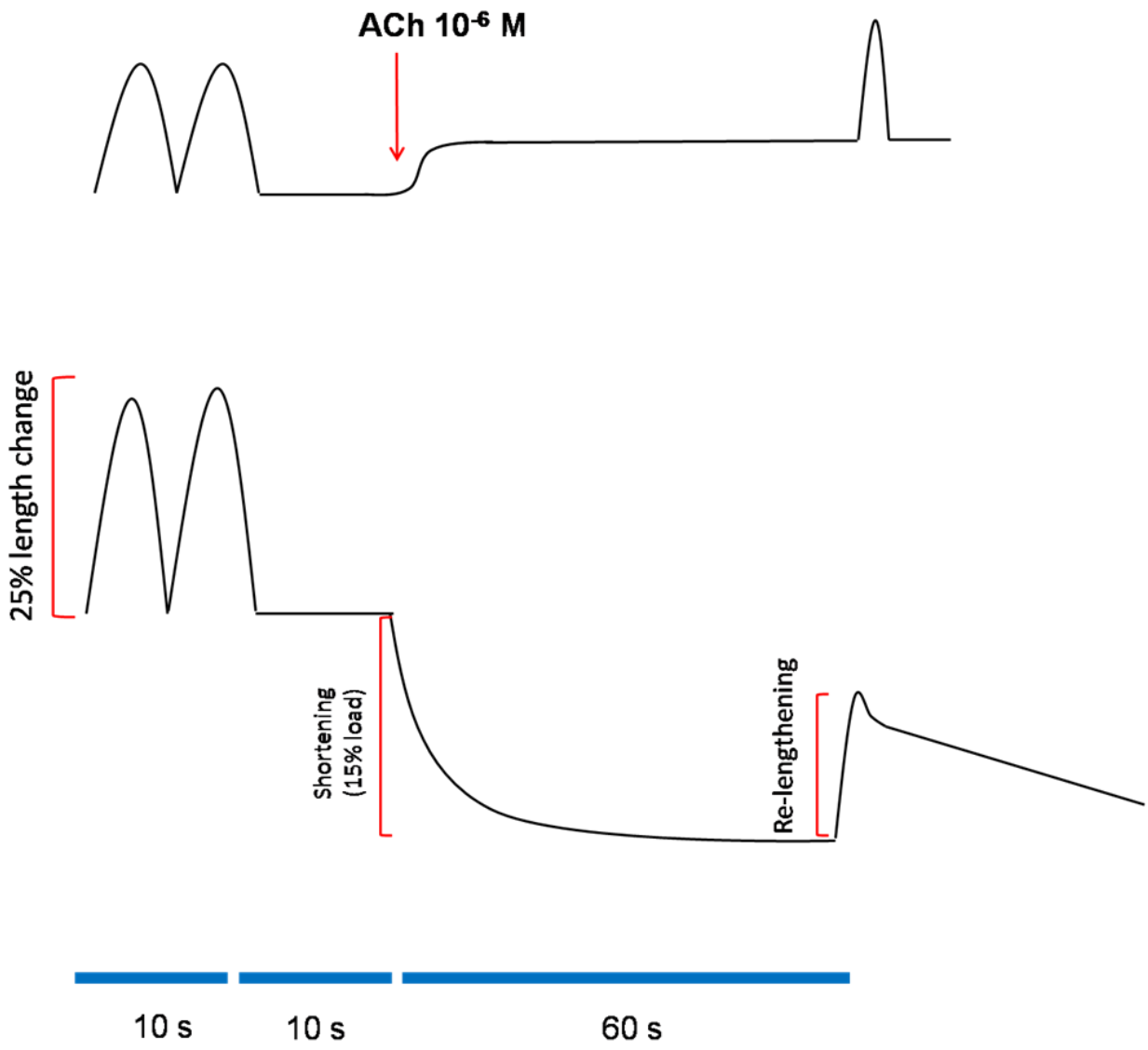

Figure 4.1 Schematic of bronchoprotection protocol. Top panel is the force trace. Bottom panel is the length trace.

This standard bronchoprotection protocol was applied to ASM tracheal strips under 4 different conditions: 1) ASM was kept at L_{ref} and two different amplitudes of stress oscillations were used for the third DI stretch. One mimicked a normal airway transmural pressure achieved during a typical inspiration to TLC (25cm H_2O) while the other amplitude mimicked a supramaximal pressure oscillation (50cm H_2O). 2) Tissue was shortened by 30% and allowed to length adapt for an hour. During the first 30 minutes the tissue was allowed to equilibrate with no stimulation and for the subsequent 30 minutes it was stimulated once every 5 minutes until a stable plateau in force was reached. 3) Tissue was stretched

by 30% and allowed to length adapt in the same manner. 4) Tissue was exposed to a low level of ACh stimulation (~$5x10^{-8}$M) and stimulated repeatedly at 5 min intervals with EFS to induce force adaptation. Once force adaptation was induced (in a similar manner to Bosse et. al. 2009 (66)) the bronchoprotective protocol was applied. In the case of force adaptation, the two prior DIs were force controlled perturbations (25 cm H2O) instead of length oscillations. This is because with increased tone a 25% length perturbation would require an applied stress greater than would be expected *in vivo* (143).

4.2.5 Calculation of Resistance Change Due to Prior DIs

A simple model of a single airway with a radius of 1mm was used to calculate the change in airflow resistance that would result from the prior DI's effect on the length changes induced by the subsequent FEV_1-like DI. It was assumed that the change in length of the ASM strip *ex vivo* was proportional to the change in circumference of the airway lumen. Airflow resistance (R) was calculated using the Poiseuille equation: $R=8\eta L/\pi r^4$, where η is the viscosity of the air, L is the length of the airway and r is the radius of the airway. Assuming that between the control and prior DI protocol the only variable that changed was the radius, we were able to calculate the change in resistance due to the prior DIs. For example, the viscosity of air and length of the airway were both set to one so that the equation simplified to $R=8/\pi r^4$. With the control radius following activation set to one, the resistance in this airway was 2.55 $cmH_2O/L/s$. Changing the radius in the prior DI setting by the same percentage as the increase in length in the ASM strips yielded the resistance in each of the test conditions. This calculation was done for all the tissue conditions (L_{ref}, 70% L_{ref}, 130% L_{ref} and force adapted) and expressed as % change from control.

4.2.6 Computational Modeling

To examine the possible role of airway reopening, a computational model of the human lung was employed to test the effect of bronchoprotection. The airway tree geometry is taken from a previously reported model (182), and each airway in that tree has dynamics similar to those described in previous reports (183–185) with explicit representations of both airway wall compliance and parenchymal tethering forces based on experimental data, as well as ASM length-tension relationships obtained from the data in this manuscript. We assumed an initially normally distributed range of ASM tension, and the degree of constriction is adjusted until the respiratory impedance reaches a prescribed level (to simulate agonist challenge). We assume that this "challenged" lung then has a bimodal distribution of radii, with closed and open populations, which can exist because of the bistability of airway radius in terms of ASM tension in the small airways (186). (Note that the model does not address

the formation of this bimodal distribution, but rather takes it as a starting point on the basis of other work (187, 188)To simulate the third DI maneuver, ASM force-length loops are fit to the experimental data collected in this study, both for the control and prior DI situations. The difference in these force-length loops were the only thing that separated the control and prior DI cases – the challenged lung is assumed to be identical in both cases. A 30 cmH_20 DI is imposed on the challenged lung, driving reopening of some closed airways; airway opening being determined by the force-length relationships. For complete model details please see appendix A.

4.2.7 Statistical Analyses

Maximal shortening, peak re-lengthening and $T_{1/2}$ were normalized to L_{ref} for each strip of muscle. Data are mean ± SEM. Analysis of time course of re-shortening was done using a repeated measures two-way ANOVA. Analysis of maximal shortening, peak re-lengthening and $T_{1/2}$ was done using a paired t-test. Analysis of the change in airflow resistance was done using a paired student's t-test. All graphs and analysis were done using Prism 5 (GraphPad Software, Inc. San Diego, CA). A $p<0.05$ was considered significant.

4.3 Results

4.3.1 Effect of Prior DIs at L_{ref}

All tissues were shortened against a 15% F_{max} load with 1 μM ACh. In tissues where the third DI was of an amplitude equivalent to 25cm H_2O, tissues without prior DIs (control) shortened by 37.0% ± 6.0% vs. tissues with prior DIs that shortened by 35.3% ± 6.0% (figure 2A, $p<0.05$). When the third DI was of an amplitude equivalent to 50cm H_2O, tissues without prior DIs (control) shortened by 37.5% ± 4.1% which was similar to tissues with prior DIs that shortened by 38.6% ± 3.4% (figure 2B, $p>0.05$). The peak strain in response to both amplitudes of DI is shown in figure 4.3. In both cases, prior DIs enhanced the re-lengthening of the tissue in response to the third DI maneuver. The 25cm H_2O DI strained the tissue by 10.1% ± 1.3% in the control intervention and by 11.3% ± 1.6% with prior DI (Figure 4.3A and B. $p<0.05$). Figure 4.3A also shows the time course of re-shortening following the DI. The two curves are significantly different ($p<0.05$) by repeated measures two-way ANOVA. The time it took to shorten to half the maximal re-shortening ($T_{1/2}$) was not significantly different between conditions (8.1 ± 1.1s prior DI vs. 7.9 ± 1.0s control, $p>0.05$.). The 50cm H_2O DI strained the tissue by 18.0% ± 1.2% in the control intervention and by 19.2% ± 1.4% in the prior DI intervention (Figure 4.3C and D, $p<0.05$). Figure 4.3C

shows the time course of re-shortening following the DI. The two curves are significantly different ($p<0.05$) by repeated measures two-way ANOVA. The $T_{1/2}$ was significantly different between control (5.8 ± 2.4s) and prior DI (6.4 ± 2.5s) interventions ($p<0.05$.).

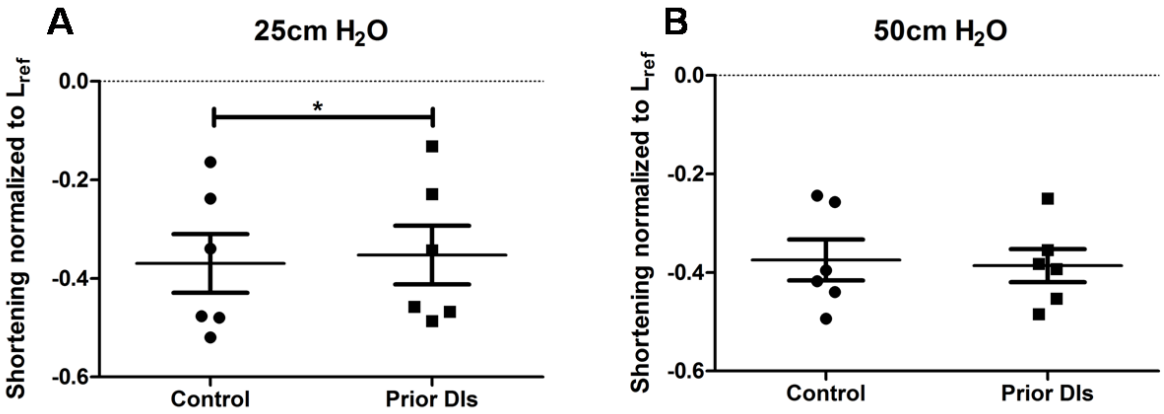

Figure 4.2 Maximal pre-FEV_1 DI shortening induced by 1 µM ACh in strips either subjected to A) a third DI of amplitude equivalent to 25cm H_2O or B) 50cm H_2O. * $p<0.05$ with paired t-test.

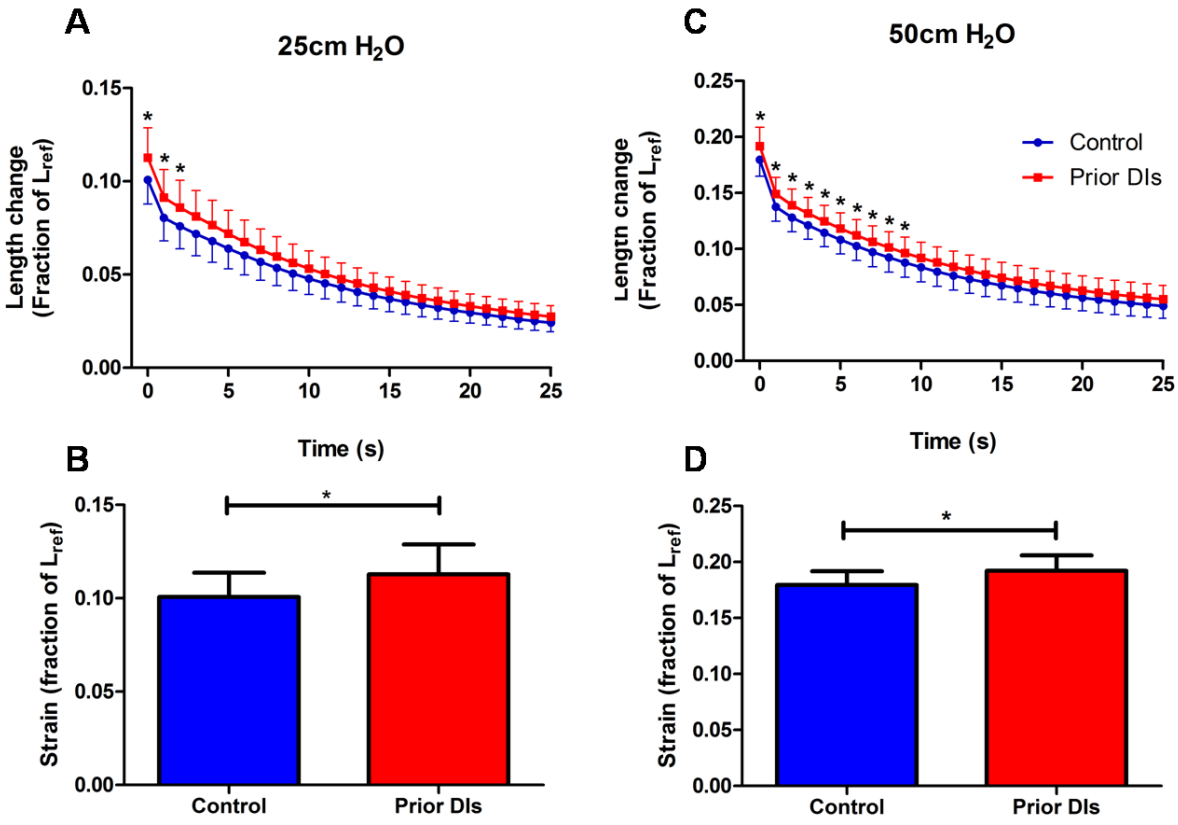

Figure 4.3 Re-shortening and strain of different amplitude FEV_1 DIs. Time course of re-shortening following FEV_1 DI equivalent to A) 25cm H_2O or C) 50cm H_2O pressure. Peak strain of tissue in response to an FEV_1 DI of B) 25cm H_2O or D) 50cm H_2O. * $p<0.05$ by repeated measures two-way ANOVA (A & C) or paired t-test (B & D).

4.3.2 Effect of Length Adaptation on Bronchoprotection

Tissues adapted to shorter (70% L_{ref}) or longer (130% L_{ref}) lengths were considered adapted when force in response to EFS plateaued to a new F_{max}. Tissues length adapted to 70% L_{ref} showed similar levels of shortening between the control and prior DI conditions (14.1% ± 0.89% vs. 13.5% ± 0.96%. $p>0.05$) (Figure 4.4A). For tissues adapted at 130% L_{ref}, shortening was also similar at 59.8% ± 4.0% for the control condition and 58.9% ± 3.6% for the prior DI condition ($p>0.05$, figure 4.4B). There appeared to be no effect of prior DIs on shortening when the data for all tissues (70% L_{ref}, 130% L_{ref} and L_{ref}) are combined (Figure 4.4C, $p>0.05$).

For tissues adapted at 70% L_{ref}, prior DIs had no effect on the subsequent strain of the third DI maneuver (8.8% ± 0.011% vs. 8.9% ± 0.011%. p>0.05) (Figure 4.5B) or the following re-shortening in response to the third DI maneuver (Figure 4.5A, p>0.05). Prior DIs did not affect the rate of re-shortening ($T_{1/2}$) following the stretch (11.5 ± 1.9s vs. 11.4 ± 1.6s. p>0.05). For tissues adapted to 130% L_{ref}, prior DIs significantly increased the length change during and after the subsequent DI as measured by a repeated measures two-way ANOVA (Figure 4.5C, p<0.01). However, the peak strain induced by the third DI maneuver (Figure 4.5D) in the prior DI protocol was not significantly greater than for the control condition (10.9% ±0.58% vs. 11.4 ± 0.50%, p>0.05). The $T_{1/2}$ was also not significantly different between the control group and prior DI group (11.2 ± 1.3s vs. 11.1 ± 1.7s. p>0.05).

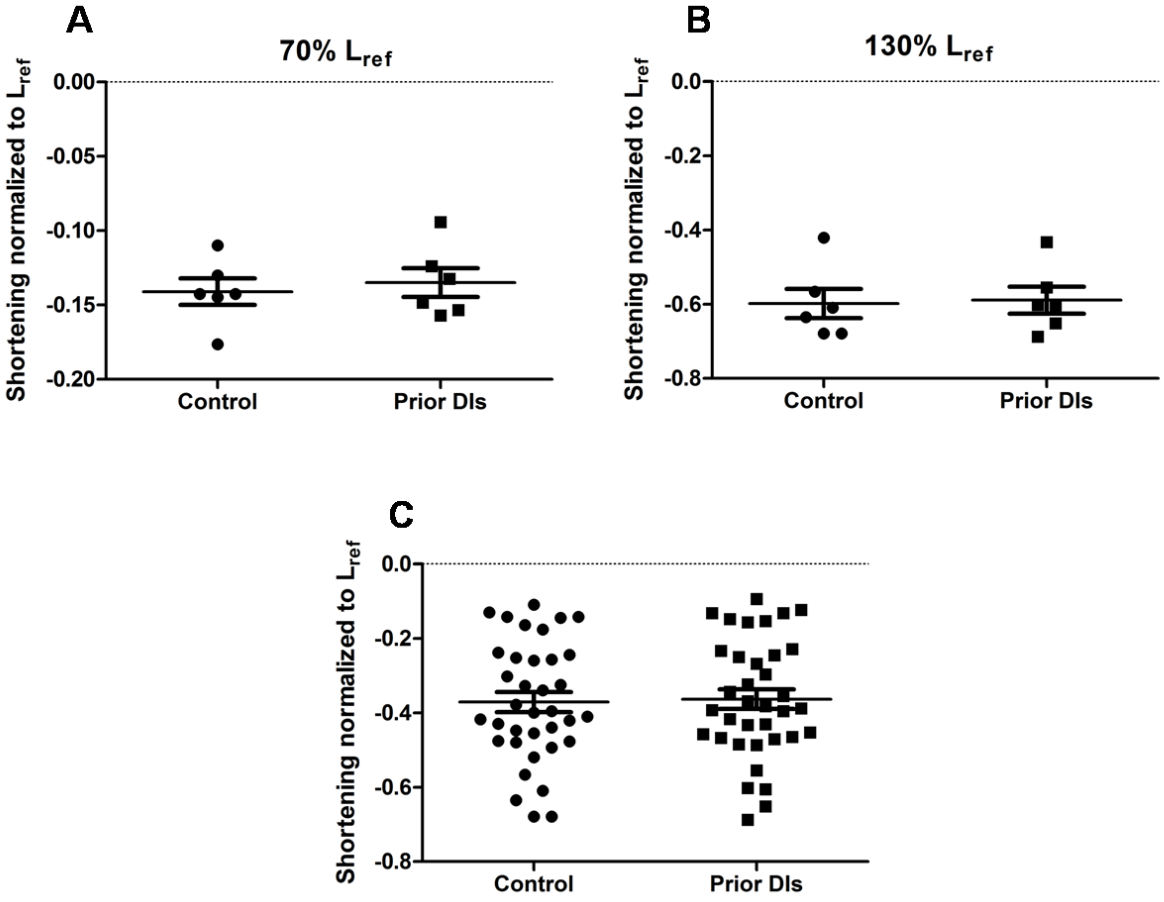

Figure 4.4 Maximal pre-FEV_1 DI shortening induced by 1 µM ACh in strips length adapted to A) 70% L_{ref} or B) 130% L_{ref}. C) Comparison of shortening in all conditions pooled.

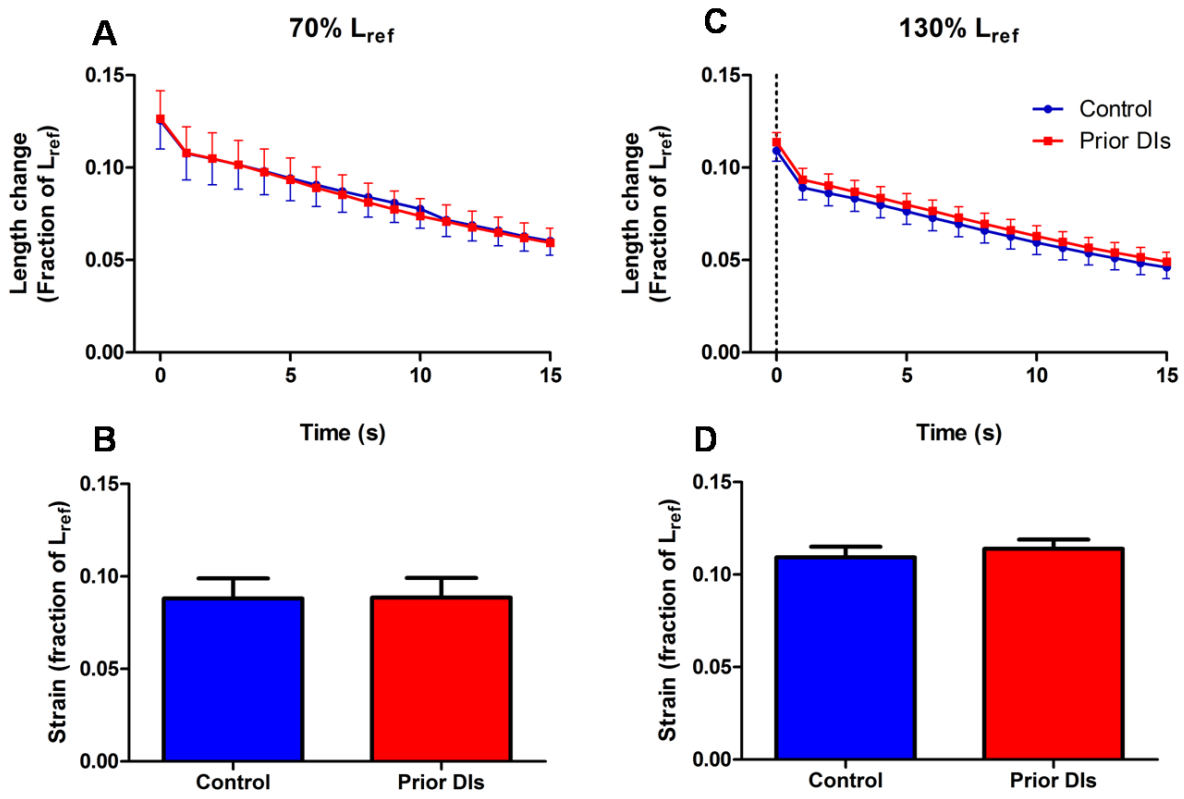

Figure 4.5 Re-shortening and strain of length adapted tissues. Time course of re-shortening following FEV_1 DI in tissues adapted to lengths of A)70% L_{ref} or C) 130% L_{ref}. Peak strain of tissue in response to an FEV_1 DI in tissue adapted to lengths of B) 70% L_{ref} or D) 1305 L_{ref}.

4.3.3 Force Adaptation and Bronchoprotection

Force adaptation was induced using 50 nM ACh and was measured and identified as an increase in EFS-induced force that rose to a new plateau following 3 to 5 EFS stimulations at 5 min intervals (Figure 4.6A). The degree of force adaptation in the two protocols was not significantly different ($p>0.05$). The shortening induced by 1µM ACh was also not significantly different between the two conditions with the control tissues shortening by an average of 34.1% ± 3.7% and tissues subjected to prior DI shortening by 32.7% ± 4.0% (Figure 4.6C, $p>0.05$). In the presence of force adaptation, prior DIs did not affect the magnitude of strain induced by the third DI maneuver nor did they affect the subsequent re-shortening (Figure 4.6B and D, $p>0.05$). The peak strain induced by the third DI maneuver was 11.0% ± 1.4% for the control and 11.2% ± 0.92% for the prior DI conditions respectively. Again, $T_{1/2}$ was not significantly different between the two conditions (4.3 ± 2.0s vs. 4.4 ± 1.3s. $p>0.05$).

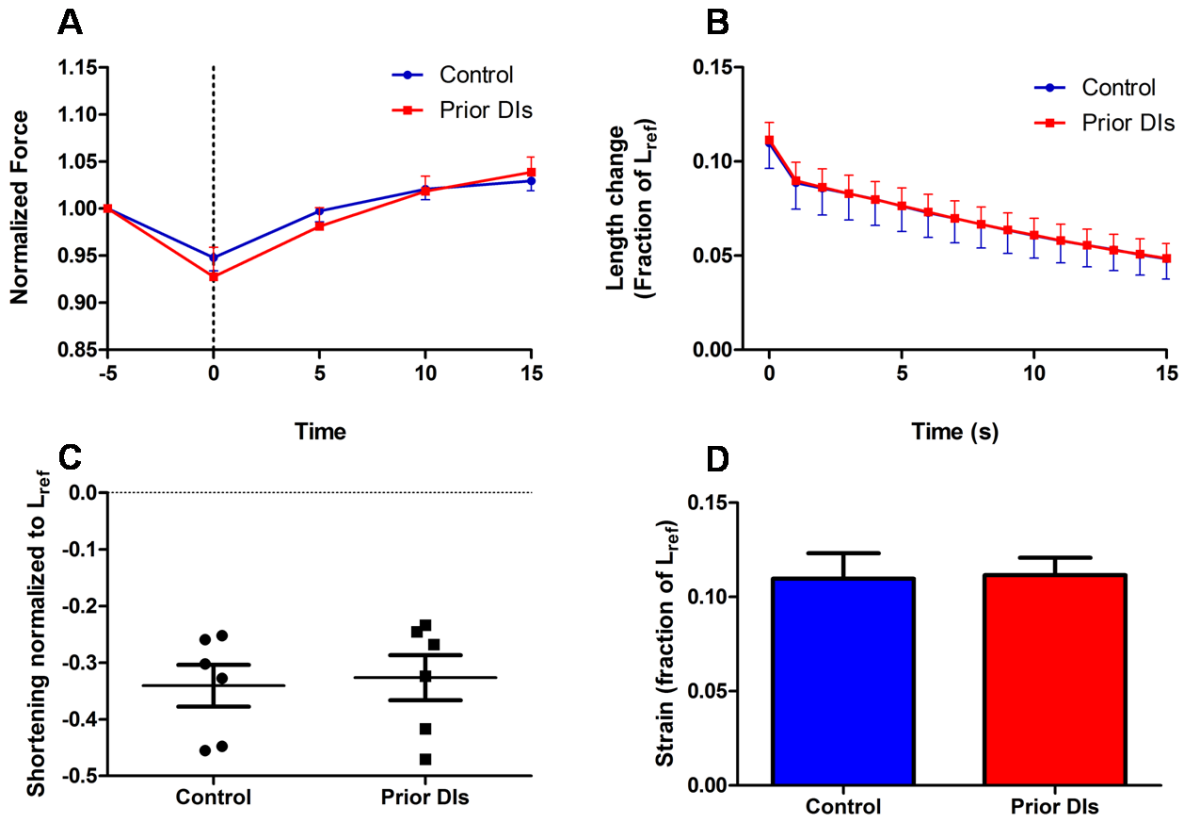

Figure 4.6 Effect of force adaptation on bronchoprotection. A) Force adaptation was induced using 50 nM ACh. Vertical dotted line indicates the first EFS after ACh administration. B) Time course of re-shortening following FEV_1 DI in tissues adapted to 50nM ACh. C) Maximal shortening pre-FEV_1 DI. D) Peak strain of tissue in response to an FEV_1 DI in tissues adapted to 50nM ACh.

4.3.4 Modeling Resistance Change

To understand the potential functional consequence of the increased strain induced by third DI maneuver following prior DIs, as well as the effect length and force adaptation had on blunting this increase, we modeled the change in resistance to airflow in a single airway. The change in resistance to airflow can be seen in Table 4.1. When the ASM tissue was at L_{ref}, the decrease in airflow resistance elicited by the DI on an ACh-constricted airway was 33.3% ± 4.73% greater with prior DIs than without prior DIs. This change in resistance was statistically significant (Figure 4.7. $p<0.001$). When the tissues were adapted to a shorter length the change in airflow resistance of an airway was not different from the control condition (1.48% ± 13.7% increase. $p>0.05$). Additionally, adaptation to longer lengths caused the prior DIs to have a non-significant effect on the reduction in airflow resistance in response to

the third DI maneuver (11.7% ± 12.6% difference. p>0.05). Induction of force adaptation also ablated the change in airflow resistance caused by the prior DIs when compared to the control (no prior DIs) condition (11.9% ± 35.6% difference. p>0.05). These values can be found in table 4.1.

Condition	Ratio of Radius (Prior DIs:Control)	Resistance	% Change
L_{ref}	1.11 ± 0.02	1.70 ± 0.12	-33.3% ± 4.73%
70% L_{ref}	1.01 ± 0.03	2.59 ± 0.35	1.48% ± 13.7%
130% L_{ref}	1.04 ± 0.04	2.25 ± 0.32	-11.7% ± 12.6%
Force Adapted	1.05 ± 0.08	2.85 ± 0.91	11.9% ± 35.6%

Table 4.1 Change in airflow resistance caused by prior DIs. Note: The resistance listed is the minimal resistance achieved during the stretch induced by the third DI maneuver in cases where the prior DIs were applied. Percent change is calculated from the difference in the minimal resistance achieved during the stretch induced by the third DI maneuver in between conditions without versus with prior DIs. Data is mean ± SE.

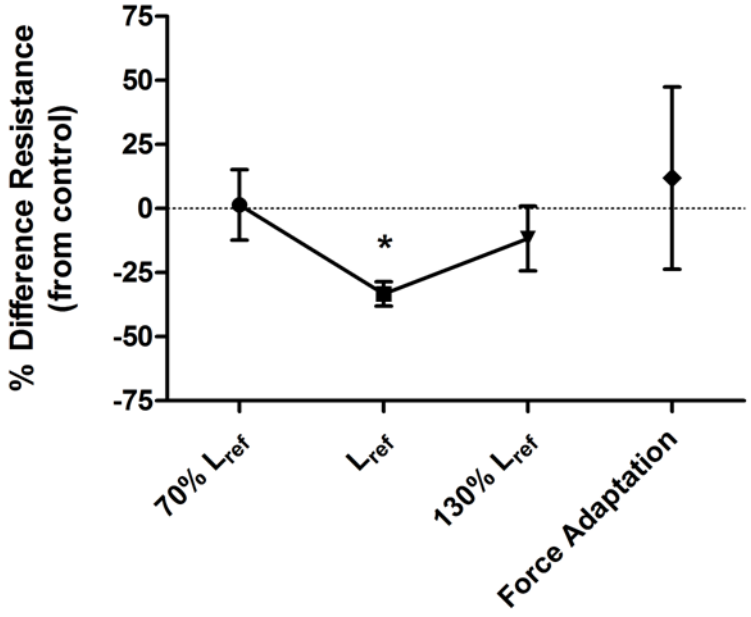

Figure 4.7 Change in airflow resistance caused by prior DIs in each condition. * $p<0.05$ vs. control paired student's t-test.

4.3.5 Modeling the Effect on Organ Scale

Using the computational model we found that the differential ASM response to prior DIs during the third DI maneuver, though modest at the tissue level, can drive additional airway reopening at the organ level. Further, we find that this additional reopening may be enough to account for significant differences in lung function post-DI and hence account for the bronchoprotective effect of prior DIs.

In the challenged lung, we assume that there is a bimodal distribution of airway radii, with a closed population and an open population. Specifically, the model challenged lung has 9305 "closed" airways out of 30941 total (30.1% closed). The central question is how many of these can be reopened by a DI, whether control or with prior DIs. Imposing a DI on this challenged lung moves some airways from the closed population to the open one; critically, the number of these reopened airways depends on the ASM force-length dynamics, and it is the alteration of these dynamics by prior DIs that allows additional reopening. In an FEV_1 DI without prior DIs, 254 of those 9305 closed airways reopen (2.7%). However, in the brochoprotective case with prior DIs, 1584 reopen (17.0%). This process is illustrated graphically in Fig. 4.8, which shows the bimodal distribution of open and closed airways in the challenged lung (dotted black line), the change in this distribution due to a DI (without prior DIs) as the

red dotted line, and the additional change due to a DI when prior DIs are present as the blue solid line (note the y-axis is on a log-scale). In terms of resistance at 1 Hz, the FEV_1 DI alone results in a 12.2% decrease relative to baseline, while adding prior DIs resulted in a 43.4% decrease. Clearly the prior DIs lead to a significant increase in the number of reopened airways, as represented by the decrease in the closed population and matching increase in the open population. These data are computed for typical parameter values, but the results are qualitatively the same within a reasonable range of parameter values – for further details, please see appendix A.

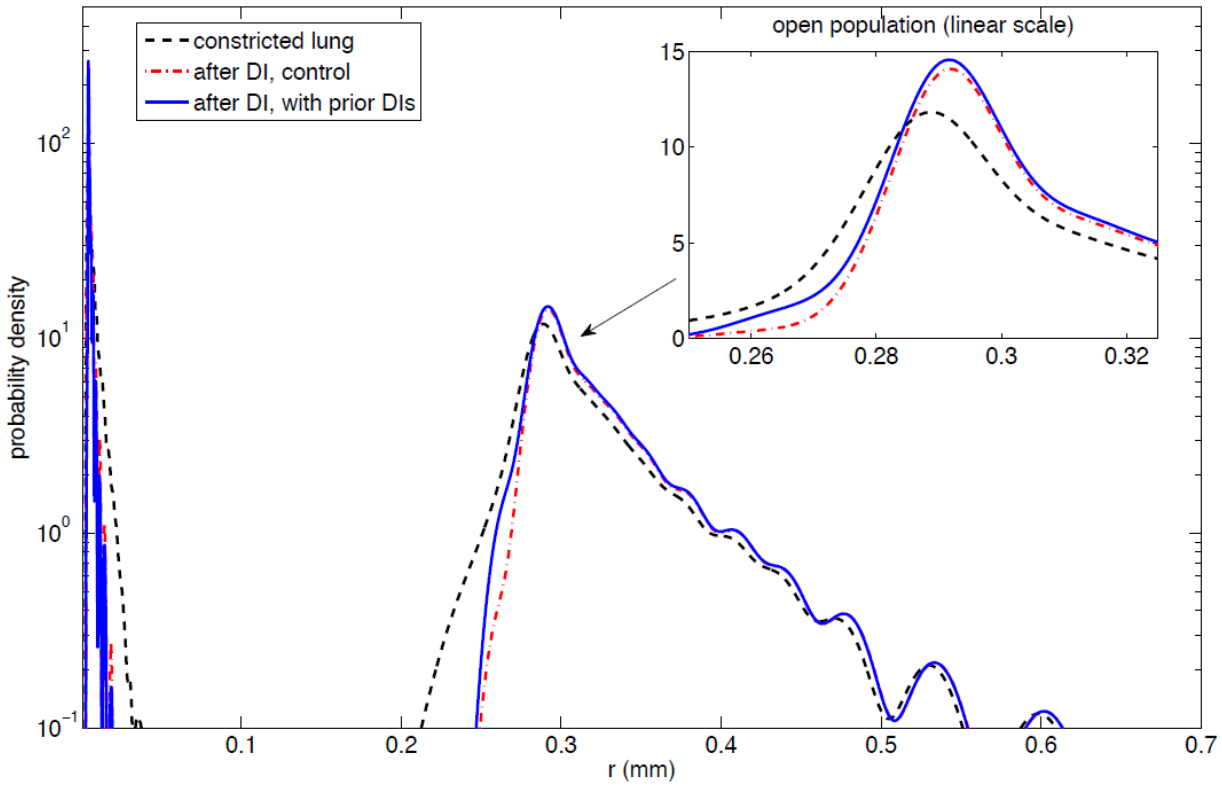

Figure 4.8 Distributions of airway radii in challenged lung, with and without DIs. The dashed black curve gives the bimodal distribution of airway radii after agonist challenge, with a population of closed airways near zero radius, and a population of open airways. Note the log scale on the vertical axis, used to visualize both modes. The inset figure gives detail of the open population on a linear scale. Imposing a DI on this challenged lung reopens some closed airways, with the new distribution given as a dashed red line: some airways move from the closed population to the open population. Similarly, the solid blue line shows the change in the distribution which occurs from a DI which after prior DIs (bronchoprotective). In this case a significant number of additional airways are transferred from the closed population (left peak) to the open population (right peak), and we propose that it is this additional reopening that is responsible for the improvement in lung function from bronchoprotective DIs. For details of the calculation of distributions please see the supplementary material.

4.5 Discussion

The purpose of this study was to test whether intrinsic properties of ASM contribute to, or are the cause of, the bronchoprotective effect of DIs seen in non-asthmatic subjects. We showed that prior DIs have no effect on the level of shortening achieved by the tissues in response to ACh which is in line with *in vivo* results showing that prior DIs do not affect airway narrowing (measured by airway conductance, partial maximal expiratory flows and FEV_1/ FVC)until a subsequent DI is taken (121, 122). Our results also indicate that prior DIs increase the compliance of an ACh-shortened ASM strips in response to a subsequent DI-like maneuver (i.e. a sudden increase in distending stress). However, the additional increase in ASM elongation engendered by the prior DIs is relatively small and is unlikely to be the sole mechanism for the bronchoprotective effect seen in non-asthmatics. This suggests that there may be other factors that are important in determining the extent by which DIs protect against a subsequent decrease in FEV_1 elicited by an inhaled challenge with a spasmogen. This point will be addressed later from a different perspective with the help of a mathematical model that simulates the behavior of a heterogeneous population of airways rather than assuming homogeneous behavior of a "typical" airway.

The results of a number of *ex vivo* studies designed to investigate how DIs play a role in the dilation of constricted airways (171, 189, 190) or ASM strips (92, 111, 114) have shown that activated ASM is difficult to stretch with simulated DIs. However the mechanisms of DI-induced bronchodilitation and bronchoprotection are likely to be different. DI-induced bronchoprotection involves application of strain to airways and ASM prior to a constricting stimulus (97). Based on the effects of prior length oscillations on subsequent ASM force generation (63, 98, 111) it was initially hypothesized that DIs might result in changes in the contractile or cytoskeletal apparatus of ASM, which decrease its contractile capacity and thus explain the protective effect of a DI. However the study from Crimi et al. (122) showed that prior DIs did not affect the magnitude of subsequent airway narrowing when tests of airway narrowing that did not require a DI were employed. Only when FEV_1 was used as a surrogate of airway narrowing was a significant effect of prior DIs apparent. These *in vivo* results suggest that the beneficial effect of prior DIs are mediated by improving the effectiveness of the post challenge DI. Our results support this conclusion in that, in general, *ex vivo* protocols that included simulated DIs prior to ACh challenge, resulted in greater effectiveness of the subsequent DI maneuver with respect to its ability to strain the ASM strip. However, the effects are relatively small and by themselves are unlikely to explain the rather substantial protective effect of prior DIs on the decline in FEV_1 when they preceded the MCh challenge.

For example, Kapsali et. al. showed that the reduction in FEV_1 of non-asthmatics was blunted by over 80% with prior DIs (108). Malmberg et al. showed a similar reduction (102). There is the possibility that *in vivo* release of mediators such as nitric oxide (NO) or prostaglandin E2 (PGE_2) upon ASM stretch may contribute to the protective and dilatory response of DIs by actively relaxing the ASM(191–193). A loss of these mediators in asthma could contribute to the loss of bronchoprotective DIs that is characteristic of the disorder.

The results of Chapman et al (121) suggest that the salutatory effects of prior DIs are in enabling more effective opening of closed airways by the post challenge FEV_1-related DI. How could prior DIs affect subsequent airway opening? Besides an effect on the compliance of the ASM, prior DIs could influence the generation of an effective transmural pressure and/or could influence the surface active properties of airway lining liquid to decrease the opening pressures of closed airways. Alternatively the small changes in ASM re-lengthening we observed may be enough to explain larger differences in the ability to recruit closed airways. Our computational model suggests that the relatively modest differences in ASM response due to prior DIs could nonetheless account for a significant bronchoprotective effect by allowing additional re-opening of closed airways during the post challenge DI. This mechanism amplifies the effect of relatively small changes in ASM behaviour by way of two sources of nonlinearity: the highly compliant small airways, and the nonlinearity of airflow with respect to airway luminal radius. This amplification mechanism offers one solution to the puzzle posed by the significant bronchoprotective effect seen *in vivo*, in contrast with the limited influence of simulated DIs in both intact airways (115, 118, 171, 189, 190) and ASM strips (143). Thus it could be that for a typical airway, a DI does very little; but by reopening some closed airways, significant changes in lung function are possible.

Wong and colleagues (124) studied mice in an attempt to explain the mechanism for DI-induced bronchoprotection. Paradoxically they found that prior DIs increased measures of airway narrowing (and the heterogeneity of narrowing) which was consistent with previous study on excised porcine bronchial segments (177). However, like the human in vivo studies, Wong and colleagues showed that a subsequent DI was more effective in dilating airways as assessed by a superior beneficial effect on pulmonary resistance measured using a forced oscillation technique. They also attempted to measure post-challenge airway distensibility by examining the relationship between airway conductance and inflation pressure. Although DIs increased the compliance of the airways pre-challenge there was no difference in distensibility post challenge in the with- and without-DI protocols. They concluded that

increased compliance of the airway wall (or ASM) is unable to explain the beneficial protective effect of deep inspirations and like other investigators they invoked the possible effect on surface tension and thus airway opening pressures (124).

In addition to studying the bronchoprotective effect of prior "DIs" on ASM shortening and re-lengthening under "normal" conditions (L_{ref} and no tone) we investigated how changes in ASM resting length (length adaptation) and baseline tone (force adaptation) effect *ex vivo* "bronchoprotection". Length adaptation is a term given to the smooth muscle's ability to maintain contractile capacity over wide ranges of lengths (63) and it has speculated that the phenomenon may contribute to AHR by allowing a chronically narrowed airway to narrow further (62). Force adaptation is a smooth muscle property whereby, in the presence of tone, the total force generating capacity of ASM increases over time. It has been speculated that in asthma the constant presence of inflammatory and contractile mediators results in force adaptation (66, 194).

Interestingly we found that both adaptation, to a shorter length and baseline tone, abolished the beneficial effects of prior "DIs". This could be in part due to an increased stiffness of the ASM at shorter lengths (195)or upon activation (196) thereby limiting either strain in response to a given stress or the maximal ASM elongation achieved by the simulated DI. This supports the concept that these phenotypic changes if present in asthmatic subjects could contribute to the relative ineffectiveness of DI-induced bronchoprotection in asthma. However adaptation of the ASM to a longer length, which would be expected to have the opposite effect, did not enhance the effectiveness of prior "DIs"; in fact the protective effect of prior "DIs" was marginal after length adaptation to longer length. This may be due to an underestimation of the required stretch for the third DI. Since the tissues were adapted to shorter or longer lengths we would need to adjust the force applied to the muscle to keep a constant pressure amplitude at the shorter or longer lengths (LaPlace's law: Tension = Pressure x Radius). The problem is that this adjustment is not as simple as increasing or decreasing the amplitude by 30% as in the case of tissues adapted to longer lengths. As a result, the amplitude we applied could underestimate the real amplitude that needs to be applied to achieve a stretch equivalent to 25cm H_2O. This would mean that this marginal protection observed could in fact be as large as the tissue at L_{ref} and that tissues adapted to longer lengths would also benefit from the bronchoprotective effect of DIs. In the case of adaptation to a shorter length, our applied distending force would be overestimating the required stretch and we still did not see any protection afforded by the DIs. Alternatively, the fixed oscillating strain that was used to simulate prior DIs (which was set to 25% of L_{ref}) represents a smaller relative length change for a

muscle adapted to an elongated length, which may explain the attenuated effect of prior DIs on the compliance of ACh-shortened ASM at 130% L_{ref}.

Loss of the bronchoprotective effect of DIs is one of the most consistent markers of asthma. In a recent *ex vivo* study the only phenotypic difference in tracheal smooth muscle mechanics between asthmatic and non-asthmatic tissues was deficient force attenuation in response to a series of simulated DIs (53). The results of that study suggest that there is an intrinsic difference in the response to oscillating strain in asthmatic ASM; a difference that could contribute to AHR. It is well known that a decline in contractile capacity is proportional to the magnitude of strain applied to the ASM (85, 116, 143, 171, 197) and that this occurs regardless of asthmatic status (190). A stiffer airway wall in asthmatics (162, 198, 199) would reduce the strain caused by breathing maneuvers and could be a cause for the loss in the bronchoprotective effect of DIs. There are a host of cytoskeletal proteins that may be important in determining ASMs response to DIs including the focal adhesion proteins vinculin and paxillin, the actin stress fiber protein zyxin (200) and the actin binding proteins actinin and filamin. The role of cytoskeletal proteins in the response to DIs is an overlooked area of research and more work needs to be done to characterize their role in the active cytoskeletal re-organization that is likely taking place during DIs. Over expression of some cytoskeletal proteins may enhance the ability of the cytoskeletal network to tolerate or recover from strain caused by DIs in asthmatics and potentially could attenuate the increased compliance in response to protective DIs. In addition, work by Laube et al. (201) and Lippmann et al. (202) has shown that while aerosol distribution in the lung is homogenous in non-asthmatics, the distribution is heterogeneous in asthmatics and concentrated in the more central airways. However, our model incorporates heterogeneity in the distribution of isometric tensions which could be the result of heterogeneous distribution of the spasmogen.

The whole lung computational model is designed specifically to test the extent to which alterations in ASM behavior, such as that caused by bronchoprotective DIs, modulates reopening of closed airways during DI. The model employs as its key elements the Lambert model for the airway wall (153) and the Lai-Fook model for parenchymal tethering (203) for individual airways in the bronchial tree, and thus bears a strong resemblance to several previous models (185, 204). The central differences are 1) we take the ASM force-length behavior directly from the experimental data for this particular protocol, rather than using a more general representation, and 2) we assume a bimodal distribution of the airway radii in the challenged lung by fiat, without reference to a specific mechanism for its formation. Thus the model is narrowly defined for addressing only the central question we consider here.

Another of the potential limitations of this study is the use of tracheal smooth muscle strips to test the bronchoprotective effect of DIs, which would normally have their major effect in smaller bronchi and bronchioles. However, the purpose of this study was to test the intrinsic properties of the ASM to prior DIs. In that respect, tracheal smooth muscle if a good model. A limitation of the apparatus used to conduct this study is that it requires that the strip length is returned to resting length after the initial DIs rather than letting it remain at the increased length (immediately post-DI) as may be occurring *in vivo.* Thus the conclusions of this paper need to be validated using a different preparation such as precision cut lung slices (PCLS). Work using precision cut lung slices may provide a better understanding on how parenchymal tethering plays a role in the protective effect of DIs. Again, the results we present show a small, but significant increase in the muscles compliance following prior DIs and it is only in the context of the whole lung that these small changes become physiologically significant as predicted by our model. Future work should be focused on determining what the main contributors to the bronchoprotective effect in the lung are and how they work in concert with ASM to protect the airways of non-asthmatics from constriction.

4.6 Conclusion

We conclude that prior DIs confer bronchoprotection by modestly increasing the compliance of contracted ASM. In turn, this increased compliance enhances the strain that the airway wall undergoes during a subsequent DI and, concomitantly, potentiates the bronchodilator effect of DI. This explains why the phenomenon only manifests itself with lung function tests that require a DI. This effect is small when looking at the tissue or airway level. However, when considering the lung as a whole, the small increase of ASM compliance could play a large effect on FEV_1 and FVC measured in patients by re-opening a greater number of closed airways. Finally, phenomena such as length and force adaptations may contribute to the lack of effectiveness of DIs in asthma by preventing the increased compliance of ASM that is normally induced by DIs that preceded the bronchoconstriction.

Chapter 5 Phenotypic Differences in the Airways of Asthmatic Subjects[5]

5.1 Introduction

Asthma is a chronic disease characterized by inflammation of the airways, airway hyperresponsiveness (AHR) and reversible airway obstruction which manifests as breathlessness and wheezing in patients. AHR is defined as an increase in the sensitivity and maximal constriction of the tracheal-bronchial tree in response to inhaled agonist (such as methacholine) (9). It has been known for a long time that excessive narrowing of airways due to contraction of the airway smooth muscle (ASM) is the major contributor to AHR (39). There is a genetic contribution to asthma and AHR and a number of specific genes have been implicated in recent genome wide association studies (141, 205–208) however the genes incriminated are mainly expressed in the airway epithelium or in cells involved in the immune system. The exception to this is ADAM33, which has been shown to be expressed in ASM and plays a role in its mechanical function (209–211). A variety of studies have shown that there is an increase in the amount of ASM surrounding the remodeled airways of asthmatics (4, 41, 53, 154) but it is unclear whether the ASM from asthmatics is phenotypically different than ASM from non-asthmatics (212). Adding to the debate has been the finding by some investigators that mRNA for contractile proteins such as myosin light chain kinase (MLCK) and myosin heavy chain (MYH11) are upregulated in asthmatic ASM (60, 61) while others have shown there to be no change (127). Recently, it has been suggested that the ASM may contribute to the airway inflammation seen in asthma and take on what is known as a synthetic phenotype (213, 214).

We hypothesized that there are changes in the ASM phenotype of asthmatic subjects which contribute to AHR and that this phenotypic change would be manifest in altered gene and protein expression. Specifically we proposed that there would be increased expression of genes involved in contraction, cytoskeletal stiffness and proliferation in the airways from asthmatic patients when compared to non-asthmatics. Using human donor lungs from asthmatic and non-asthmatic patients, we measured the relative expression of over 100 genes potentially involved in the ASM's role in AHR. The genes included those related to contraction and contractile regulation, cytoskeletal organization and its regulation, calcium handling, and growth and proliferation. Some of these genes and proteins have been

[5] A version of this chapter will be submitted for publication. Christopher D. Pascoe, Bryna A. Arsenault, Tillie L Hackett, Chun Y. Seow, Peter D. Paré. 2014

studied by other groups in the past (MLCK, MYH11) while others have never been studied in the context of asthma. Our results show that there is no evidence for a difference in the relative expression of genes directly involved in ASM contraction such as MLCK or MYH11, but there is decreased relative expression of many genes involved in contractile regulation, cytoskeletal regulation and calcium handling. There was increased relative expression in genes related to cytoskeletal maintenance; in particular, we found increased relative expression of both Zyxin and Smoothelin mRNA and protein expression in the ASM of asthmatics. Both of these genes bind to actin (200, 215) and may be important in maintaining actin stress fibers.

5.2 Methods

5.2.1 Subject Selection and RNA Isolation

The studies were performed on the airway tissue from 24 human lungs; 12 with and 12 without a history of asthma. The lungs were donated for research and obtained from the International Institute for the Advancement of Medicine (IIAM, Edison, NJ, USA; www.iiam.org). Non-asthmatic donor deaths were primarily due to head trauma while 8 of the 12 asthmatic subjects died during exacerbations of their asthma. Subject demographics and clinical details can be seen in table 5.1. The study was approved by the University of British Columbia/St Paul's Hospital ethics committee.

After surgical removal the lungs were flushed with Custodiol HTK solution (Odyssey Pharmaceuticals, East Hanover, NJ, USA) and transported on ice by plane. The average time between harvesting and arrival at the University of British Columbia was 15–20 h. The mechanical properties of the tracheal muscle from the donor lungs were measured as previously described (53).

Following harvesting of the tracheal preparations the lungs were immediately inflated with a mixture of cryoprotectant and saline and frozen over liquid nitrogen fumes. The frozen lungs were then sliced into ~2 cm slices using a band saw and multiple random 2 cm diameter cores of frozen lung tissue were obtained using a power driven hole saw. Frozen cores from the donor lungs were sectioned on a cryostat at a thickness of 10µm and placed on a plain glass slide (figure 5.1). Two cores from each of the lungs of 12 asthmatics and 12 non-asthmatics were used for this study for a total of 48 samples. A total of 20 sections per subject were cut and stored at -80^{o}C until RNA was isolated. Sections 1, 5, 10, 15 and 20 were stained with hematoxylin and eosin (H&E) for morphometric measurements while the remaining 15 sections had their airways and a small amount of surrounding parenchyma

macroscopically dissected using a scalpel (Fisher Scientific No. 11) for RNA isolation. Airways were only isolated if they were continuous from section one to 20. Large vessels were avoided. RNA was isolated using the Qiagen RNeasy Mini Kit according to directions. RNA quality and quantity was measured using the NanoDrop 8000 UV-Vis Spectrophotometer. Samples were used if they had an A260/280 ratio over 1.8 as suggested by Nanostring®. Each sample of RNA was diluted to a concentration of 17ng/µL as specified by Nanostring and stored at -80^{o}C in 0.5 ml RNase free microfuge tubes. A preliminary sample of RNA from the frozen lung sections was run on the Agilent® bioanalyzer to check for RNA integrity. The sample trace can be seen in appendix B (Figure B1).

Gender	Age	Weight (kg)	Height (cm)	Ethnicity	Cause of Death	Patient Medical History	Known Medication	Terminal Medication
Non-Asthmatics								
M	20	86	185	Caucasian	Head Trauma, MVA	Cigarettes 2/week; Vodka half bottle/week; Marijuana weekly	None	Vasopressors
F	4	17.5	104	Hispanic	Head Trauma	None	None	Steroids and vasopressors
M	22	112	193	Caucasian	Head Trauma	Occasional marijuana	None	Vasopressors
F	63	77	159	Caucasian	Gastrointestinal Bleed	Hypertension for 2 years	Pain medications, Antihypertensive	Antihypertensive
M	14	50	165	Caucasian	Head Trauma, MVA	None	None	Vasodilator
F	19	87	165	Caucasian	Head Trauma, MVA	Beer/Hard Liquor 1-2x/month for 2 years	None	Steroids and vasopressors
F	20	72.2	165	Caucasian	Head Trauma	Cigarettes <1PPD for 2 years, Marijuana	Inhalents, Pain medication	Vasopressors
M	24	81.8	175	Hispanic	Head Trauma	Alcohol on weekends	None	Vasopressors
M	12	48.1	160	Caucasian	Head Trauma, MVA	None	None	Vasopressors
F	42	90	178	Caucasian	Head Trauma, MVA	Hypertension for 1 year	Antihypertensive	Steroids and vasopressors
F	47	82	167.5	Caucasian	CVA	None	None	Amiodarone
M	47	105	167.5	Caucasian	CNS Tumor	Heart Murmur	Vasopressors, Solumedrol	Albuterol

Gender	Age	Weight (kg)	Height (cm)	Ethnicity	Cause of Death	Patient Medical History	Known Medication	Terminal Medication
Asthmatics								
F	8	30.5	117	Hispanic	Asthma Attack	Asthma diagnosed age 3. RSV age 2	Albuterol, Singular, Rantadine	Steroids and vasopressors
M	11	65.3	152.5	Caucasian	Head Trauma	Asthma diagnosed age 6	None	Steroids and vasopressors
F	21	55	170	Caucasian	Drug Overdose (Tylenol)	Asthma; Cervical Cancer free 1 year; Cigarettes 2PPD for 6 years	Aspirin, Albuterol, Advair	N/A
F	15	56	162.5	Caucasian	Anoxia, Probable Asthma Attack	Asthma; cigarettes <1PPD for 1 year; Marijuana 2x/week	Singular, Advair, Claritin, Flovent, Albuterol, Ritalin, Solumedrol, Albuterol	Steroids and vasopressors
M	11	69	170	Caucasian	Anoxia, Probable Asthma Attack	Asthma diagnosed age 2	Albuterol	Vassopressors
F	26	91.6	168	Caucasian	Anoxia, Probable Asthma Attack	Asthma since childhood; cigarettes 1 pack/week since 16; heavy drinker	Albuterol, Advair, Lorazepam, Xanax	Vassopressors
M	10	43	157.5	Caucasian	Asthma Attack	Asthma diagnosed age 4	Advair, Allegra, Albuterol	Steroids and vasopressors
M	25	103	185	Hispanic	Anoxia, Suicide	Asthma diagnosed age 11; cigarettes 2 PPD for 12 years; Marijuana 6x/day for 12 years	Albuterol, Advair, Naproxen and Trazodone	Steroids and vasopressors

Gender	Age	Weight (kg)	Height (cm)	Ethnicity	Cause of Death	Patient Medical History	Known Medication	Terminal Medication
F	15	67	177.8	Caucasian	Asthma Attack	Asthma diagnosed at birth	Prednisone, Albuterol	Steroids and vasopressors
M	36	91	173	Caucasian	Head Trauma	Asthma; Chewing Tobacco daily	Roxicodone and unknown inhaler	Steroids and vasopressors
M	23	52.6	152.4	Hispanic	Asthma Attack	Asthma diagnosed at birth; Seizures 2-3x age 1 & 2	Unknown inhaler	Steroids and vasopressors
M	20	81.2	172.7	Caucasian	Asthma Attack	Asthma diagnosed at birth; Recreational Marijuana	None	Steroids and vasopressors

Table 5.1 Subject demographics and clinical details. PPD – packs per day. NA - not available

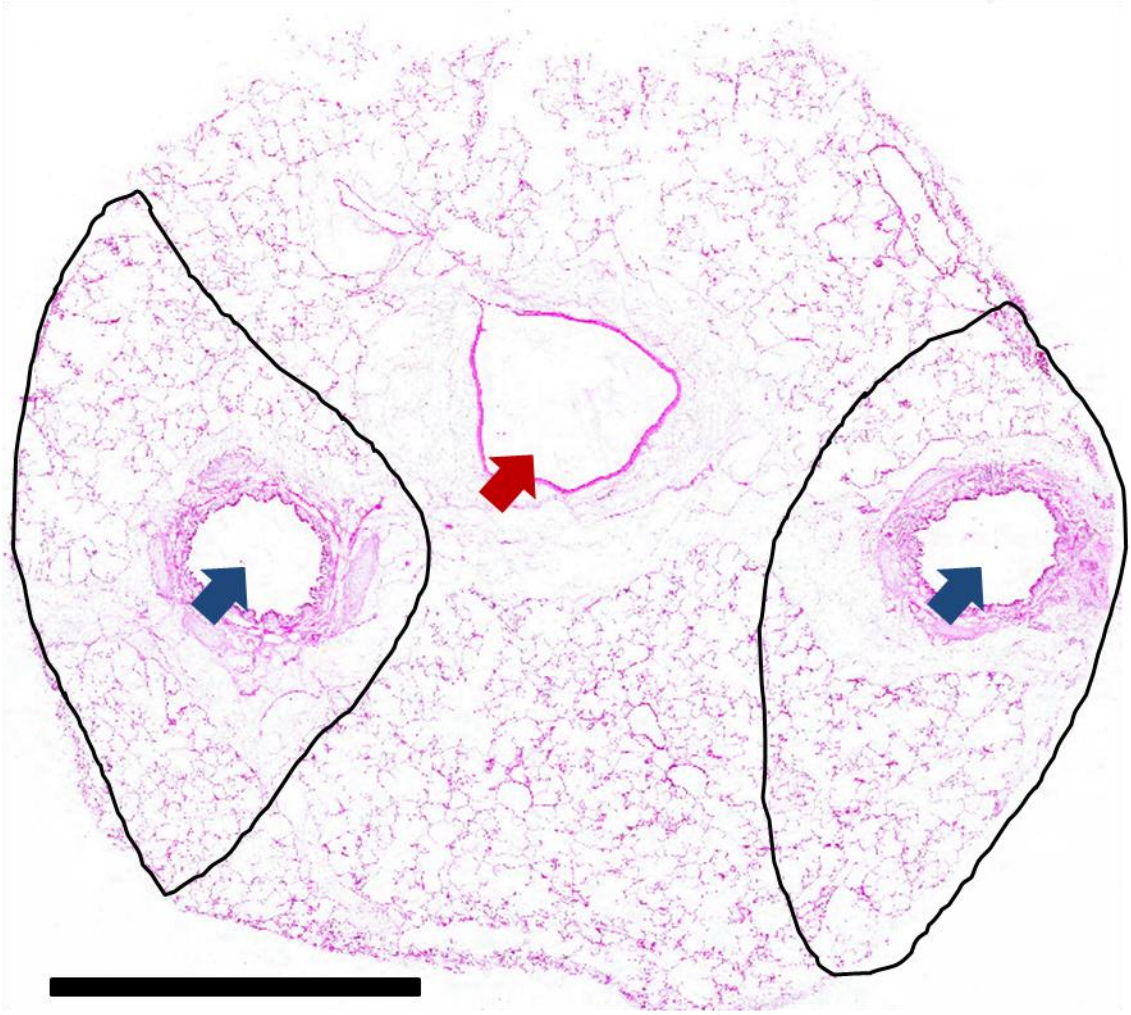

Figure 5.1 Section of a frozen human lung core cut at 10µm thick. Blue arrows points to airways. Red arrow points to blood vessel. Black outline indicates tissue taken for isolation of total airway RNA. Scale bar is 5mm.

5.2.2 Quantification of Remodeling Changes in Airways

Quantification of ASM area, epithelial area, total airway wall area, basement membrane thickness and collagen area was done to determine the degree of airway remodeling within the airways and to allow for correlation with gene expression results. As described, every 5th slide was stained with H&E to visualize the airways and after they were digitally scanned airway wall compartments were quantified using the Aperio® system (Leica Biosystems, Germany). ASM area, epithelial area and total airway wall area were quantified using a point counting method, where a grid of approximately 4000

points was overlaid onto each airway of interest and the points falling on the area of interest were counted (Image Pro Plus ®, Media Cybernetics, Maryland). The measurements for all airways were normalized to the internal perimeter (P_i) of the airway and averaged across all the sections for each subject . The P_i was measured by tracing along the lumen side of the epithelium. For the measurement of basement membrane thickness and collagen area, an additional two sections were cut from each core (same as used for RNA isolation and other measurements) to stain with Masson's trichrome (basement membrane) and Picrosirius red (collagen). To quantify the basement membrane thickness, a random series of line segments was placed over each image and the thickness of the basement membrane was measured at the points where any line segment crossed over the basement membrane. All thickness measurements were made perpendicular to the epithelium. A minimum of 40 measurements were made for each airway. For the measurement of collagen content in the airway, Picrosirius red stained slides were visualized under polarized light where the picrosirius red stain shows birefringence. The collagen shows up red on a black background and using color segmentation in Image Pro Plus®, the amount of collagen per airway was quantified. All measurements were carried out in a blinded manner.

5.2.3 Gene Expression Analysis

Expression of mRNA for 99 candidate genes and 5 housekeeping genes (POLR2A, GUSB, GNB2L1, RPL19, and TBP) was measured using the Nanostring nCounter® system. A custom codeset panel was developed to analyze gene expression on the 48 samples. Samples were shipped to Nanostring on dry ice and data were received as an excel spreadsheet. Data were normalized in accordance with Nanostrings guidelines. This included normalization to the 5 most stable housekeeping genes as determined by calculation of the percent coefficient of variation (% CV) between samples. See table B1 in appendix B for a complete list of genes including housekeeping genes.

Housekeeping genes were selected by conducting a separate study using 3 asthmatic and 3 non-asthmatic airway sections in technical duplicates. Total RNA isolated from the whole tissue (airway, parenchyma and vessels) was sent to Nanostring for analysis. Using the reference panel from Nanostring®, the expression of 18 commonly used housekeeping genes was measured and the percent coefficient of variation (%CV) compared across all 6 subjects. The top 4 genes that had the lowest %CV were selected to be added to the final gene expression panel. These were: RNA Polymerase R2A (POLR2A – 36.3% CV), TATA box binding protein (TBP – 40.1% CV), Ribosomal Protein L19 (RPL19 – 53.9% CV), and β-Glucuronidase (GUSB, 57.6% CV). These 4 genes were also selected because they spanned a range of counts from low (average 198 counts for GUSB) to high (average 22,486 counts for

RPL19). These 4 housekeeping genes were added to another 8 for a total of 12 housekeeping genes in the final panel. This was done to confirm that we could select the best housekeeping genes for our study. The 4 originally selected best housekeeping genes were in the top 5 lowest %CV values and an additional housekeeping gene not originally in the 18 from the separate study was added since it fell within the top 5 housekeeping genes. The 5 housekeeping genes used in this study and their %CV are: POLR2A (14.6%), RPL19 (16.2%), GUSB (17.1%), GNB2L1 (Guanine nucleotide-binding protein subunit beta-2-like 1, 19.3%), and TBP (20.0%). Again these 5 housekeeping genes spanned a range of counts from low to high.

5.2.4 Candidate Gene Selection

The Nanostring nCounter® platform allows users to build a custom panel of up to 800 genes for a more directed hypothesis driven approach to gene expression analysis than microarray or RNA-seq. We selected our genes based our hypotheses. They fell into the following categories: 1) genes involved in the contraction and relaxation of ASM and its regulation, 2) genes involved in the structure of the cytoskeleton and its regulation, 3) genes involved in growth and proliferation, and 4) genes involved in calcium handling. All of the genes selected were thought to be expressed in the ASM and were biologically plausible candidates for a role in the development of AHR or remodeling changes within the airway. Genes like MYH11, MLCK, SM-22 or actin have been previously examined by other groups (60, 61, 127). Many of the genes in the contractile machinery group were taken from the Krypto Encyclopedia of Genes and Genomes (KEGG) pathway for vascular smooth muscle contraction. Genes within this pathway are involved in either contraction or relaxation of smooth muscle and so have the potential to play a role in AHR in asthma. Genes within the cytoskeletal group were selected based on previous work by Gunst et al. (216) and Rosner et al. (200). All genes in this group were shown to be important in transmitting ASM force to the external environment at adherens junctions, in maintaining the actin filament lattice or were shown to interact directly with cytoskeletal proteins. Similarly, work by Sieck et al. (217) led to our selection of CD38 and other calcium handling proteins that have been shown to be expressed in cultured ASM cells (218). Finally, work showing the role of the myocardin pathway in proliferation of ASM cells (219) led to the selection of genes in this pathway involved in growth and proliferation in ASM.

5.2.5 Immunohistochemsitry

Protein expression and localization of Zyxin (ZYX), Filamin B (FLNB), CD38 and Smoothelin (SMTN) was verified by immunohistochemistry (IHC) on formalin fixed paraffin embedded (FFPE) sections from each of the 24 subjects used for RNA analyses. The antibodies for ZYX (ab110202), FLNB (ab84905), CD38 (ab93941) and SMTN (ab8969) were ordered from Abcam Inc.® (Cambridge UK). Sections of 4µm thickness were cut from the lung cores. FFPE sections were deparaffinized in CitriSolv (Fisher Scientific) and brought to water using a graded series of alcohol. Sections were then autoclaved (Bench Top Tuttnauer 2340M autoclave) on a 22-minute cycle in Citrate buffer, pH6, and were then left to cool for 20 minutes. All the IHC staining was carried out on a Dako Autostainer Universal Staining System and all incubations throughout the staining run were carried out at room temperature. After cooling, the slides were loaded onto the Autostainer and incubated in Background Sniper (BS966: Biocare Medical; Concord, CA, USA) for 15 minutes to help reduce non-specific binding. The sections were incubated with the primary antibody at 1/200 dilution for 45 minutes. Detection was performed using the MACH3 Universal AP staining kit (Biocare Medical). Slides were covered with MACH3 Universal AP Polymer (M4U536) for 10 minutes each. Finally, the sections were incubated with Vulcan Fast Red as chromagen (Biocare, FR805) for 12 minutes and then counterstained with diluted Gill's III Hematoxylin (SurgiPath) for 2 minutes. As negative control, normal mouse serum was used at the same concentration as the primary antibody. Positive controls were as follows: CD38 and FLNB – lung carcinoma, SMTN – vascular smooth muscle, ZYX – breast tissue. Sample positive and negative control stains can be seen in Appendix B (Figure B4). The degree of staining was quantified for the whole airway, ASM bundles and epithelial layer.

5.2.6 Quantification of IHC Staining

Quantification of the staining was done using the positive pixel count algorithm that is part of the Aperio Image Scope® software. The area of interest for each of the analyzed layers (whole airway, ASM, epithelium) were traced to confine the algorithm to the correct tissue compartment. The algorithm variables, which were set to minimize non-specific identification of staining, were determined separately for each protein of interest. This was done by iteratively applying the algorithm to both the positive and negative controls and maximizing the selection of the positive area while minimizing the non-specific signal on the the negative slide. The hue value, width and saturation levels where repeatedly adjusted until the ratio of the signal in the positive control and negative control was maximized. Hue values usually centered around a value of 0.98 on a color wheel where 0 is red, 0.33 is

green and 0.66 is blue. Hue widths and saturation levels where set for each individual stain and where dependent on the shade of pink on the slide with pale pink needing lower saturation values or a wider range of hues and vibrant pinks needing a higher saturation value or narrower range of hues. For each tissue compartment analyzed, the percent positivity was recorded. The percent positivity is the percentage of the traced area that is positive for the color of interest (in this case pink). One section per subject was stained and analyzed this way. All measurements were carried out in a blinded manner.

5.2.7 Statistical Analyses

The normalized gene expression values for mRNA expression were compared between asthmatic (n=12) and non-asthmatic subjects (n=12) and between non-asthmatic, non-fatal asthmatic (n=4) and fatal asthmatic subjects (n=8) using a generalized linear model with a gamma distribution. Sample distribution can be seen in Appendix B (Figure B2). Statistical analysis for gene expression results was performed in collaboration with the Center for Health Evaluation & Outcome Sciences (CHEOS). Data are plotted as box and whisker plots. Data for airway wall compartment dimensions are presented as mean ± SEM and comparison between groups was done using Student's t-test. Measurements of airway wall compartment areas were normalized to the internal perimeter (Pi) to correct for airway size. Correlations of levels of expression of MYH11 and FLNB with ASM volume were done on the raw un-normalized data. For IHC, the percent positivity of protein staining in each of the airway wall compartments was measured and compared between asthmatic (n=12) and non-asthmatic subjects (n=12) and between non-asthmatic, non-fatal asthmatic (n=4) and fatal asthmatic (n=8) subjects using Student's t-test. Data are plotted or listed as mean ± SEM. A p-value less than 0.05 was considered significantly different. Multiple comparison corrections were not applied to gene expression data. Since genes were picked primarily based on *a priori* hypotheses, no correction for multiple testing was applied. Rather, genes were split into their specific hypothesis groups and analyzed. Since gene expression results need to be verified by protein expression analysis, we chose to determine which of our results were likely to be true positives and biologically plausible by examining the protein expression within our samples. This served two purposes, to confirm the changes in gene expression where not due to transient changes following the harvesting of the organ (220) and to localize the proteins within the airway. This type of analysis lies somewhere between a fully unbiased approach like RNA-seq or microarray and a targeted gene expression analysis like qPCR and as such deciding whether to apply multiple comparison corrections was difficult. Data were plotted using GraphPad version 5.04, La Jolla California USA.

5.3 Results

5.3.1 Quantification of Airway Remodeling

The total number of airways analyzed in non-asthmatic subjects was 53 with an average of 2.2 ± 0.72 airways per subject and 52 airways in asthmatic subjects with an average of 2.2 ± 0.96 airways per subjects ($p>0.05$). The average airway size (measured by Pi) of non-asthmatic subjects was 5.3 ± 1.5mm (geometric mean 4.9 ± 1.3mm) and in asthmatic subjects was 5.1 ± 2.8mm (geometric mean 4.0 ± 1.7mm) ($p>0.05$ for both arithmetic mean and geometric mean). Airway wall compartment areas for asthmatics and non-asthmatics were quantified (figure 5.2) on digitally scanned slides. Airway wall area per unit length of internal perimeter was significantly greater in asthmatics (0.22 ± 0.024 mm^2/mm) than in non-asthmatics (0.13 ± 0.019 mm^2/mm, $p<0.01$). There was also an increase in the ASM area per unit internal perimeter (0.018 ± 0.0024 mm^2/mm vs. 0.011 ± 0.0015 mm^2/mm, $p<0.05$) and in the basement membrane thickness (6.9 ± 0.81 mm vs. 3.9 ± 0.73 mm, $p<0.01$) in asthmatics when compared to non-asthmatics. Epithelial area per unit internal perimeter was not significantly increased in asthmatics (0.030 ± 0.0037 mm^2/mm) when compared to non-asthmatics (0.022 ± 0.0023 mm^2/mm, $p =0.086$). Neither was the total collagen area (including basement membrane) changed in asthmatics vs. non-asthmatics (0.073 ± 0.011 mm^2/mm vs. 0.051 ± 0.010 mm^2/mm, $p>0.16$). Total ASM volume, which is the total section thickness (number of sections times section thickness) multiplied by the ASM area per section, in isolated tissue was found to correlate with MYH11 expression ($R^2=0.127$, $p=0.013$) but not with FLNB expression ($R^2=0.0047$, $p=0.642$) as shown in figure 5.2 F & G.

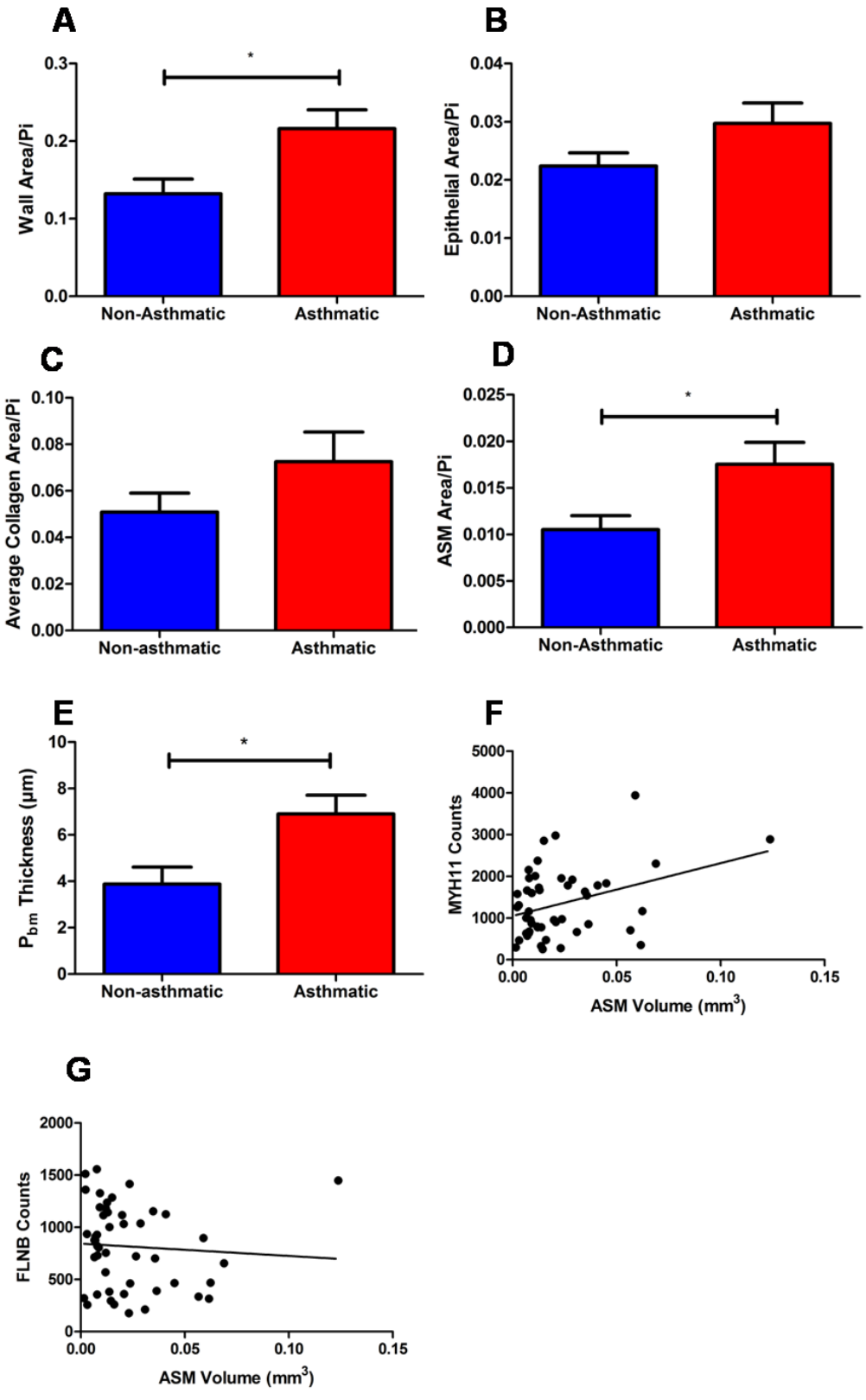
A
Wall Area/Pi
0.3
0.2
0.1
0.0
*
Non-Asthmatic
Asthmatic
B
Epithelial Area/Pi
0.04
0.03
0.02
0.01
0.00
Non-Asthmatic
Asthmatic
C
Average Collagen Area/Pi
0.10
0.08
0.06
0.04
0.02
0.00
Non-asthmatic
Asthmatic
D
ASM Area/Pi
0.025
0.020
0.015
0.010
0.005
0.000
*
Non-Asthmatic
Asthmatic
E
P_{bm} Thickness (µm)
10
8
6
4
2
0
*
Non-asthmatic
Asthmatic
F
MYH11 Counts
5000
4000
3000
2000
1000
0
0.00
0.05
0.10
0.15
ASM Volume (mm^3)
G
FLNB Counts
2000
1500
1000
500
0
0.00
0.05
0.10
0.15
ASM Volume (mm^3)

Figure 5.2 Remodeling changes and correlation to gene expression. A) Airway wall area B) Epithelial area C) Collagen area D) ASM area per unit internal perimeter (Pi) in asthmatics (red) vs. non-asthmatics (blue). E) Basement membrane thickness (P_{bm}). F) Correlation of total ASM volume (ASM area multiplied by total thickness of all sections) with MYH11 counts and G) FLNB counts. * $p<0.05$ by t-test. n=12 for both asthmatic and non-asthmatic.

5.3.2 Gene Expression Changes in Asthmatic Airways

Gene expression changes in all 99 genes analyzed are summarized in a volcano plot (figure 5.3) with the candidate gene category designated by a specific color. It is evident that the majority of candidate genes were down regulated in asthmatics as indicated by the leftward shift of the data points. Table 5.2 shows the counts for all genes that showed a nominally significant difference in expression between subject groups as well as genes where changes in expression have been previously reported or for which expression differences have been suggested as important in terms of ASM phenotype in asthma. The genes shown in bold are those that were chosen for further exploration by IHC staining and quantification. Of particular importance is the observation that there were no significant changes in the expression of smooth muscle myosin light chain kinase (MYLK1, 2267 ± 227.7 counts vs. 1680 ± 246.8 counts), myosin heavy chain (MYH11, 1564 ± 212.0 counts vs. 1328 ± 232.4 counts), transgelin/SM22 (TAGLN, 4422 ± 619.0 counts vs. 3527 ± 488.2 counts), or α-smooth muscle actin (ACTA2, 4774 ± 587.1 counts vs. 4626 ± 732.2 counts) between non-asthmatics and asthmatics respectively ($p>0.05$ for all). For these genes there was also no difference in expression in the subset of fatal asthmatics versus non-asthmatics (see table 5.2). There were significant changes in a number of candidate genes related to cytoskeletal structure and regulation, calcium handling and growth and proliferation.

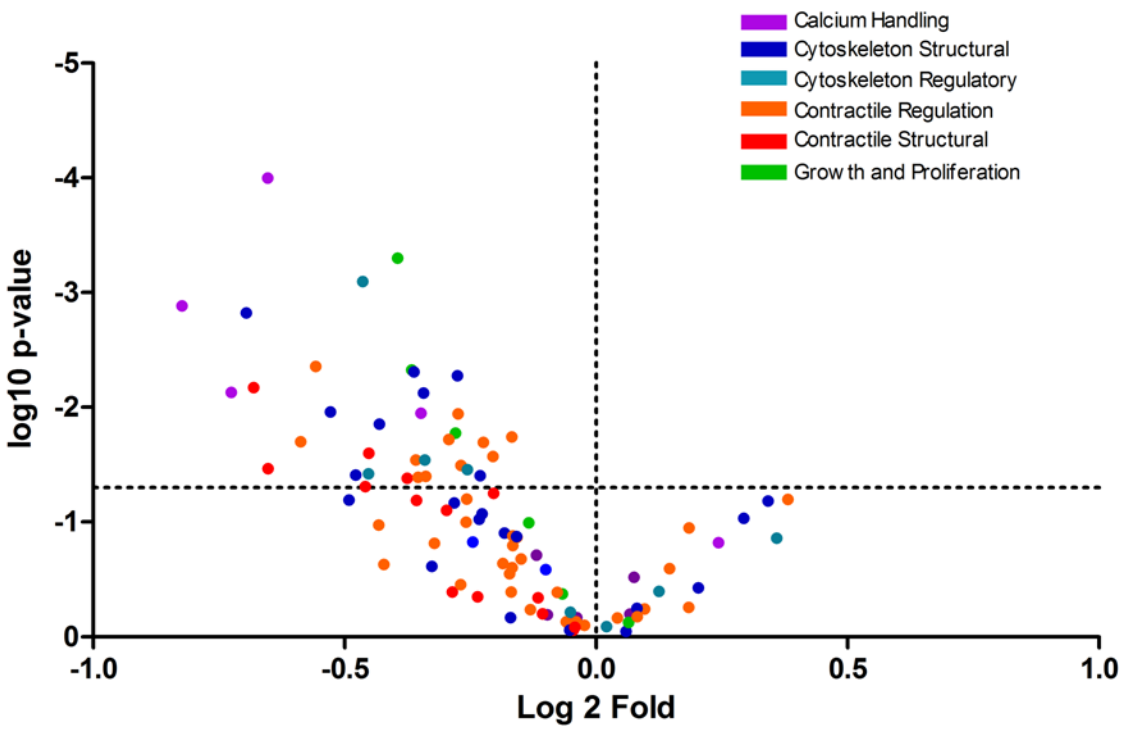

Figure 5.3 Volcano plot showing the relative expression of genes in data set. Vertical dotted line indicates zero fold change. Horizontal dotted line indicates p-value of 0.05. Genes are coloured relatie to their function in ASM (see legend). Some of the genes may fall into more than one category but have only been put under the most appropriate one. N=12 non-asthmatics and 12 asthmatics.

Four genes were chosen for analysis at the protein level based on the significant differences and/or the potential biological significance of the genes. These four genes were filamin B (FLNB, 1063 ± 93.89 counts vs. 656 ± 61.4 counts, p=0.002), cyclic ADP ribose hydrolase (CD38, 996 ± 74.0 counts vs. 633 ± 39.8 counts, p=0.0001), zyxin (ZYX, 4385 ± 421.0 counts vs. 5375 ± 420.9 counts, p=0.092), and smoothelin (SMTN, 276 ± 24.9 counts vs. 350 ± 30.5 counts, p=0.066) in non-asthmatics vs. asthmatics respectively (table 5.2 and figure 5.4). The latter two genes were selected despite not showing a significant difference between asthmatic and non-asthmatic subjects since the trend in their expression was opposite to the majority of smooth muscle specific candidates and because of their potential role in regulating cytoskeletal stiffness in ASM. In fact there was a differential increase in the expression of SMTN in fatal asthmatics when compared to non-asthmatics (table 5.2). A complete list of all gene counts and p-values can be found in appendix A.

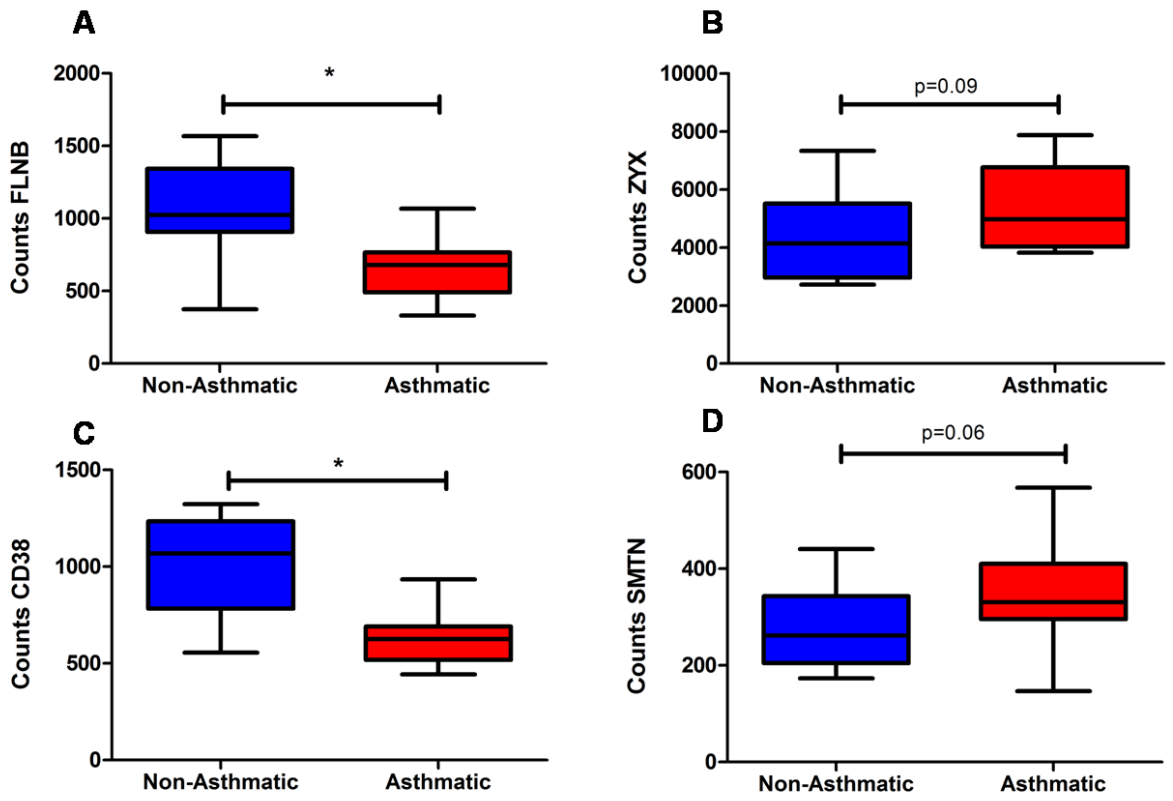

Figure 5.4 Expression of select genes from data set. A) FLNB – Filamin B, * p<0.01. B) ZYX – Zyxin. C) CD38 – Cyclic ADP ribose hydrolase, * p<0.01. D) SMTN – Smoothelin. N=12 non-asthmatics and 12 asthmatics for each.

		Gene counts				p-values	
Gene	**Description**	**Non-Asthmatic**	**Asthmatic**	**Fatal Asthmatic**	**Non-Fatal Asthmatic**	**Non-Asthmatic vs. Asthmatic**	**Non-Asthmatic vs. Fatal Asthmatic**
MYLK1	Myosin Light Chain Kinase – Smooth Muscle	2267 ± 227.7	1680 ± 246.8	1695 ± 278.3	1651 ± 554.9	0.106	0.158
MYH11	Myosin Heavy Chain 11	1564 ± 212.0	1328 ± 232.4	1402 ± 299.2	1179 ± 406.3	0.445	0.646
TAGLN	Transgelin (SM22)	4422 ± 619.0	3527 ± 488.2	3179 ± 378	4223 ± 1308	0.242	0.124
ACTA2	Alpha Actin 2	4774 ± 587.1	4626 ± 732.2	4130 ± 561.3	5619 ± 1983	0.874	0.505
FLNB	**Filamin B**	1063 ± 93.89	656 ± 61.4	711 ± 71.1	547 ± 109	**0.002**	**0.011**
CD38	**Cyclic ADP Ribose Hydrolase**	996 ± 74.0	633 ± 39.8	646 ± 57.7	608 ± 40.0	**<0.0001**	**0.001**
ZYX	**Zyxin**	4385 ± 421.0	5375 ± 420.9	5288 ± 581.4	5548 ± 597.1	0.092	0.162
SMTN	**Smoothelin**	276 ± 24.9	350 ± 30.5	384 ± 32.3	282 ± 55.2	0.066	**0.019**

Table 5.2 Summary of gene expression results. For full table of gene expression counts see appendix A. Significance was determined using a generalized linear model. $p<0.05$ denotes significance.

5.3.3 Protein Expression Changes in Asthmatic Airways

In order to validate the gene expression changes we identified, IHC staining and quantification on sections of FFPE airways from the same subjects was performed. CD38, which has been previously shown to be expressed in cultured ASM cells (217), was localized to the epithelium with no expression appearing in the ASM (Figure 5.5A). The expression of CD38 within the epithelium appeared cytoplasmic and diffuse. Similarly, FLNB expression was localized to the epithelial layer with minimal expression appearing in the ASM (Figure 5.5B). SMTN expression was localized to the ASM and appeared throughout the bundles, as expected, with minimal staining in the epithelial layer (Figure 5.5C). Finally, ZYX was ubiquitously expressed in all tissue compartments of the airway (Figure 5.5D). ZYX staining appeared punctuate in inflammatory cells in the airway wall, while in the epithelium and ASM it appeared more diffuse. There was no apparent preferential staining to either the basal or apical surface of the epithelium.

Quantification results are summarized in table 5.3. Briefly, there was no significant difference in the expression of CD38 in the airway wall (6.8 ± 1.4% vs. 7.2 ± 1.0%), epithelium (15.5 ± 3.4% vs. 13.5 ± 2.0%, Figure 5.6A), ASM (0.5 ± 0.2% vs. 0.6 ± 0.2%), or "other" wall components (4.1 ± 0.7% vs. 5.4 ± 0.9%) between non-asthmatics and asthmatics respectively ($p>0.05$ for all). There was also no difference when comparing there measurements in non-asthmatics and fatal asthmatics ($p>0.05$). FLNB expression was also not significantly different in the airway wall (8.5 ± 2.1% vs. 10.4 ± 1.5%), epithelium (20.4± 2.6% vs. 24.8 ± 3.6%, Figure 5.6B), ASM (1.7 ± 0.4% vs. 1.5 ± 0.3%) or "other wall" components (4.0 ± 0.5% vs. 5.2 ± 0.6%) between non-asthmatics and asthmatics respectively ($p>0.05$ for all). Similarly, there was no significant difference in the expression between fatal asthmatics and non-asthmatics. Expression of SMTN was increased, although not significantly, in the airway wall of asthmatics vs. non-asthmatics (7.4 ± 1.8%vs. 3.4 ± 0.6%, $p=0.051$). There was no significant difference in the expression of SMTN in the epithelium (3.0 ± 0.4% vs. 2.2 ± 0.3%) and other wall components (2.1 ± 0.3% vs. 3.1 ± 0.8%) in non-asthmatics vs. asthmatics respectively ($p>0.05$), however SMTN expression in the ASM of asthmatics (30.0 ± 5.7%) was significantly increased when compared to non-asthmatics (11.2 ± 2.5%, $p<0.01$. Figure 5.6C). Expression of SMTN was increased in fatal-asthmatics over non-asthmatics for both the airway wall (8.7 ± 2.7% vs. 3.4 ± 0.6%, $p<0.05$) and ASM (32.2 ± 8.0% vs. 11.2 ± 2.5%, $p<0.01$). Expression of SMTN in the epithelium was undetectable at the levels above the negative control. SMTN expression in the "other" wall components was not significantly different in the airways of fatal asthmatics ($p>0.05$). ZYX protein expression was not significantly different in the airway wall (15.3 ± 1.8% vs. 20.1 ± 2.3%),

ASM (17.0 ± 2.0% vs. 21.5 ± 1.5%), epithelial layer (14.1 ± 2.0% vs. 17.6 ± 2.7%) or other wall components (16.0 ± 1.9% vs. 20.8 ± 2.5%) in non-asthmatics vs. asthmatics ($p>0.05$). In fatal asthmatics, ZYX expression was significantly increased ($p<0.05$) compared to expression in the airway wall of non-asthmatics (22.7 ± 2.7% vs. 15.3 ± 1.8%) and in the ASM (23.2 ± 1.6% vs. 17.0 ± 2.0%, Figure 5.6D). Similarly ZYX expression was significantly increased in the "other" airway wall compartment (23.8 ± 3.0 vs. 16.0 ± 1.9%). There was no significant difference in the expression of ZYX in the epithelium of fatal asthmatics over non-asthmatics.

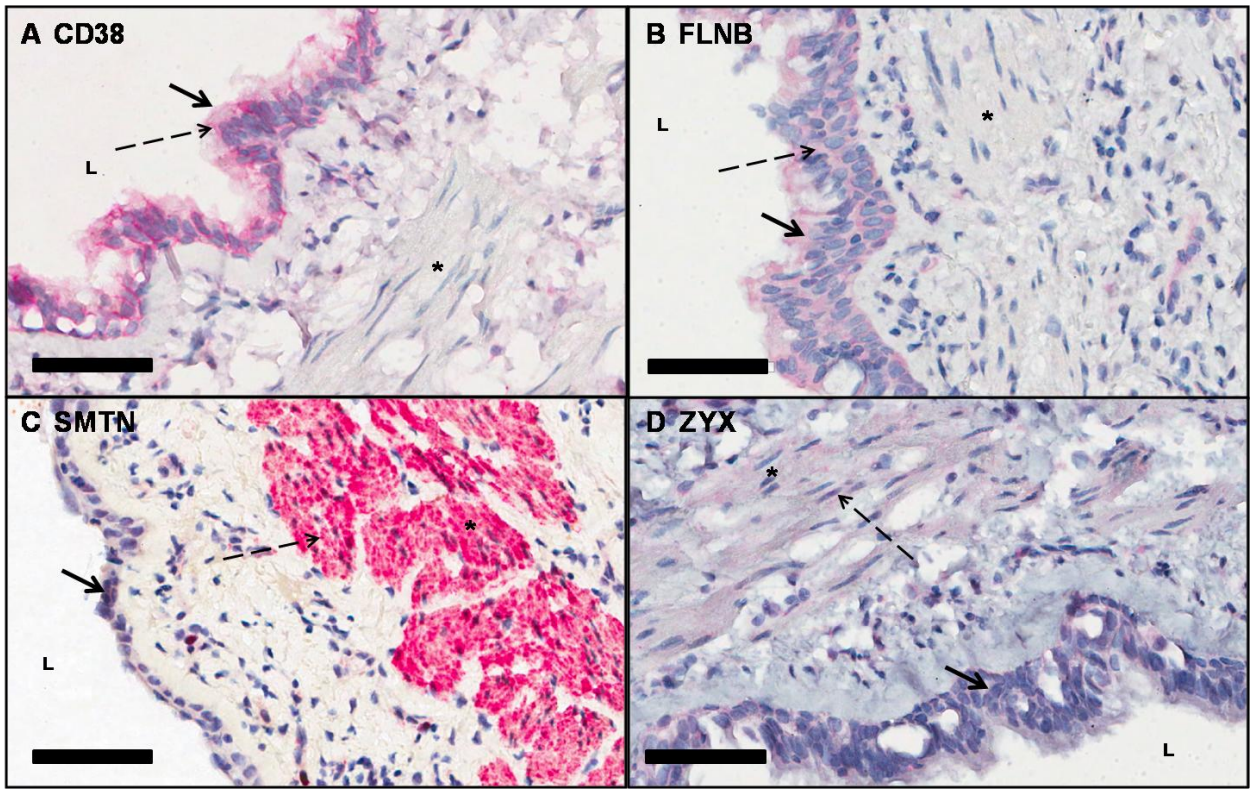

Figure 5.5 Sample images of IHC stains for A) CD38, B) FLNB, C) SMTN, D) ZYX. Asterisk labels ASM layer. Arrow points to epithelial area. L denotes lumen of each airway. Black scale bar represent 60 µm Positive cells are noted with a dashed arrow.

		CD38	FLNB	SMTN	ZYX
% Airway +	Non-Asthmatic	6.8 ± 1.4	8.5 ± 1.2	3.4 ± 0.58	15.3 ± 1.78
	Asthmatic	7.2 ± 1.0	10.4 ± 1.50	7.4 ± 1.8	20.1 ± 2.29
	Fatal-Asthmatic	6.4 ± 1.1	10.8 ± 2.19	8.8 ± 2.7*	22.7 ± 2.75*
	Non-Fatal Asthmatic	8.6 ± 2.0	9.7 ± 1.5	4.9 ± 1.1	14.9 ± 2.95
% Epithelium +	Non-Asthmatic	15.5 ± 3.44	20.4 ± 2.57	3.0 ± 0.42	14.1 ± 2.05
	Asthmatic	13.5 ± 1.98	24.8 ± 3.57	2.2 ± 0.31	17.6 ± 2.71
	Fatal-Asthmatic	10.3 ± 1.56	25.0 ± 5.25	1.7 ± 0.30	19.5 ± 3.72
	Non-Fatal Asthmatic	19.8 ± 3.48	24.4 ± 3.45	2.9 ± 0.47	13.8 ± 2.99
% ASM +	Non-Asthmatic	0.5 ± 0.2	1.7 ±0.35	11.2 ±2.49	17.0 ± 1.97
	Asthmatic	0.6 ± 0.2	1.5 ± 0.32	30.0 ± 5.70*	21.5 ± 1.47
	Fatal-Asthmatic	0.7 ± 0.2	1.2 ± 0.29	32.2 ± 8.01*	23.2 ± 1.61*
	Non-Fatal Asthmatic	0.5 ± 0.2	2.0 ± 0.74	23.4 ± 7.56	18.1 ± 2.39
% Other +	Non-Asthmatic	4.1 ± 0.74	4.0 ± 0.51	2.1 ± 0.27	16.0 ± 1.88
	Asthmatic	5.4 ± 0.86	5.2 ± 0.59	3.1 ± 0.77	20.8 ± 2.49
	Fatal-Asthmatic	5.5 ± 1.1	5.5 ± 0.82	3.7 ± 1.0	23.8 ± 2.97*
	Non-Fatal Asthmatic	5.2 ± 1.4	4.7 ± 0.69	2.2 ± 0.35	14.9 ± 3.06

Table 5.3 Summary of IHC quantification results. * $p<0.05$ vs. Non-asthmatics.

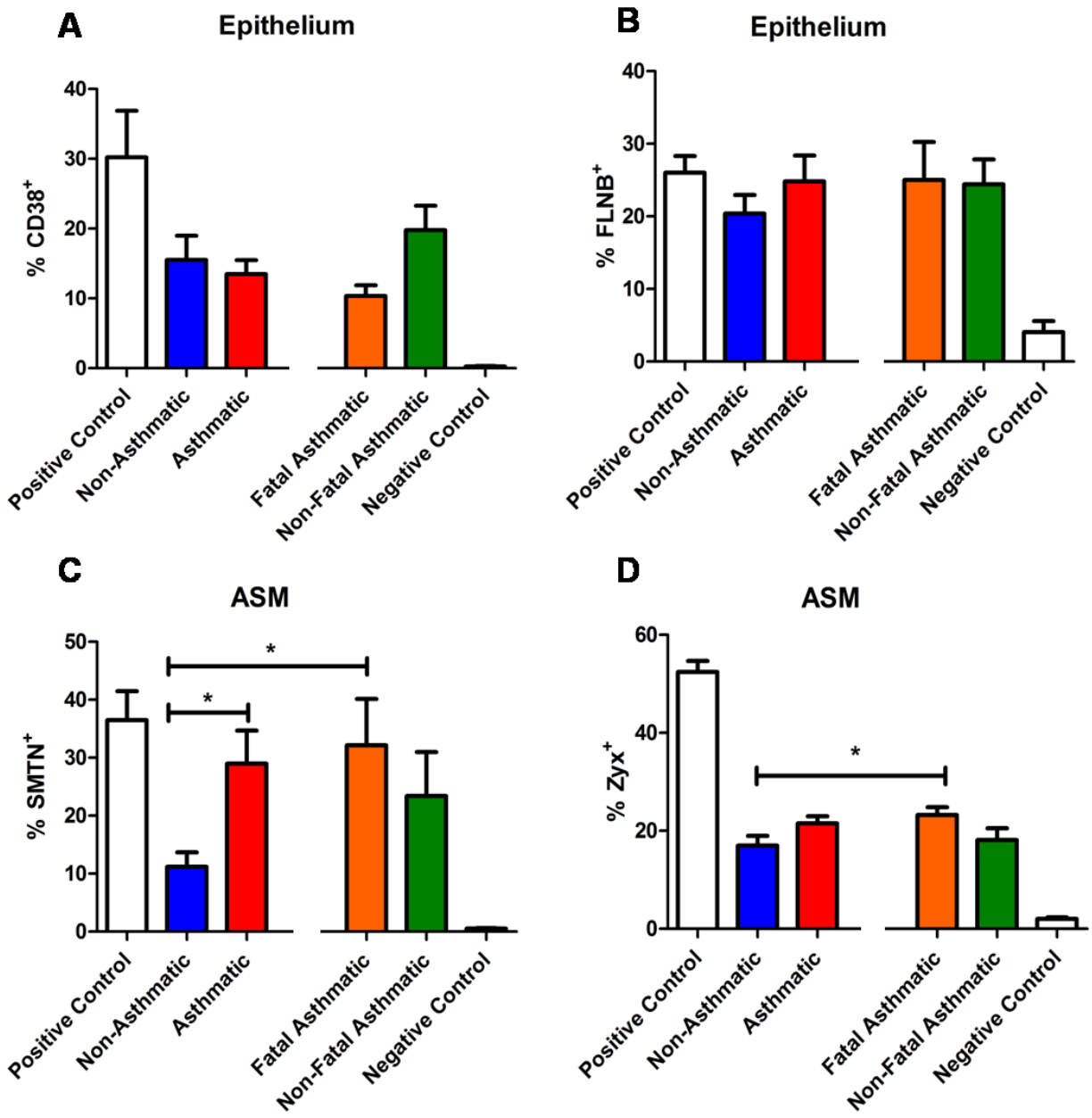

Figure 5.6 IHC quantification results. A) CD38 in the epithelium of non-asthmatics (n=12), asthmatics (n=12), fatal asthmatics (n=8) and non-fatal asthmatics (n=4). B) FLNB in the epithelium of non-asthmatics (n=12), asthmatics (n=12), fatal asthmatics (n=8) and non-fatal asthmatics (n=4). C) SMTN in the ASM of non-asthmatics (n=11), asthmatics (n=11), fatal asthmatics (n=7) and non-fatal asthmatics (n=4). D) ZYX in the ASM of non-asthmatics (n=12), asthmatics (n=12), fatal asthmatics (n=8) and non-fatal asthmatics (n=4). * $p<0.05$. All values expressed as percent positive area.

5.4 Discussion

In this study we aimed to quantify the expression of genes and proteins that could be important in AHR in asthma. The genes were chosen because they were hypothesized to be important in some aspect of ASM function and were broadly grouped into 6 categories: contractile apparatus structure, contractile regulation, cytoskeletal structure, cytoskeletal regulation, calcium handling, and growth/proliferation. Although some of the candidate genes had been previously implicated in asthma, many were previously unexplored in the context of asthma. We can see in appendix B, that expression between cores from the same subjects was more correlated than between cores from different subjects (Figure B3) indicating that the technical variability in the assay was less than the biological variability. For the most part, the results of this study do not support our initial hypotheses that an increase in the expression of genes involved in contractile function, cytoskeletal stiffness or smooth muscle proliferation would be evident in the airways of asthmatic subjects. In fact the only significant differences in gene expression were less expression of a number of genes in the asthmatic tissue.

Previous investigators have examined the phenotype of asthmatic ASM at the structural, functional and gene expression level in an attempt to incriminate ASM in the pathogenesis of airway hyperresponsiveness which is recognized as a key feature of asthma. Many of these studies have yielded conflicting results. While some groups have shown an increase in ASM force production (48) or shortening and shortening velocity (60, 221), others have shown no differences in the contractile function of ASM from asthmatics (50, 52–54). Most recently Chin et al showed no difference in stress generation, shortening velocity or the extent of maximal unloaded shortening in the trachealis muscle of asthmatics compared to non-asthmatic subjects, in whom we have examined bronchial gene expression (12).

The results of previous studies have also been discordant with respect to the relative levels of expression of genes and proteins that could implicate changes in ASM contractility as the basis of AHR. Increased expression of MLCK mRNA has been found by some (60, 61, 222) while MLCK protein expression was shown to be increased in sensitized ASM from normal subjects (223) and in severe asthmatics compared to controls and mild asthmatic (222). It was postulated that increased amounts of this kinase would allow the muscle to shorten faster and/or more forcefully. However additional studies have failed to unequivocally incriminate MLCK (127, 221). We found no significant difference in the expression of MYLK1 mRNA in either asthmatics or fatal asthmatics as compared to non-asthmatics. Protein expression in our samples was not quantified because there was no difference in MYLK1 mRNA

expression nor trend towards a difference, unlike SMTN and ZYX. Myosin heavy chain (MYH11) is another attractive candidate for involvement in AHR. MYH11 comes in multiple isoforms known as SM1, SM2, SMA and SMB (224). The isoforms are not mutually exclusive with SM1 or SM2 pairing up with either SMA or SMB to form SM1A, SM2A, SM1B, and SM2B (224). There is evidence that that ASM and other types of smooth muscle containing the SMB insert isoform can shorten faster (225, 226), and that this is primarily by increased ATPase activity (130, 227) and increased actin filament propulsion (61). This led to the hypothesis that differences in the levels of the isoforms could contribute to increased shortening velocity in asthmatic ASM. Although some investigators did not detect a difference in SMB expression (127) or couldn't detect this isoform at all (60); Léguillette et al. (61) showed an increase in the expression of SMB mRNA in asthmatic bronchial biopsies. It is possible that failure to detect SMB in the past was technical since the SMB insert is only 21 base pairs long (224). In our study, we did not see a difference in the total expression of MYH11; however we were unable to detect the different isoforms with the technology we used so it is possible that there could be different ratios of the isoforms leading to changes in ASM mechanics. Additional proteins that have been hypothesized to directly affect the contractile ability of the ASM (61, 127, 136) were not differentially expressed in the airways of asthmatic subjects (Table 5.2 and Appendix B). These include no difference in the expression of MLCP, transgelin (SM22) or α-smooth muscle actin.

Calcium handling within the ASM tissue has also been an area of interest as calcium is an essential player in the contraction cascade in ASM (reviewed in (228)). There are numerous proteins involved in calcium handling within the ASM cell including calmodulin, calponin and CD38. Recently, work on cultured ASM cells and in mouse models of asthma have implicated CD38 in the development of AHR. CD38 is an enzyme that is important in the conversion of NAD^+ into cyclic ADP-ribose (cADPR), which helps to liberate calcium from endoplasmic reticulum stores via the ryanodine receptor (229). It has been suggested that the expression of this protein in ASM cells is important for the release of Ca^{2+} during contraction (217) and that knocking it out can abolish AHR in a mouse model of asthma (230). This was the reasoning behind selecting it for analysis; however, there was a significant decrease in its mRNA expression in the asthmatic samples and IHC showed no CD38 expression in the ASM layer. It is possible that the decreased expression of CD38 mRNA is the result of steroid treatment in the asthmatic subjects. To date, there have been no studies comparing the expression of CD38 in intact ASM tissues and in cultured ASM cells (231), it may simply be an artifact of the culturing process. Western blot analysis of CD38 protein expression in whole human ASM tissue preparations may help answer this question. We saw abundant expression of CD38 in the epithelium (Figure 5.6) so it may be possible for

the cADPR to be secreted (232) and then act upon the ASM layer without the need for CD38 to be expressed by ASM tissues. The discrepancy between mRNA counts and protein expression in our samples could be explained by steroid responsiveness in the CD38 gene(233).

The second category of genes that we studied relate to the smooth muscle cytoskeleton. The cytoskeleton resists cell distortion and could insulate the ASM from the functional changes produced by cellular strain. *In vivo* an attenuated ability of DIs to reverse or prevent bronchoconstriction is a characteristic feature of asthma (97) and may be related to the phenomenon of AHR. Resistance to the salutatory effects of strain could, in theory, be due to differences in the expression and/or function of the proteins involved in ASM contraction or ASM stiffness. The cytoskeleton could play an important role in the resistance of ASM to stretch and so we included key genes involved in the cytoskeleton and its regulation among our candidates. Interestingly, the only difference that was observed in the mechanics of the trachealis muscle strips from these same subjects in the study of Chin et al (53) was a decrease in the effectiveness of simulated deep inspirations (DIs) to lessen subsequent force production in the asthmatic ASM compared to non-asthmatic. It was noted by investigators that when non-asthmatic subjects refrained from taking DIs they became hyperresponsive to methacholine (95, 110, 119, 234) and this led to the idea that DIs are important in limiting airway narrowing. If ASM force generating capacity in asthmatics is the same as in non-asthmatics, as suggested by some studies (50, 53), then it is possible that a failure to dilate the airways results in AHR. Stiffening of the muscle so that is no longer responds to DIs may explain why asthmatics fail to dilate their airways in response to DIs (92, 99, 171, 189, 197). It has been recently shown that ASM stiffness is modifiable by calcium and Rho kinase (235, 236) and alterations to these pathways may account for failure of DIs to dilate asthmatic airways. It has also been shown that when actin polymerization was inhibited by latrunculin B, large DI-like oscillations were able to re-lengthen contractile agonist- induced shortening in ASM. However when actin filaments were stabilized by jasplakinolide, the same oscillations were unable to re-lengthen the ASM tissue (237). This intuitively leads to the hypothesis that the results seen by Chin et al. (53) may be due to alterations in actin filament stability or to changes in the proteins that stabilize actin. Although we found no significant difference in the level of expression of the candidate genes involved in the cytoskeleton or its regulation we observed that two cytoskeletal genes, ZYN and SMTN tended to show increased expression in asthma in the face of a general decrease in expression of most genes.

ZYX is a protein that may have an important role in determining the ASMs response to strain (200) and its increased expression could help explain the results seen by Chin et al. (53) where asthmatic ASM was more resistant to length oscillations than non-asthmatic ASM. ZYX protein was significantly

increased in the ASM of fatal asthmatics. Rosner et al. have shown that knock down of ZYX protein results in a tissue that cannot fully regain its force generating capacity following oscillatory strains imposed on the muscle (200). It is possible that over expression of ZYX could do the opposite and make the muscle less compliant and less responsive to oscillating stresses that mimic deep inspirations leading to a either greater resistance to or faster recovery from oscillation-induced relaxation in ASM. Validation of our protein expression result on a larger cohort of better phenotyped asthmatics would be beneficial.

SMTN is a cytoskeletal protein that has been shown to be specific for mature smooth muscle cells (215). It is often used as a marker for smooth muscle cells in tissues but its function are relatively unknown. It is known to bind actin and may play a role in muscle contraction(238) since knock out of SMTN-A in mice results in impairment of intestinal muscle contraction (238). It would therefore not be a great stretch to hypothesize that increased SMTN expression could lead to increased levels of contraction in ASM. While one would expect the levels of SMTN to increase simply because there is more muscle in asthmatic airways, in our study, the measurement was percent positivity in which the positive staining was normalized to the area of muscle and therefore this result indicates an increase in SMTN per unit muscle. SMTN gene expression was one of the only genes in our study that increased in asthmatics (although not significantly) and its protein expression was significantly increased. More studies need to be done to determine the function of SMTN (239) and its role in ASM contraction and to determine if over expression of it can result in a hypercontractile phenotype.

Another protein identified by our experiments that was thought to bind to actin and perhaps be important in determining the ASM response to DIs is FLNB. FLNB is a member of the filamin family which consists of FLNA, FLNB and FLNC (240). The filamins are actin cross linkers that can associate with many other proteins responsible for cell adhesion, spreading and migration (240). No role for the filamins in asthma or AHR has been shown, however there has been research identifying the requirement of FLNA for the organization of epithelium and development of cell to cell connections in a knockout mouse (241). Our data did not show a difference in the protein expression of FLNB even though the gene expression levels were decreased in asthmatics. Again these results could indicate responsiveness to the terminal administration of steroids. FLNB is an attractive target to help explain the loss of epithelial integrity in asthma (242) since its family members play important roles in vascular endothelial integrity (241); however it does not appear to be expressed in the ASM. Again, western blot analysis of ASM tissues would help further prove its absence in the ASM layer. The discrepancy between protein quantification and mRNA counts in our study again could be due to steroid treatment affecting the steroid responsive elements in the filamin gene promoter (243).

One of the limitations of our study is the use of whole airway RNA and not just RNA from the ASM. While laser capture microdissection of ASM from human airways has been done (244) it requires the amplification of RNA which can introduce skewing of relative mRNA amounts and the loss of up to 30% of differentially expressed genes (245). Another problem posed by microdissection is the isolation of ASM from non-asthmatic subjects. While asthmatic subjects have abundant ASM around their airways (4), non-asthmatic airways have little making it difficult to identify and isolate. This further compounds the problem of low RNA yields. By using the whole airway in our sample, we were able to ensure enough RNA to perform the quantification using the Nanostring nCounter ® system and were able to determine the location of the proteins in the airways using IHC. While IHC is only semi-quantitative, it shows which cells express the gene and gives us a good idea of where to focus future protein analysis efforts when samples become available. It should be noted that the majority of the asthmatic patients were fatal asthmatics and were on steroids either for the management of the disease or during their fatal attack. It has been shown that factors such as hypoxia, time from death to tissue fixation or freezing and post mortem drug treatment can affect mRNA expression (246) in tissues taken for research purposes. Post mortem events (terminal medication and hypoxia) also affect transcript turnover (247) making it more likely that mRNA transcript levels are altered before analysis can be done. As such, the gene expression results could be confounded. mRNA degradation is unlikely in the tissues because the cryopreservative maintains mRNA integrity and tissues are handled as if they were being transplanted. Since it would take much longer for the terminal events to modify protein levels this shows the importance of the exploration of protein expression to confirm the results. An additional limitation is that since the majority of the subjects in the asthmatic group were individuals who died of their disease, a rare occurrence, the results may not be generalizable to more mild asthmatic patients. It should also be noted that it would be possible to have increased airway narrowing or closure by ASM contraction in asthma without having hypercontractile ASM thanks to the geometric effect of airway remodeling (248, 249). It could even be possible to have a slightly less contractile ASM cell that acts in concert with the increased ASM mass to narrow the airways more than would be expected from a less contractile muscle layer (152).

5.5 Conclusion

This study is the first to show changes in expression of previously unexplored cytoskeletal proteins that may be important in the response of the ASM to oscillatory strain. Specifically, over expression of Zyxin and Smoothelin might help explain why asthmatic subjects do not respond to deep

inspirations and the signaling pathways involved with each protein may prove to be viable targets to treat AHR. There was no significant difference in the expression of many previously explored contractile genes and this observation raises the possibility that differences between asthmatic and non-asthmatic ASM may lie within the cytoskeleton.

Chapter 6 Conclusions and Future Directions

6.1 Introduction

ASM has long been implicated in asthma (39) and through the years many different hypotheses were brought forth to explain how it may contribute to both asthma and AHR. This thesis aimed to show two things: 1) ASM possess the ability to stiffen and become hypercontractile in response to contractile agonists including acetylcholine and that this ability can act to prevent the normal dilatory responses to DIs seen in non-asthmatics. This loss of dilating effect of DIs could contribute to the development of AHR. 2) There are changes to the gene and protein networks involved in cytoskeletal reinforcement that can contribute to AHR by stiffening the ASM cell and resisting the dilatory response of DIs. The findings in this thesis suggest that no drastic changes in the contractile machinery of the ASM are necessary to induce AHR in asthma. Instead, coupling the ability of the ASM to adapt to both a shortened length and to contractile agonists with changes in the expression of proteins important in maintaining the actin cytoskeleton following oscillatory perturbations could account for some of the features of AHR including the loss of the DI induced bronchodilation similar to what is seen in the study by Chin et al. (53). It is likely a synergistic interaction between the intrinsic plasticity of the muscle to contractile agonists (termed force adaptation) and the expression changes in the cytoskeletal network that acts to further aggravate AHR and prevent the beneficial effects of DIs.

6.2 Changes in ASM following Activation: Force Adaptation and ASM Stiffening.

Force adaptation, first discussed by Bossé et al. (66) in 2009, has been suggested to be a potential player in the development of AHR in asthmatics. With the plethora of inflammatory mediators and potential contractile agonists that exist within the airways of asthmatics, it seems plausible that force adaptation could occur *in vivo*, although currently there is no research that has tested for its occurrence. The research presented in chapter two takes force adaptation from the realm of a static muscle into the realm of the dynamic airway by applying tension oscillations that mimic those seen within a breathing lung. Previous research called into question the validity of force adaptation under conditions that more closely mimicked the dynamic environment of the lung (114) however this research used length oscillations in activated tissue to mimic the breathing patterns, and as discussed in chapter two, in an activated muscle the amount of pressure that would need to be applied to the airway to get 25% strain would be unphysiologic and necessitates the use of tension oscillations, to allow the strain applied to the muscle to be dictated by the level of activation in the tissue. While it is not a

perfect model of the *in vivo* setting, we feel it is closer than the application of length oscillations to the tissue. Force adaptation may be how ASM in asthma obtains its hypercontractile phenotype and may also explain why studies, for the most part, have failed to detect increases in the force or stress that asthmatic ASM produces *ex vivo*. The increase in force gained from adaptation to baseline tone disappears when that baseline tone or its mediator (ACh for example) is removed. A further limitation of the model is that when tissues are removed from asthmatic lungs, they are removed from the inflammatory environment and so the increase in force we expect to see, if brought on by force adaptation, may disappear. Future work studying increases in asthmatic ASM stress should focus on maintaining the *in vivo* setting and could be done by incubating the strips of muscle in asthmatic serum or inflammatory mediators. Along the same line of thought, if force adaptation is the reason for the increase in force production in asthmatic ASM and if force adaptation can be induced by inflammation, then treatments that reduce inflammation in the airways should help to alleviate the effects of force adaptation. Based on our results, we would say that force adaptation can occur *in vivo* and is likely to play a role in the development of AHR.

ASM activation is also known to lead to ASM stiffening (196) and in chapter three we clearly see that the strains imposed by tension oscillations drop off steeply after ASM activation and that, when in isolation from histories of large amplitude strains, breathing maneuvers can do little to dilate contracted muscle. In fact, stiffness increase in the ASM seems to precede the development of force. Airway stiffness has become an area of increasing interest lately as a target for asthma treatment (250). It could be that ASM from asthmatics subjects is stiffer at rest or at low levels of activation, which do not result in substantial airway narrowing, and this acts to limit the effectiveness of DI's at dilating airways. Our work in chapter three also indicates that strain is the important variable in determining how effective breathing pressures are at dilating a narrowed airway. This has been known for a while when studies using length oscillations were able to relax contracted ASM (85, 111, 114) however the data from chapter three shows that very little activation is needed to significantly decrease the strain on the muscle by applied tension oscillations. This means that if we hope to treat asthma and AHR we need to make breathing maneuvers more effective and dilating the airways. Recent work has shown that a portion of ASM stiffness can be regulated by inhibiting Rho-kinase or removal of calcium (235). Other work recently has also shown that Rho-kinase is important in modulating ACh induced stiffening of airways (236). Treatment of this pathway is not currently feasible but future treatment of it may help to treat the stiffer asthmatic airways and make DIs more effective. Pairing this with current treatments that decrease ASM activation could act to synergistically make DIs more effective at dilating airways.

6.3 Deep inspirations: Bronchoprotection and Bronchodilation

In chapter three, we were able to show that increasing ASM activation limited the effectiveness of DIs to relax ASM, a phenomenon similar to the loss of bronchodilation in asthmatic subjects, but what about the loss of bronchoprotective effects of DIs in asthmatics? In chapter four we see that prior DI's act to make the muscle more compliant to subsequent stretches making them more effective at dilating the airways. This result could help explain the results seen in chapter three where a history of oscillation makes apparently small strains effective at reducing the contractile capacity of the muscle. The increased compliance of the ASM strips from the prior DIs is significant but small and only once the results are analyzed at the level of a whole lung (mathematically modeled) do we see larger, more relevant results. Many recent studies using force or pressure oscillations to mimic *in vivo* breathing oscillations (including ours in this thesis) have shown very little effect and have come to the conclusion that once the ASM is activated, there is very little that breathing can do to reverse the airway narrowing (118, 171, 189, 197). The results of our modeling work suggest that those studies may hold more promising conclusions if the results of their studies were extrapolated to the whole lung. This is often a difficult step and it is where mathematical modeling may help us better understand ASM and airway mechanics at the level of the whole lung.

The two prior chapters showed how ASM activation can lead to force adaptation and increasing stiffness of the muscle and we suggested that alterations in the stiffness of the ASM may explain the loss of DI induced bronchodilation and bronchoprotection. In chapter four, we see that changing the ASM stiffness by adaptation to shorter lengths or inducing baseline tone abolishes the effect of prior DI's on the increased compliance of the ASM and therefore, the bronchoprotective effect of these DIs. Again, our results point to the idea that if we can modulate the stiffness in the airways of asthmatics, we could return the dilating capacity or protective effects of DIs. The results from the first three research chapters suggest that the ASM can contribute to AHR without a need for changes to the phenotype of asthmatic ASM.

6.4 Changes to Phenotype of ASM Contributing to AHR

While it is possible that ASM can contribute to AHR without the need for intrinsic phenotypic changes, it is likely that there is some phenotypic change within the airways or ASM of asthmatics that make them more prone to developing AHR (251). While most research has been focused on the role of classical contractile machinery proteins like MLCK, MYH11 or actin, we saw in chapter five no evidence

for a change in the expression of these contractile proteins. There are, however, plenty of other proteins that could potentially play a role in the development of AHR including proteins involved in: cytoskeleton (252), adhesion complexes (216), and calcium handling (253). Proteins identified in our study that bind to and stabilize actin cytoskeletal filaments, such as Zyxin and Smoothelin (200, 215) could prove important in showing how increased ASM stiffness can limit the effectiveness of strains on ASM such as seen in the study by Chin et. al. (53). Coupling changes in the expression of these proteins with the changes that occur within ASM following activation could explain why DIs are not effective in dilating asthmatic airways. Studies focusing on the role of these two proteins in ASM and how they play a role in contraction are still needed but they may prove to be targets for the treatment of AHR or for the improvement in DI induced bronchodilation or bronchoprotection.

Smoothelin is a relatively unknown protein whose primary role so far has been to identify mature ASM cells or tissues. Smoothelin does appear to have a role smooth muscle function as loss of the protein in other forms of smooth muscle leads to almost a complete loss in contractile function (238). It stands to reason that over expression of a protein this essential to contractile function in smooth muscle would likely lead to some form of altered contractility. Similarly, Zyxin is a protein whose function has been known for some time in other tissues (254) but has only recently been explored for a role in ASM contractility. Loss of Zyxin seems to increase the ASMs susceptibility to oscillations, so again it stands to reason that more Zyxin would perhaps increase the resistance of ASM to oscillations. Work needs to be done to determine how over expression of these two proteins may change the muscles response to oscillation. These are studies which should be undertaken in order to grow our understanding of the role of actin binding proteins in AHR and response to oscillations.

Although we were unable to find changes to the expression of ‘classical’ contractile proteins MLCK and myosin, it is still theoretically possible to get increased ASM shortening and airway narrowing from ASM that is normally contractile. It has been discussed in this thesis that the amount of ASM surrounding the airways of asthmatics is greater than in non-asthmatics and so the cross sectional area of ASM in asthmatic airways is likely to be greater. If every ASM cell in that asthmatic bundle could contract with the same force as a non-asthmatic ASM cell, the ASM from the asthmatic would contract with a greater force without needing to produce more force per unit muscle. Add to this the geometric effects of such ASM remodeling (248), and you get a recipe for increased airway narrowing without a change in the contractile capacity of the ASM in asthma. What about if some of the ASM cells in

asthmatics were less contractile? This idea would hold true as long as the majority of the cells were still normally contractile.

It has come to light that cultured ASM cells can take on a different phenotype that has been termed the synthetic or proliferative phenotype (137). There is no current evidence of this phenotype occurring *in vivo* although it is unlikely that the contractile phenotype or the synthetic phenotypes are mutually exclusive populations of ASM tissues. It is far more likely that they exist together in some combination (255) that could lead to the increased ASM mass seen in asthma, inflammation or perhaps some form of hypercontractility. In order to measure the presence of synthetic ASM cells ASM bundle, *in situ* RNA hybridization may prove to be a useful tool. We did not measure for markers of the synthetic ASM phenotype like eotaxin or caveolin, in part because our samples contained other tissue types, but we did measure many of the contractile proteins that were suggested to be decreased in the synthetic phenotype. While we did not see significant down regulation in many of these genes, the data had a general shift towards the left with most of the genes being down regulated and we did see decreased expression of vimentin and caldesmon. This could be evidence of the synthetic phenotype existing *in vivo*, although more definitive studies are needed. If ASM tissues are a mixed population of cells consisting of contractile phenotypes and synthetic or proliferative phenotypes then it may explain how the inflammatory environment around and in the ASM band is induced and maintained. It would also lend feasibility to the idea of force adaptation in the ASM bundle of asthmatics since the mediators necessary to induce the phenomenon would be present thanks to neighboring synthetic ASM cells secreting them. If we could target and inhibit this transition towards the synthetic phenotype, we may be able to stop inflammation in the ASM bundle and inhibit the proliferation that occurs during the remodeling of the ASM layer.

6.5 Summary

In conclusion, the work from this thesis has shown that ASM hypercontractility likely results from the contribution of multiple different mechanisms. There are intrinsic muscle phenomenon, such as ASM stiffening or force adaptation, that in the context of an inflamed airway may run amok and contribute to AHR. Additionally, changes in the expression of proteins involved in actin binding, cytoskeleton dynamics or calcium handling may augment normal muscle behaviors to make them detrimental. It is also possible that a shift in the phenotype of populations of ASM within the airway towards proliferative or synthetic phenotypes may perpetuate lung inflammation. All together, the stiffening of the airway by force adaptation and contractile activation which is brought on by

inflammation (potentially from synthetic ASM cells) and changes to actin binding protein expression can act together to prevent DIs from dilating the airways as they do in non-asthmatics and can synergistically interact to induce AHR.

References

1. Government of Canada SC. Asthma, by sex, provinces and territories (Number of persons). 2013;at <http://www.statcan.gc.ca/tables-tableaux/sum-som/l01/cst01/health50a-eng.htm>. Accessed August 2014.

2. Sadatsafavi M, Lynd L, Marra C, Carleton B, Tan WC, Sullivan S, FitzGerald JM. Direct health care costs associated with asthma in British Columbia. *Can Respir J J Can Thorac Soc* 2010;17:74–80.

3. WHO | Asthma. *WHO* at <http://www.who.int/topics/asthma/en/>. Accessed August 2014.

4. James AL, Elliot JG, Jones RL, Carroll ML, Mauad T, Bai TR, Abramson MJ, McKay KO, Green FH. Airway smooth muscle hypertrophy and hyperplasia in asthma. *Am J Respir Crit Care Med* 2012;185:1058–64.

5. NAYLOR B. The shedding of the mucosa of the bronchial tree in asthma. *Thorax* 1962;17:69–72.

6. Aikawa T, Shimura S, Sasaki H, Ebina M, Takishima T. Marked goblet cell hyperplasia with mucus accumulation in the airways of patients who died of severe acute asthma attack. *Chest* 1992;101:916–921.

7. Roche WR, Beasley R, Williams JH, Holgate ST. Subepithelial fibrosis in the bronchi of asthmatics. *Lancet* 1989;1:520–524.

8. Redington AE, Howarth PH. Airway wall remodelling in asthma. *Thorax* 1997;52:310–312.

9. Woolcock AJ, Salome CM, Yan K. The shape of the dose-response curve to histamine in asthmatic and normal subjects. *Am Rev Respir Dis* 1984;130:71–5.

10. Lötvall J, Inman M, O'Byrne P. Measurement of airway hyperresponsiveness: new considerations. *Thorax* 1998;53:419–424.

11. Johnson M. Beta2-adrenoceptors: mechanisms of action of beta2-agonists. *Paediatr Respir Rev* 2001;2:57–62.

12. Cazzola M, Page CP, Calzetta L, Matera MG. Pharmacology and therapeutics of bronchodilators. *Pharmacol Rev* 2012;64:450–504.

13. Barnes PJ. Inhaled Glucocorticoids for Asthma. *N Engl J Med* 1995;332:868–875.

14. Durham A, Adcock IM, Tliba O. Steroid resistance in severe asthma: current mechanisms and future treatment. *Curr Pharm Des* 2011;17:674–684.

15. Dahlén S-E. Treatment of asthma with antileukotrienes: first line or last resort therapy? *Eur J Pharmacol* 2006;533:40–56.

16. Berger W, De Chandt MTM, Cairns CB. Zileuton: clinical implications of 5-Lipoxygenase inhibition in severe airway disease. *Int J Clin Pract* 2007;61:663–676.

17. Scow DT, Luttermoser GK, Dickerson KS. Leukotriene inhibitors in the treatment of allergy and asthma. *Am Fam Physician* 2007;75:65–70.

18. Alexander H, Paddock R. Bronchial asthma: response to pilocarpine and epinephrine. *Arch Intern Med* 1921;27:184–191.

19. Weiss S, Robb G., Ellis L. The systematic effects of histamine in man. *Arch Intern Med* 1932;49:360–396.

20. Starr I. Acetyl-[beta]-methylcholin its action on paroxysmal tachycardia and peripheral vascular disease, with a discussion of its action in other conditions.

21. Philippot DL. Asthmatic crisis produced by aerosols of carbaminolycholine in man treated by aerosols of amphetamine: study of action of these substances by determination of useful respiratory volume. *Presse Médicale* 1941;49:

22. Curry JJ. The action of histamine on the respiratory tract in normal and asthmatic subjects. *J Clin Invest* 1946;25:785–91.

23. Herxheimer HS. The effect of slow reacting substance (srs-a) in guinea pigs and asthmatic patients. *Physiol* 1962;165:

24. Mathe AA, Hedqvist P, Holmgren A, Svanborg N. Bronchial hyperreactivity to prostaglandin F 2 and histamine in patients with asthma. *Br Med J* 1973;1:193–6.

25. McNeill RS, Ingram CG. Effect of propranolol on ventilatory function. *Am J Cardiol* 1966;18:473–5.

26. Wells J RE, Walker JE, Hickler RB. Effects of cold air on respiratory air flow resistance in patients with respiratory tract disease. *New Engl J Med* 1960;263:

27. NADEL JA, SALEM H, TAMPLIN B, TOKIWA Y. Mechanism of bronchoconstriction during inhalation of sulfur dioxide. *J Appl Physiol* 1965;20:164–167.

28. Dubois AB, Dautrebande L. Acute Effects of Breathing Inert Dust Particles and of Carbachol Aerosol on Mechanical Characteristics of Lungs in Man: Changes in Response After Inhaling Sympathomimetic Aerosols. *J Clin Invest* 1958;37:1746–1755.

29. McNeill RS, Nairn JR, Millar JS, Ingram CG. Exercise-induced asthma. *Quart J Med* 1966;35:

30. De Vries K, Booij-Noord H, Goei JT, Grobler NJ, Sluiter HJ, Tammeling GJ, Orie NG. *Hyperreactivity of the bronchial tree to drugs chemical and physical agents*. The Netherlands: 1964.

31. Parker CD, Bilbo RE, Reed CE. Methacholine aerosol as test for bronchial asthma. *Arch Intern Med* 1965;115:452–458.

32. Simonsson BG. Clinical and Physiological Studies on Chronic Bronchitis. *Allergy* 1965;20:325–348.

33. Woolcock AJ, Anderson SD, Peat JK, Du Toit JI, Zhang YG, Smith CM, Salome CM. Characteristics of bronchial hyperresponsiveness in chronic obstructive pulmonary disease and in asthma. *Am Rev Respir Dis* 1991;143:1438–1443.

34. Moore BJ, Hilliam CC, Verburgt LM, Wiggs BR, Vedal S, Paré PD. Shape and position of the complete dose-response curve for inhaled methacholine in normal subjects. *Am J Respir Crit Care Med* 1996;154:642–648.

35. De Vries K, Goei JT, Booy-Noord H, Orie NG. Changes during 24 hours in the lung function and histamine hyperreactivity of the bronchial tree in asthmatic and bronchitic patients. *Int Arch Allergy Appl Immunol* 1962;20:93–101.

36. Kerrebijin KF, Orie NG., Lende van der R. *Endogenous factors in childhood (NSLD: methodological aspects in population studies) in Bronchitis*. Roayl VanGorcum: 1970.

37. Cockcroft DW, Ruffin RE, Dolovich J, Hargreave FE. Allergen-induced increase in non-allergic bronchial reactivity. *Clin Allergy* 1977;7:503–13.

38. Juniper EF, Frith PA, Hargreave FE. Long-term stability of bronchial responsiveness to histamine. *Thorax* 1982;37:288–91.

39. Floyer SJ. *A treatise of the asthma divided into four parts*. 1698.

40. HH S. *On Asthma: Its pathology and treatment.* John Churchill; 1859.

41. HL KK. The pathology of bronchial asthma. *Archs Intern Med* 1922;30:

42. Schild HO, Hawkins DF, Mongar JL, Herxheimer H. Reactions of isolated human asthmatic lung and bronchial tissue to a specific antigen; histamine release and muscular contraction. *Lancet* 1951;2:376–82.

43. Benson MK. Bronchial hyperreactivity. *Br J Chest* 1975;69:227–39.

44. Benson MK. Proceedings: The influence of bronchomotor tone on bronchial reactivity. *Clin Sci Mol Med* 1974;47:13P.

45. Simonsson BG, Jacobs FM, Nadel JA. Role of autonomic nervous system and the cough reflex in the increased responsiveness of airways in patients with obstructive airway disease. *J Clin Invest* 1967;46:1812–1818.

46. Szentivanyi A. The beta adrenergic theory of the atopic abnormality in bronchial asthma. *J Allergy* 1968;42:203–232.

47. Freedman BJ. The functional geometry of the bronchi. The relationship between changes in external diameter and calibre, and a consideration of the passive role played by the mucosa in bronchoconstriction. *Bull Physiopathol Respir Nancy* 1972;8:545–52.

48. Bai TR. Abnormalities in airway smooth muscle in fatal asthma. *Am Rev Respir Dis* 1990;141:552–7.

49. Bramley AM, Thomson RJ, Roberts CR, Schellenberg RR. Hypothesis: excessive bronchoconstriction in asthma is due to decreased airway elastance. *Eur Respir J* 1994;7:337–41.

50. Bai TR. Abnormalities in airway smooth muscle in fatal asthma. A comparison between trachea and bronchus. *Am Rev Respir Dis* 1991;143:441–3.

51. Cerrina J, Le Ladurie MR, Labat C, Raffestin B, Bayol A, Brink C. Comparison of human bronchial muscle responses to histamine in vivo with histamine and isoproterenol agonists in vitro. *Am Rev Respir Dis* 1986;134:57–61.

52. Cerrina J, Labat C, Haye-Legrande I, Raffestin B, Benveniste J, Brink C. Human isolated bronchial muscle preparations from asthmatic patients: effects of indomethacin and contractile agonists. *Prostaglandins* 1989;37:457–69.

53. Chin LY, Bosse Y, Pascoe CD, Hackett TL, Seow CY, Pare PD. Mechanical properties of asthmatic airway smooth muscle. *Eur Respir J* 2012;40:45–54.

54. Whicker SD, Armour CL, Black JL. Responsiveness of bronchial smooth muscle from asthmatic patients to relaxant and contractile agonists. *Pulm Pharmacol* 1988;1:25–31.

55. Moreno RH, Hogg JC, Pare PD. Mechanics of airway narrowing. *Am Rev Respir Dis* 1986;133:1171–80.

56. James AL, Pare PD, Hogg JC. The mechanics of airway narrowing in asthma. *Am Rev Respir Dis* 1989;139:242–6.

57. Wiggs BR, Bosken C, Pare PD, James A, Hogg JC. A model of airway narrowing in asthma and in chronic obstructive pulmonary disease. *Am Rev Respir Dis* 1992;145:1251–8.

58. Lambert RK, Wiggs BR, Kuwano K, Hogg JC, Pare PD. Functional significance of increased airway smooth muscle in asthma and COPD. *J Appl Physiol* 1993;74:2771–81.

59. Oliver MN, Fabry B, Marinkovic A, Mijailovich SM, Butler JP, Fredberg JJ. Airway hyperresponsiveness, remodeling, and smooth muscle mass: right answer, wrong reason? *Am J Respir Cell Mol Biol* 2007;37:264–72.

60. Ma X, Cheng Z, Kong H, Wang Y, Unruh H, Stephens NL, Laviolette M. Changes in biophysical and biochemical properties of single bronchial smooth muscle cells from asthmatic subjects. *Am J Physiol Lung Cell Mol Physiol* 2002;283:L1181–9.

61. Léguillette R, Laviolette M, Bergeron C, Zitouni N, Kogut P, Solway J, Kachmar L, Hamid Q, Lauzon A-M. Myosin, Transgelin, and Myosin Light Chain Kinase. *Am J Respir Crit Care Med* 2009;179:194–204.

62. Bosse Y, Sobieszek A, Pare PD, Seow CY. Length adaptation of airway smooth muscle. 2008;5:62–7.

63. Wang L, Paré PD, Seow CY. Selected Contribution: Effect of chronic passive length change on airway smooth muscle length-tension relationship. *J Appl Physiol* 2001;90:734–740.

64. Pratusevich VR, Seow CY, Ford LE. Plasticity in canine airway smooth muscle. *J Gen Physiol* 1995;105:73–94.

65. Bossé Y, Chapman DG, Paré PD, King GG, Salome CM. A “Good” muscle in a “Bad” environment: the importance of airway smooth muscle force adaptation to airway hyperresponsiveness. *Respir Physiol Neurobiol* 2011;179:269–75.

66. Bossé Y, Chin LY, Paré PD, Seow CY. Adaptation of airway smooth muscle to basal tone: relevance to airway hyperresponsiveness. *Am J Respir Cell Mol Biol* 2009;40:13–8.

67. Webb RC. Smooth Muscle Contraction and Relaxation. *Adv Physiol Educ* 2003;27:201.

68. Schittny JC, Miserocchi G, Sparrow MP. Spontaneous peristaltic airway contractions propel lung liquid through the bronchial tree of intact and fetal lung explants. *Am J Respir Cell Mol Biol* 2000;23:11–18.

69. Mitzner W. Airway Smooth Muscle. *Am J Respir Crit Care Med* 2004;169:787–790.

70. Lei M, Ghezzo H, Chen MF, Eidelman DH. Airway smooth muscle orientation in intraparenchymal airways. *J Appl Physiol Bethesda Md 1985* 1997;82:70–77.

71. Barnes PJ. Autonomic Pharmacology of the Airways. *Pharmacology of the Respiratory Tract* 1993;67:

72. Chung KF, Barnes PJ. Role of inflammatory mediators in asthma. *Br Med Bull* 1992;48:135–148.

73. Floreani AA, Rennard SI. Experimental treatments for asthma. *Curr Opin Pulm Med* 1997;3:30–41.

74. Barnes PJ, Chung KF, Page CP. Inflammatory Mediators. *Pharmacol Rev* 1991;

75. Hynes TR, Block SM, White BT, Spudich JA. Movement of myosin fragments in vitro: domains involved in force production. *Cell* 1987;48:953–963.

76. Kureishi Y, Kobayashi S, Amano M, Kimura K, Kanaide H, Nakano T, Kaibuchi K, Ito M. Rho-associated Kinase Directly Induces Smooth Muscle Contraction through Myosin Light Chain Phosphorylation. *J Biol Chem* 1997;272:12257–12260.

77. Dimopoulos GJ, Semba S, Kitazawa K, Eto M, Kitazawa T. Ca2+-Dependent Rapid Ca2+ Sensitization of Contraction in Arterial Smooth Muscle. *Circ Res* 2007;100:121–129.

78. Csapo AI. Smooth muscle as a contractile unit. *Physiol Rev Suppl* 1962;5:7–33.

79. Stephens NL, Kroeger E, Mehta JA. Force-velocity characteristics of respiratory airway smooth muscle. *J Appl Physiol* 1969;26:685–92.

80. Kuo KH, Herrera AM, Wang L, Pare PD, Ford LE, Stephens NL, Seow CY. Structure-function correlation in airway smooth muscle adapted to different lengths. *Am J Physiol Cell Physiol* 2003;285:C384–90.

81. Herrera AM, McParland BE, Bienkowska A, Tait R, Pare PD, Seow CY. "Sarcomeres" of smooth muscle: functional characteristics and ultrastructural evidence. *J Cell Sci* 2005;118:2381–92.

82. Stephens NL, Van Niekerk W. Isometric and isotonic contractions in airway smooth muscle. *Can J Physiol Pharmacol* 1977;55:833–838.

83. Gunst SJ, Meiss RA, Wu MF, Rowe M. Mechanisms for the mechanical plasticity of tracheal smooth muscle. *Am J Physiol* 1995;268:C1267–1276.

84. Liu JC-Y, Rottler J, Wang L, Zhang J, Pascoe CD, Lan B, Norris BA, Herrera AM, Paré PD, Seow CY. Myosin filaments in smooth muscle cells do not have a constant length. *J Physiol* 2013;1–48.doi:10.1113/jphysiol.2013.264168.

85. Wang L, Paré PD, Seow CY. Effects of length oscillation on the subsequent force development in swine tracheal smooth muscle. *J Appl Physiol Bethesda Md 1985* 2000;88:2246–50.

86. McParland BE, Tait RR, Pare PD, Seow CY. The role of airway smooth muscle during an attack of asthma simulated in vitro. *Am J Respir Cell Mol Biol* 2005;33:500–4.

87. Oliven A, Supinski GS, Kelsen SG. Functional adaptation of diaphragm to chronic hyperinflation in emphysematous hamsters. *J Appl Physiol Bethesda Md 1985* 1986;60:225–231.

88. Farkas GA, Roussos C. Diaphragm in emphysematous hamsters: sarcomere adaptability. *J Appl Physiol* 1983;54:1635–1640.

89. Kelsen SG, Wolanski T, Supinski GS, Roessmann U. The effect of elastase-induced emphysema on diaphragmatic muscle structure in hamsters. *Am Rev Respir Dis* 1983;127:330–334.

90. Shrager JB, Kim D-K, Hashmi YJ, Stedman HH, Zhu J, Kaiser LR, Levine S. Sarcomeres are added in series to emphysematous rat diaphragm after lung volume reduction surgery. *Chest* 2002;121:210–215.

91. Naghshin J, Wang L, Pare PD, Seow CY. Adaptation to chronic length change in explanted airway smooth muscle. *J Appl Physiol* 2003;95:448–53; discussion 435.

92. Pascoe CD, Jiao Y, Seow CY, Pare PD, Bosse Y. Force Oscillations Simulating Breathing Maneuvers do not Prevent Force Adaptation. *Am J Respir Cell Mol Biol* 2012;doi:10.1165/rcmb.2011-0429OC.

93. Fish JE, Peterman VI, Cugell DW. Effect of deep inspiration on airway conductance in subjects with allergic rhinitis and allergic asthma. *J Allergy Clin Immunol* 1977;60:41–46.

94. Fish JE, Kehoe TJ, Cugell DW. Effect of deep inspiration on maximum expiratory flow rates in asthmatic subjects. *Respir Int Rev Thorac Dis* 1978;36:57–63.

95. Skloot G, Permutt S, Togias A. Airway hyperresponsiveness in asthma: a problem of limited smooth muscle relaxation with inspiration. *J Clin Invest* 1995;96:2393–403.

96. Wang L, Pare PD. Deep inspiration and airway smooth muscle adaptation to length change. 2003;137:169–78.

97. Skloot G, Togias A. Bronchodilation and bronchoprotection by deep inspiration and their relationship to bronchial hyperresponsiveness. *Clin Rev Allergy Immunol* 2003;24:55–71.

98. Shen X, Wu MF, Tepper RS, Gunst SJ. Mechanisms for the mechanical response of airway smooth muscle to length oscillation. *J Appl Physiol* 1997;83:731–8.

99. Fredberg JJ, Inouye DS, Mijailovich SM, Butler JP. Perturbed equilibrium of myosin binding in airway smooth muscle and its implications in bronchospasm. *Am J Respir Crit Care Med* 1999;159:959–67.

100. Lim TK, Pride NB, Ingram RH Jr. Effects of volume history during spontaneous and acutely induced air-flow obstruction in asthma. *Am Rev Respir Dis* 1987;135:591–596.

101. Gayrard P, Orehek J, Grimaud C, Charpin J. Bronchoconstrictor effects of a deep inspiration in patients with asthma. *Am Rev Respir Dis* 1975;111:433–9.

102. Malmberg P, Larsson K, Sundblad BM, Zhiping W. Importance of the time interval between FEV1 measurements in a methacholine provocation test. *Eur Respir J* 1993;6:680–6.

103. Moore BJ, Verburgt LM, King GG, Paré PD. The effect of deep inspiration on methacholine dose-response curves in normal subjects. *Am J Respir Crit Care Med* 1997;156:1278–81.

104. Shen X, Gunst SJ, Tepper RS. Effect of timing of deep inspiration on airway response to methacholine challenge in mature and immature rabbits. *Am J Respir Crit Care Med* 1999;159:959–967.

105. Chandy DC-BR, Schachter EN, Skloot GS. Differences between the bronchoprotective effect of fast and slow deep inspiration. *Am J Respir Crit Care Med* 1999;159:

106. Scichilone N, Kapsali T, Permutt S, Togias A. Deep inspiration-induced bronchoprotection is stronger than bronchodilation. *Am J Respir Crit Care Med* 2000;162:910–6.

107. Scichilone N, Permutt S, Togias A. The lack of the bronchoprotective and not the bronchodilatory ability of deep inspiration is associated with airway hyperresponsiveness. *Am J Respir Crit Care Med* 2001;163:413–9.

108. Kapsali T, Permutt S, Laube B, Scichilone N, Togias A. Potent bronchoprotective effect of deep inspiration and its absence in asthma. *jap.physiology.org* 2000;89:711–720.

109. Brown RH, Scichilone N, Mudge B, Diemer FB, Permutt S, Togias A. High-resolution computed tomographic evaluation of airway distensibility and the effects of lung inflation on airway caliber in healthy subjects and individuals with asthma. *Am J Respir Crit Care Med* 2001;163:994–1001.

110. Jensen A, Atileh H, Suki B, Ingenito EP, Lutchen KR. Selected contribution: airway caliber in healthy and asthmatic subjects: effects of bronchial challenge and deep inspirations. *J Appl Physiol* 2001;91:506–15; discussion 504–5.

111. Fredberg JJ, Inouye D, Miller B, Nathan M, Jafari S, Raboudi SH, Butler JP, Shore SA. Airway smooth muscle, tidal stretches, and dynamically determined contractile states. *Am J Respir Crit Care Med* 1997;156:1752–9.

112. Wang L, Chitano P, Murphy TM. Length oscillation induces force potentiation in infant guinea pig airway smooth muscle. *Am J Physiol Lung Cell Mol Physiol* 2005;289:L909–15.

113. Weist A, Williams T, Kisling J, Clem C, Tepper RS. Volume history and effect on airway reactivity in infants and adults. *J Appl Physiol* 2002;93:1069–74.

114. Raqeeb A, Solomon D, Paré PD, Seow CY. Length oscillation mimicking periodic individual deep inspirations during tidal breathing attenuates force recovery and adaptation in airway smooth muscle. *J Appl Physiol* 2010;109:1476–1482.

115. LaPrad AS, West AR, Noble PB, Lutchen KR, Mitchell HW. Maintenance of airway caliber in isolated airways by deep inspiration and tidal strains. *J Appl Physiol* 2008;105:479–85.

116. Noble PB, McFawn PK, Mitchell HW. Responsiveness of the isolated airway during simulated deep inspirations: effect of airway smooth muscle stiffness and strain. *J Appl Physiol* 2007;103:787–95.

117. Noble PB, Jones RL, Needi ET, Cairncross A, Mitchell HW, James AL, McFawn PK. Responsiveness of the human airway in vitro during deep inspiration and tidal oscillation. *J Appl Physiol* 2011;110:1510–8.

118. LaPrad AS, Szabo TL, Suki B, Lutchen KR. Tidal stretches do not modulate responsiveness of intact airways in vitro. *J Appl Physiol* 2010;109:295–304.

119. King GG, Moore BJ, Seow CY, Pare PD. Time course of increased airway narrowing caused by inhibition of deep inspiration during methacholine challenge. *Am J Respir Crit Care Med* 1999;160:454–7.

120. King GG, Moore BJ, Seow CY, Pare PD. Airway narrowing associated with inhibition of deep inspiration during methacholine inhalation in asthmatics. *Am J Respir Crit Care Med* 2001;164:216–8.

121. Chapman DG, Berend N, King GG, McParland BE, Salome CM. Deep inspirations protect against airway closure in nonasthmatic subjects. *J Appl Physiol* 2009;107:564–9.

122. Crimi E, Pellegrino R, Milanese M, Brusasco V. Deep breaths, methacholine, and airway narrowing in healthy and mild asthmatic subjects. *J Appl Physiol* 2002;93:1384–90.

123. Slats AM, Janssen K, van Schadewijk A, van der Plas DT, Schot R, van den Aardweg JG, de Jongste JC, Hiemstra PS, Mauad T, Rabe KF, Sterk PJ. Bronchial inflammation and airway responses to deep inspiration in asthma and chronic obstructive pulmonary disease. *Am J Respir Crit Care Med* 2007;176:121–8.

124. Wong RS, Larcombe AN, Fernandes LB, Zosky GR, Noble PB. The mechanism of deep inspiration-induced bronchoprotection: evidence from a mouse model. *Eur Respir J* 2012;40:982–9.

125. Kuo KH, Wang L, Pare PD, Ford LE, Seow CY. Myosin thick filament lability induced by mechanical strain in airway smooth muscle. *J Appl Physiol* 2001;90:1811–6.

126. Sellers JR, Spudich JA, Sheetz MP. Light chain phosphorylation regulates the movement of smooth muscle myosin on actin filaments. *J Cell Biol* 1985;101:1897–1902.

127. Woodruff PG, Dolganov GM, Ferrando RE, Donnelly S, Hays SR, Solberg OD, Carter R, Wong HH, Cadbury PS, Fahy JV. Hyperplasia of smooth muscle in mild to moderate asthma without changes in cell size or gene expression. *Am J Respir Crit Care Med* 2004;169:1001–6.

128. Rovner AS, Thompson MM, Murphy RA. Two different heavy chains are found in smooth muscle myosin. *Am J Physiol* 1986;250:C861–870.

129. Babij P, Kelly C, Periasamy M. Characterization of a mammalian smooth muscle myosin heavy-chain gene: complete nucleotide and protein coding sequence and analysis of the 5’ end of the gene. *Proc Natl Acad Sci U S A* 1991;88:10676–10680.

130. Rovner AS, Freyzon Y, Trybus KM. An insert in the motor domain determines the functional properties of expressed smooth muscle myosin isoforms. *J Muscle Res Cell Motil* 1997;18:103–110.

131. Jarai G, Sukkar M, Garrett S, Duroudier N, Westwick J, Adcock I, Chung KF. Effects of interleukin-1beta, interleukin-13 and transforming growth factor-beta on gene expression in human airway smooth muscle using gene microarrays. *Eur J Pharmacol* 2004;497:255–265.

132. Lee JH, Kaminski N, Dolganov G, Grunig G, Koth L, Solomon C, Erle DJ, Sheppard D. Interleukin-13 induces dramatically different transcriptional programs in three human airway cell types. *Am J Respir Cell Mol Biol* 2001;25:474–485.

133. Syed F, Panettieri RA Jr, Tliba O, Huang C, Li K, Bracht M, Amegadzie B, Griswold D, Li L, Amrani Y. The effect of IL-13 and IL-13R130Q, a naturally occurring IL-13 polymorphism, on the gene expression of human airway smooth muscle cells. *Respir Res* 2005;6:9.

134. McKay S, Hirst SJ, Haas MB, de Jongste JC, Hoogsteden HC, Saxena PR, Sharma HS. Tumor necrosis factor-alpha enhances mRNA expression and secretion of interleukin-6 in cultured human airway smooth muscle cells. *Am J Respir Cell Mol Biol* 2000;23:103–111.

135. Hakonarson H, Maskeri N, Carter C, Grunstein MM. Regulation of TH1- and TH2-type cytokine expression and action in atopic asthmatic sensitized airway smooth muscle. *J Clin Invest* 1999;103:1077–1087.

136. Woodruff PG. Gene expression in asthmatic airway smooth muscle. *Proc Am Thorac Soc* 2008;5:113.

137. Halayko AJ, Salari H, Ma X, Stephens NL. Markers of airway smooth muscle cell phenotype. *Am J Physiol* 1996;270:L1040–1051.

138. Ma X, Wang Y, Stephens NL. Serum deprivation induces a unique hypercontractile phenotype of cultured smooth muscle cells. *Am J Physiol - Cell Physiol* 1998;274:C1206–C1214.

139. Halayko AJ, Camoretti-Mercado B, Forsythe SM, Vieira JE, Mitchell RW, Wylam ME, Hershenson MB, Solway J. Divergent differentiation paths in airway smooth muscle culture: induction of functionally contractile myocytes. *Am J Physiol* 1999;276:L197.

140. Wjst M, Sargurupremraj M, Arnold M. Genome-wide association studies in asthma: what they really told us about pathogenesis. *Curr Opin Allergy Clin Immunol* 2013;13:112–118.

141. Van Eerdewegh P, Little RD, Dupuis J, del Mastro RG, Falls K, Simon J, Torrey D, Pandit S, McKenny J, Braunschweiger K, Walsh A, Liu Z, Hayward B, Folz C, Manning SP, Bawa A, Saracino L, Thackston M, Benchekroun Y, Capparell N, Wang M, Adair R, Feng Y, Dubois J, FitzGerald MG, Huang H, Gibson R, Allen KM, Pedan A, *et al.* Association of the ADAM33 gene with asthma and bronchial hyperresponsiveness. *Nature* 2002;418:426.

142. Haitchi HM, Powell RM, Shaw TJ, Howarth PH, Wilson SJ, Wilson DI, Holgate ST, Davies DE. ADAM33 expression in asthmatic airways and human embryonic lungs. *Am J Respir Crit Care Med* 2005;171:958–965.

143. Pascoe CD, Seow CY, Paré PD, Bossé Y. Decrease of airway smooth muscle contractility induced by simulated breathing maneuvers is not simply proportional to strain. *J Appl Physiol* 2013;1–10.

144. Kesler BS, Mazzone SB, Canning BJ. Nitric oxide-dependent modulation of smooth-muscle tone by airway parasympathetic nerves. *Am J Respir Crit Care Med* 2002;165:481–488.

145. White J, Eiser NM. The role of histamine and its receptors in the pathogenesis of asthma. *Br J Chest* 1983;77:215–26.

146. Lam S, Chan H, LeRiche JC, Chan-Yeung M, Salari H. Release of leukotrienes in patients with bronchial asthma. *J Allergy Clin Immunol* 1988;81:711–7.

147. Mattoli S, Soloperto M, Marini M, Fasoli A. Levels of endothelin in the bronchoalveolar lavage fluid of patients with symptomatic asthma and reversible airflow obstruction. *J Allergy Clin Immunol* 1991;88:376–84.

148. Murray JJ, Tonnel AB, Brash AR, Roberts LJ, Gosset P, Workman R, Capron A, Oates JA. Release of prostaglandin D2 into human airways during acute antigen challenge. *N Engl J Med* 1986;315:800–4.

149. Bossé Y, Chin LY, Paré PD, Seow CY. Chronic activation in shortened airway smooth muscle: a synergistic combination underlying airway hyperresponsiveness? *Am J Respir Cell Mol Biol* 2010;42:341–8.

150. Gump A, Haughney L, Fredberg J. Relaxation of activated airway smooth muscle: relative potency of isoproterenol vs. tidal stretch. *J Appl Physiol Bethesda Md 1985* 2001;90:2306–2310.

151. Gunst SJ. Contractile force of canine airway smooth muscle during cyclical length changes. *J Appl Physiol* 1983;55:759–769.

152. Wiggs BR, Moreno R, Hogg JC, Hilliam C, Paré PD. A model of the mechanics of airway narrowing. *J Appl Physiol* 1990;69:849–860.

153. Lambert RK, Wilson TA, Hyatt RE, Rodarte JR. A computational model for expiratory flow. *J Appl Physiol* 1982;52:44–56.

154. Kuwano K, Bosken CH, Pare PD, Bai TR, Wiggs BR, Hogg JC. Small airways dimensions in asthma and in chronic obstructive pulmonary disease. *Am Rev Respir Dis* 1993;148:1220–5.

155. Brown RH, Kaczka DW, Mitzner W. Effect of parenchymal stiffness on canine airway size with lung inflation. *PloS One* 2010;5:e10332.

156. Bosse Y, D. Pare P. Airway Smooth Muscle Responsiveness: The Origin of Airway Hyperresponsiveness in Asthma? *Curr Respir Med Rev* 2011;7:289–301.

157. Mitchell HW, Gray PR. Uncoupling in the wall of the cartilaginous bronchus of the pig produced by smooth muscle contraction. *Pulm Pharmacol* 1996;9:29–34.

158. Saez AM, Schellenberg RR, Ludwig MS, Meiss RA, Paré PD. Tissue elastance influences airway smooth muscle shortening: comparison of mechanical properties among different species. *Can J Physiol Pharmacol* 2002;80:865–71.

159. Mauad T, Silva LFF, Santos MA, Grinberg L, Bernardi FDC, Martins MA, Saldiva PHN, Dolhnikoff M. Abnormal alveolar attachments with decreased elastic fiber content in distal lung in fatal asthma. *Am J Respir Crit Care Med* 2004;170:857–862.

160. Paré PD, Bai TR. The consequences of chronic allergic inflammation. *Thorax* 1995;50:328–332.

161. Raboudi SH, Miller B, Butler JP, Shore SA, Fredberg JJ. Dynamically Determined Contractile States of Airway Smooth Muscle. *Am J Respir Crit Care Med* 1998;158:S176–S178.

162. Pyrgos G, Scichilone N, Togias A, Brown RH, Pyrgos G, Scichilone N, Togias A, Brown RH. Bronchodilation response to deep inspirations in asthma is dependent on airway distensibility and air trapping. *J Appl Physiol* 2011;110:472–479.

163. Bosse Y, Pare P, Bosse Y. Airway Smooth Muscle in Asthma Symptoms: Culprit but Maybe Innocent. In: Irusen E, editor. *Lung Dis - Sel State Art Rev* InTech; 2012. at <http://www.intechopen.com/books/lung-diseases-selected-state-of-the-art-reviews/airway-smooth-muscle-in-asthma-symptoms-culprit-but-maybe-innocent>.

164. Saxena H, Deshpande D, Tiegs B, Yan H, Battafarano R, Burrows W, Damera G, Panettieri R, DuBose Jr T, An S, Penn R. The GPCR OGR1 (GPR68) mediates diverse signalling and contraction of airway smooth muscle in response to small reductions in extracellular pH. *Br J Pharmacol* 2012;166:981–990.

165. Dowell ML, Lavoie TL, Lakser OJ, Dulin NO, Fredberg JJ, Gerthoffer WT, Seow CY, Mitchell RW, Solway J. MEK modulates force-fluctuation-induced relengthening of canine tracheal smooth muscle. *Eur Respir J* 2010;36:630–7.

166. Latourelle J, Fabry B, Fredberg JJ. Dynamic equilibration of airway smooth muscle contraction during physiological loading. *J Appl Physiol* 2002;92:771–779.

167. Lavoie TL, Dowell ML, Lakser OJ, Gerthoffer WT, Fredberg JJ, Seow CY, Mitchell RW, Solway J. Disrupting actin-myosin-actin connectivity in airway smooth muscle as a treatment for asthma? 2009;6:295–300.

168. Mitchell RW, Dowell ML, Solway J, Lakser OJ. Force Fluctuation–induced Relengthening of Acetylcholine-contracted Airway Smooth Muscle. *Proc Am Thorac Soc* 2008;5:68–72.

169. Chin LY, Bosse Y, Jiao Y, Solomon D, Hackett TL, Pare PD, Seow CY. Human airway smooth muscle is structurally and mechanically similar to that of other species. *Eur Respir J* 2010;36:170–7.

170. Noble PB, Hernandez JM, Mitchell HW, Janssen LJ. Deep inspiration and airway physiology: human, canine, porcine, or bovine? *J Appl Physiol* 2010;109:938–939.

171. Lavoie TL, Krishnan R, Siegel HR, Maston ED, Fredberg JJ, Solway J, Dowell ML. Dilatation of the Constricted Human Airway by Tidal Expansion of Lung Parenchyma. *Am J Respir Crit Care Med* 2012;1–8.doi:10.1164/rccm.201202-0368OC.

172. Fredberg JJ. Airway narrowing in asthma: does speed kill? *Am J Physiol - Lung Cell Mol Physiol* 2002;283:L1179–L1180.

173. Zhang W, Gunst SJ. Interactions of Airway Smooth Muscle Cells with Their Tissue Matrix. *Proc Am Thorac Soc* 2008;5:32–39.

174. Salerno FG, Pellegrino R, Trocchio G, Spanevello A, Brusasco V, Crimi E. Attenuation of induced bronchoconstriction in healthy subjects: effects of breathing depth. *J Appl Physiol* 2005;98:817–821.

175. Milanese M, Saporiti R, Bartolini S, Pellegrino R, Baroffio M, Brusasco V, Crimi E. Bronchodilator effects of exercise hyperpnea and albuterol in mild-to-moderate asthma. *J Appl Physiol* 2009;107:494–499.

176. Crimi E, Pellegrino R, Smeraldi A, Brusasco V. Exercise-induced bronchodilation in natural and induced asthma: effects on ventilatory response and performance. *J Appl Physiol* 2002;92:2353–2360.

177. Noble PB, McFawn PK, Mitchell HW. Intraluminal pressure oscillation enhances subsequent airway contraction in isolated bronchial segments. *J Appl Physiol* 2004;96:1161–1165.

178. Chapman DG, Brown NJ, Salome CM. The dynamic face of respiratory research: understanding the effect of airway disease on a lung in constant motion. *Pulm Pharmacol Ther* 2011;24:505–512.

179. Orehek J, Charpin D, Velardocchio JM, Grimaud C. Bronchomotor effect of bronchoconstriction-induced deep inspirations in asthmatics. *Am Rev Respir Dis* 1980;121:297–305.

180. Bai TR, Bates JHT, Brusasco V, Camoretti-Mercado B, Chitano P, Deng LH, Dowell M, Fabry B, Ford LE, Fredberg JJ, Gerthoffer WT, Gilbert SH, Gunst SJ, Hai C-M, Halayko AJ, Hirst SJ, James AL, Janssen LJ, Jones KA, King GG, Lakser OJ, Lambert RK, Lauzon A-M, Lutchen KR, Maksym GN, Meiss RA, Mijailovich SM, Mitchell HW, Mitchell RW, *et al.* On the terminology for describing the length-force relationship and its changes in airway smooth muscle. *J Appl Physiol* 2004;97:2029–2034.

181. Gunst SJ, Wu M-F. Selected Contribution: Plasticity of airway smooth muscle stiffness and extensibility: role of length-adaptive mechanisms. *J Appl Physiol* 2001;90:741–749.

182. Tawhai MH, Nash MP, Hoffman EA. An imaging-based computational approach to model ventilation distribution and soft-tissue deformation in the ovine lung. *Acad Radiol* 2006;13:113–120.

183. Donovan GM, Kritter T. Spatial pattern formation in the lung. *J Math Biol* 2014;doi:10.1007/s00285-014-0792-9.

184. Donovan GM, Sneyd J, Tawhai MH. The importance of synergy between deep inspirations and fluidization in reversing airway closure. *PloS One* 2012;7:e48552.

185. Politi AZ, Donovan GM, Tawhai MH, Sanderson MJ, Lauzon A-M, Bates JHT, Sneyd J. A multiscale, spatially distributed model of asthmatic airway hyper-responsiveness. *J Theor Biol* 2010;266:614–624.

186. Affonce DA, Lutchen KR. New perspectives on the mechanical basis for airway hyperreactivity and airway hypersensitivity in asthma. *J Appl Physiol* 2006;101:1710–1719.

187. Anafi RC, Wilson TA. Airway stability and heterogeneity in the constricted lung. *J Appl Physiol* 2001;91:1185–1192.

188. Venegas JG, Winkler T, Musch G, Vidal Melo MF, Layfield D, Tgavalekos N, Fischman AJ, Callahan RJ, Bellani G, Scott Harris R. Self-organized patchiness in asthma as a prelude to catastrophic shifts. *Nature* 2005;434:777–782.

189. Harvey BC, Parameswaran H, Lutchen KR. Can tidal breathing with deep inspirations of intact airways create sustained bronchoprotection or bronchodilation? *J Appl Physiol* 2013;115:436–45.

190. Noble PB, Jones RL, Cairncross A, Elliot JG, Mitchell HW, James AL, McFawn PK. Airway narrowing and bronchodilation to deep inspiration in bronchial segments from subjects with and without reported asthma. *J Appl Physiol* 2013;114:1460–1471.

191. Brown RH, Mitzner W. Airway response to deep inspiration: role of nitric oxide. *Eur Respir J* 2003;22:57–61.

192. Copland IB, Reynaud D, Pace-Asciak C, Post M. Mechanotransduction of stretch-induced prostanoid release by fetal lung epithelial cells. *Am J Physiol Lung Cell Mol Physiol* 2006;291:L487–495.

193. Piper P, Vane J. The Release of Prostaglandins from Lung and Other Tissues. *Ann N Y Acad Sci* 1971;180:363–385.

194. Bosse Y, Pare PD. Histamine And Endogenously Produced Spasmogenic Prostaglandins Increase The Strength Of Airway Smooth Muscle. *J Allergy Clin Immunol* 2012;129:Abstract 52.

195. Bossé Y, Solomon D, Chin LYM, Lian K, Paré PD, Seow CY. Increase in passive stiffness at reduced airway smooth muscle length: potential impact on airway responsiveness. *Am J Physiol Lung Cell Mol Physiol* 2010;298:L277–287.

196. Hubmayr RD, Shore SA, Fredberg JJ, Planus E, Panettieri RA, Moller W, Heyder J, Wang N. Pharmacological activation changes stiffness of cultured human airway smooth muscle cells. *Am J Physiol* 1996;271:C1660–1668.

197. Ansell TK, McFawn PK, Mitchell HW, Noble PB. Bronchodilatory response to deep inspiration in bronchial segments: the effects of stress vs. strain. *J Appl Physiol* 2013;115:505–13.

198. Brown NJ, Salome CM, Berend N, Thorpe CW, King GG. Airway distensibility in adults with asthma and healthy adults, measured by forced oscillation technique. *Am J Respir Crit Care Med* 2007;176:129–137.

199. Johns DP, Wilson J, Harding R, Walters EH. Airway distensibility in healthy and asthmatic subjects: effect of lung volume history. *J Appl Physiol* 2000;88:1413–1420.

200. Rosner SR, Blankman E, Jensen CC, Krishnan R, Beckerle MC, Fredberg JJ, Smith M. Bronchospasm, Deep Inspirations And The Paradoxical Role Of Zyxin. American Thoracic Society; 2014. p. A3667–A3667.

201. Laube BL, Norman PS, Adams III GK. The effect of aerosol distribution on airway responsiveness to inhaled methacholine in patients with asthma. *J Allergy Clin Immunol* 1992;89:510–518.

202. Lippmann M. Regional Deposition of Particles in the Human Respiratory Tract. *Compr Physiol* John Wiley & Sons, Inc.; 2010. at <http://onlinelibrary.wiley.com/doi/10.1002/cphy.cp090114/abstract>.

203. Lai-Fook SJ. A continuum mechanics analysis of pulmonary vascular interdependence in isolated dog lobes. *J Appl Physiol* 1979;46:419–429.

204. Lambert RK, Wilson TA. Smooth muscle dynamics and maximal expiratory flow in asthma. *J Appl Physiol* 2005;99:1885–1890.

205. Moffatt MF, Kabesch M, Liang L, Dixon AL, Strachan D, Heath S, Depner M, von Berg A, Bufe A, Rietschel E, Heinzmann A, Simma B, Frischer T, Willis-Owen SA, Wong KC, Illig T, Vogelberg C, Weiland SK, von Mutius E, Abecasis GR, Farrall M, Gut IG, Lathrop GM, Cookson WO. Genetic variants regulating ORMDL3 expression contribute to the risk of childhood asthma. *Nature* 2007;448:470.

206. Allen M, Heinzmann A, Noguchi E, Abecasis G, Broxholme J, Ponting CP, Bhattacharyya S, Tinsley J, Zhang Y, Holt R, Jones EY, Lench N, Carey A, Jones H, Dickens NJ, Dimon C, Nicholls R, Baker C, Xue L, Townsend E, Kabesch M, Weiland SK, Carr D, von Mutius E, Adcock IM, Barnes PJ, Lathrop GM, Edwards M, Moffatt MF, *et al.* Positional cloning of a novel gene influencing asthma from chromosome 2q14. *Nat Genet* 2003;35:258.

207. Zhang Y, Leaves NI, Anderson GG, Ponting CP, Broxholme J, Holt R, Edser P, Bhattacharyya S, Dunham A, Adcock IM, Pulleyn L, Barnes PJ, Harper JI, Abecasis G, Cardon L, White M, Burton J, Matthews L, Mott R, Ross M, Cox R, Moffatt MF, Cookson WOCM. Positional cloning of a quantitative trait locus on chromosome 13q14 that influences immunoglobulin E levels and asthma. *Nat Genet* 2003;34:181–186.

208. Belgrave D, den Dekker H, Husby A, Sevelsted A. A genome-wide association study identifies CDHR3 as a susceptibility locus for early childhood asthma with severe exacerbations. *Nature* 2013;1–8.

209. Lin F, Song A, Wu J, Jiang X, Long J, Chen J, Duan Y, Shi Y, Deng L. ADAM33 protein expression and the mechanics of airway smooth muscle cells are highly correlated in ovalbumin-sensitized rats. *Mol Med Rep* 2013;8:1209–1215.

210. Linhong Deng, Jiaoyue Long, Yiyuan Duan, Jun Chen, Feng Lin, Rong Xu, Xuemei Jiang. Soluble ADAM33 Determines Mechanical Behaviors Of Airway Smooth Muscle Cells. *A108 Airw SMOOTH MUSCLE NEW WAYS RELAX BEHAVE* American Thoracic Society; 2013. p. A2277–A2277.at

<http://www.atsjournals.org/doi/abs/10.1164/ajrccm-conference.2013.187.1_MeetingAbstracts.A2277>.

211. Linhong Deng, Jiaoyue Long, Yiyuan Duan, Jun Chen, Feng Lin, Rong Xu, Xuemei Jiang. Modulation Of ADAM33 Gene Expression Alters Biomechanical Behavior Of Airway Smooth Muscle Cells. *C30 ROLE SMOOTH MUSCLE CELL Airw Dis* American Thoracic Society; . p. A4132–A4132.at <http://www.atsjournals.org/doi/abs/10.1164/ajrccm-conference.2012.185.1_MeetingAbstracts.A4132>.

212. Gunst SJ, Panettieri RA, Pare PD, Mitzner W. Alterations in Airway Smooth Muscle Phenotype Do/Do Not Cause Airway Hyperresponsiveness in Asthma. *J Appl Physiol* 2012;at <http://jap.physiology.org/content/early/2012/04/12/japplphysiol.00483.2012.abstract>.

213. Halayko A, Tran T, Gosens R. Phenotype and functional plasticity of airway smooth muscle: role of caveolae and caveolins. *Proc Am* 2008;1–9.

214. Wright DB, Trian T, Siddiqui S, Pascoe CD, Johnson JR, Dekkers BGJ, Dakshinamurti S, Bagchi R, Burgess JK, Kanabar V, Ojo OO. Phenotype modulation of airway smooth muscle in asthma. *Pulm Pharmacol Ther* 2013;26:42–9.

215. Loop FT van der, Schaart G, Timmer ED, Ramaekers FC, Eys GJ van. Smoothelin, a novel cytoskeletal protein specific for smooth muscle cells. *J Cell Biol* 1996;134:401–411.

216. Gunst SJ, Zhang W. Actin cytoskeletal dynamics in smooth muscle: a new paradigm for the regulation of smooth muscle contraction. *Am J Physiol - Cell Physiol* 2008;295:C576–C587.

217. Sieck GC, White TA, Thompson MA, Pabelick CM, Wylam ME, Prakash YS. Regulation of store-operated Ca2+ entry by CD38 in human airway smooth muscle. *Am J Physiol - Lung Cell Mol Physiol* 2008;294:L378–L385.

218. Sathish V, Thompson M, Sinha S, Sieck G. Inflammation, caveolae and CD38-mediated calcium regulation in human airway smooth muscle. *Biophys Acta BBA* 2013;1–6.

219. Wang D-Z, Olson EN. Control of smooth muscle development by the myocardin family of transcriptional coactivators. *Curr Opin Genet Dev* 2004;14:558.

220. Gupta S, Halushka MK, Hilton GM, Arking DE. Postmortem cardiac tissue maintains gene expression profile even after late harvesting. *BMC Genomics* 2012;13:26.

221. Matsumoto H, Moir LM, Oliver BGG, Burgess JK, Roth M, Black JL, McParl BE, McParland BE. Comparison of gel contraction mediated by airway smooth muscle cells from patients with and without asthma. *Thorax* 2007;62:848–854.

222. Benayoun L, Druilhe A, Dombret M-C, Aubier M, Pretolani M. Airway Structural Alterations Selectively Associated with Severe Asthma. *Am J Respir Crit Care Med* 2003;167:1360–1368.

223. Ammit AJ, Armour CL, Black JL. Smooth-muscle myosin light-chain kinase content is increased in human sensitized airways. *Am J Respir Crit Care Med* 2000;161:257–63.

224. Babu GJ, Warshaw DM, Periasamy M. Smooth muscle myosin heavy chain isoforms and their role in muscle physiology. *Microsc Res Tech* 2000;50:532–540.

225. Babu GJ, Loukianov E, Loukianova T, Pyne GJ, Huke S, Osol G, Low RB, Paul RJ, Periasamy M. Loss of SM-B myosin affects muscle shortening velocity and maximal force development. *Nat Cell Biol* 2001;3:1025.

226. Karagiannis P, Babu GJ, Periasamy M, Brozovich FV. Myosin heavy chain isoform expression regulates shortening velocity in smooth muscle: studies using an SMB KO mouse line. *J Muscle Res Cell Motil* 2004;25:149–158.

227. Lauzon AM, Tyska MJ, Rovner AS, Freyzon Y, Warshaw DM, Trybus KM. A 7-amino-acid insert in the heavy chain nucleotide binding loop alters the kinetics of smooth muscle myosin in the laser trap. *J Muscle Res Cell Motil* 1998;19:825–837.

228. Jude JA, Wylam ME, Walseth TF, Kannan MS. Calcium Signaling in Airway Smooth Muscle. *Proc Am Thorac Soc* 2008;5:15–22.

229. Lee HC. Structure and Enzymatic Functions of Human CD38. *Mol Med* 2006;12:317–323.

230. Deshpande DA, White TA, Guedes AGP, Milla C, Walseth TF, Lund FE, Kannan MS. Altered airway responsiveness in CD38-deficient mice. *Am J Respir Cell Mol Biol* 2005;32:149–156.

231. Deshpande DA, Dogan S, Walseth TF, Miller SM, Amrani Y, Panettieri RA, Kannan MS. Modulation of calcium signaling by interleukin-13 in human airway smooth muscle: role of CD38/cyclic adenosine diphosphate ribose pathway. *Am J Respir Cell Mol Biol* 2004;31:36–42.

232. Franco L, Bruzzone S, Song P, Guida L, Zocchi E, Walseth TF, Crimi E, Usai C, De Flora A, Brusasco V. Extracellular cyclic ADP-ribose potentiates ACh-induced contraction in bovine tracheal smooth muscle. *Am J Physiol Lung Cell Mol Physiol* 2001;280:L98–L106.

233. Tliba O, Cidlowski JA, Amrani Y. CD38 expression is insensitive to steroid action in cells treated with tumor necrosis factor-alpha and interferon-gamma by a mechanism involving the up-regulation of the glucocorticoid receptor beta isoform. *Mol Pharmacol* 2006;69:588–596.

234. Brusasco V, Crimi E, Barisione G, Spanevello A, Rodarte JR, Pellegrino R. Airway responsiveness to methacholine: effects of deep inhalations and airway inflammation. *J Appl Physiol Bethesda Md 1985* 1999;87:567–573.

235. Raqeeb A, Jiao Y, Syyong HT, Pare PD, Seow CY. Regulatable stiffness in relaxed airway smooth muscle: a target for asthma treatment? *J Appl Physiol* 2012;112:337–46.

236. Lan B, Wang L, Zhang J, Pascoe CD, Norris BA, Liu JC-Y, Solomon D, Pare PD, Deng L, Seow CY. Rho-kinase mediated cytoskeletal stiffness in skinned smooth muscle. *J Appl Physiol Bethesda Md 1985* 2013;doi:10.1152/japplphysiol.00654.2013.

237. Dowell ML, Lakser OJ, Gerthoffer WT, Fredberg JJ, Stelmack GL, Halayko AJ, Solway J, Mitchell RW. Latrunculin B increases force fluctuation-induced relengthening of ACh-contracted, isotonically shortened canine tracheal smooth muscle. *J Appl Physiol* 2005;98:489–497.

238. Niessen P, Rensen S, van Deursen J, De Man J, De Laet A, Vanderwinden J-M, Wedel T, Baker D, Doevendans P, Hofker M, Gijbels M, van Eys G. Smoothelin-a is essential for functional intestinal smooth muscle contractility in mice. *Gastroenterology* 2005;129:1592–1601.

239. Van Eys GJ, Niessen PM, Rensen SS. Smoothelin in Vascular Smooth Muscle Cells. *Trends Cardiovasc Med* 2007;17:26–30.

240. Nakamura F, Stossel TP, Hartwig JH. The filamins: organizers of cell structure and function. *Cell Adhes Migr* 2011;5:160–9.

241. Feng Y, Chen M, Moskowitz I. Filamin A (FLNA) is required for cell–cell contact in vascular development and cardiac morphogenesis. *Proc Of* 2006. p. 19836–19841.at <http://www.pnas.org/content/103/52/19836.short>.

242. Lambrecht BN, Hammad H. The airway epithelium in asthma. *Nat Med* 2012;18:684–692.

243. Feng Y, Walsh CA. The many faces of filamin: A versatile molecular scaffold for cell motility and signalling. *Nat Cell Biol* 2004;6:1034–1038.

244. Yick CY, Zwinderman AH, Kunst PW, Grünberg K, Mauad T, Chowdhury S, Bel EH, Baas F, Lutter R, Sterk PJ. Gene expression profiling of laser microdissected airway smooth muscle tissue in asthma and atopy. *Allergy* 2014;n/a–n/a.doi:10.1111/all.12452.

245. Boelens MC, Meerman GJ te, Gibcus JH, Blokzijl T, Boezen HM, Timens W, Postma DS, Groen HJ, Berg A van den. Microarray amplification bias: loss of 30% differentially expressed genes due to long probe – poly(A)-tail distances. *BMC Genomics* 2007;8:277.

246. Li JZ, Vawter MP, Walsh DM, Tomita H, Evans SJ, Choudary PV, Lopez JF, Avelar A, Shokoohi V, Chung T, Mesarwi O, Jones EG, Watson SJ, Akil H, Bunney WE, Myers RM. Systematic changes in gene expression in postmortem human brains associated with tissue pH and terminal medical conditions. *Hum Mol Genet* 2004;13:609–616.

247. Wang Y, Liu CL, Storey JD, Tibshirani RJ, Herschlag D, Brown PO. Precision and functional specificity in mRNA decay. *Proc Natl Acad Sci* 2002;99:5860–5865.

248. Paré PD, Roberts CR, Bai TR, Wiggs BJ. The functional consequences of airway remodeling in asthma. *Monaldi Arch Chest Dis Arch Monaldi Mal Torace Fondazione Clin Lav IRCCS Ist Clin Tisiol E Mal Appar Respir Univ Napoli Secondo Ateneo* 1997;52:589–596.

249. McParland BE, Macklem PT, Pare PD. Airway wall remodeling: friend or foe? *J Appl Physiol* 2003;95:426–34.

250. Seow CY. Passive stiffness of airway smooth muscle: the next target for improving airway distensibility and treatment for asthma? *Pulm Pharmacol Ther* 2013;26:37–41.

251. Gunst SJ, Reynold A. Panettieri J. Point:Counterpoint: Alterations in airway smooth muscle phenotype do/do not cause airway hyperresponsiveness in asthma. *J Appl Physiol* 2012;113:837–839.

252. Deng L, Fairbank NJ, Fabry B, Smith PG, Maksym GN. Localized mechanical stress induces time-dependent actin cytoskeletal remodeling and stiffening in cultured airway smooth muscle cells. *Am J Physiol - Cell Physiol* 2004;287:C440–C448.

253. Janssen LJ. Calcium handling in airway smooth muscle: mechanisms and therapeutic implications. *Can Respir J J Can Thorac Soc* 1998;5:491–498.

254. Cattaruzza M, Lattrich C, Hecker M, Cattaruzza M, Lattrich C, Hecker M. Focal Adhesion Protein Zyxin Is a Mechanosensitive Modulator of Gene Expression in Vascular Smooth Muscle Cells. *Hypertension* 2004;43:726–730.

255. Sukkar MB, Stanley AJ, Blake AE, Hodgkin PD, Johnson PRA, Armour CL, Hughes JM. "Proliferative" and "synthetic" airway smooth muscle cells are overlapping populations. *Immunol Cell Biol* 2004;82:471–478.

256. Chiu WW-C. *Multi-scale Models of Respiratory Impedance and Bimodal Ventilation*. Bioengineering, University of Auckland; 2011.

257. Lutchen KR, Costa KD. Physiological interpretations based on lumped element models fit to respiratory impedance data: use of forward-inverse modeling. *IEEE Trans Biomed Eng* 1990;37:1076–1086.

Appendices

Appendix A

Supplement to chapter 4.

Mathematical Model

This section describes the details of the whole lung computational model. The purpose of this model is to ascertain how alterations to the ASM force-length behavior caused by prior DIs, as measured in this work, might regulate the re-opening of closed airways during a DI. Thus the model begins from a bi-stable, constricted state, assumed to result from agonist challenge. The existence of such a state is predicated on the work of others who have considered how such a state might form (186–188). From such a bistable, constricted state, we then examine the reopening which occurs in response to a DI in both the bronchoprotective and control cases.

The airway tree employed in the computational model is derived from Tawhai et al. (182) with large orders extracted from CT imaging and the remainder generated by a computational algorithm. The lung considered thus has 30,941 airways, up to Horsfield order 24.

The dynamics of each individual airway are assumed to be

$$\frac{dr}{dt}=\varrho(\Phi(r)-r) \qquad [1]$$

where r is the luminal radius (183, 184). The function $\Phi(r)$ describes the steady state behaviour of the airway, due to a combination of the Lambert model for the airway wall (153), the Lai-Fook model for parenchymal tethering (203) and the Laplace law. Thus

$$\Phi(r)=R(P(r)) \qquad [2]$$

by composition where the airway wall mechanics are given by Lambert model (153) as

$$R(P)=\begin{cases} \sqrt{R_i^2(1-P/P_1)^{-n_1}}; & P\leq 0 \\ \sqrt{r_{imax}^2-(r_{imax}^2-R_i^2)(1-P/P_2)^{-n_2}}; & P>0 \end{cases} \qquad [3]$$

and the transmural pressure is

$$P(r)=P_0-\frac{\kappa(r_{sm})\times(r_m-r_w)}{r_{sm}}+\tau(r). \qquad [4]$$

The parenchymal tethering $\tau(r)$ is given by Lai-Fook (203) as

$$\tau(r)=2\mu\left(\left(\frac{R_{ref}-r_i}{R_{ref}}\right)+1.5\left(\frac{R_{ref}-r_i}{R_{ref}}\right)^2\right) \qquad [5]$$

and the smooth muscle radius is

$$r_{sm} =(r_w+r_m)/2, \text{ where} \qquad [6]$$

$$r_w =R_i\sqrt{(1+\varepsilon_w)^2+(r/R_i)^2-1} \text{ and} \qquad [7]$$

$$r_m =R_i\sqrt{(1+\varepsilon_w+\varepsilon_m)^2+(r/R_i)^2-1}. \qquad [8]$$

The ASM force-length behaviour is captured by the term $\kappa(r_{sm})$ and depends on the smooth muscle length. We fit the experimental data (force-length curves during force-controlled DI, from this manuscript) as

$$\kappa_u=\hat{\kappa}\times\left(1-p_1\sqrt{1-L_0}+p_1\sqrt{L-L_0}\right) \qquad [9]$$

in the stretching phase, and

$$\kappa_d=\hat{\kappa}\times\left(p_1\sqrt{1-L_0}+p_1\sqrt{L-L_0}+p_2\sqrt{L-L}\right) \qquad [10]$$

when re-shortening. Here $L=2\pi r_{sm}$ and normalized to reference length, and $\hat{L}$ is the maximum length for each airway during the maneuver.

The agonist challenged lung state is determined by assuming that the $\hat{\kappa}$ are drawn from a normal distribution with prescribed coefficient of variation (cv). The mean of this distribution is then adjusted to reach the target respiratory resistance (5 cm H_20 at 1 Hz). If the resulting ASM tension for an individual airway lies in the region with both open and closed branches, a branch is selected at random with equal probability. Simulations with varied cv were also carried out to test the effects of this parameter (see below).

Deep inspirations were simulated by making the parameters P_0 and μ time dependent, with a sinusoidal deep breath of duration 8 sec and depth 30 cmH_2O.

Individual airway radius and ASM force from the simulations is shown in Fig. A1; these correspond to the distributions shown in Fig. 8, but now give individual force-radius points for each airway, rather than distributions. The left panel shows the small airways in the challenged state, with a clear bimodal pattern. The center panel shows the changes due to a DI, without prior DIs (control), with the grey lines showing the overall change for each airway from the beginning of the DI to the end, and the grey crosses the final distribution after the end of the DI. Thus lines crossing from the closed population to the open population are the reopening airways. The right panel gives the same information in black for the DI with prior DIs (bronchoprotective). Clearly there is additional reopening, and the mechanism for this is the response of the ASM to the DI-induced stretch – specifically, the extent to which airway dilation increases ASM force, as represented by the slope of the response to DI in the force-radius plane. If the slope is steeper (e.g. the ASM force at the end of the DI is lower), then a larger fraction of the airways from the closed population reach the stable, open branch and stay there (hence that airway has reopened).

Respiratory resistance is calculated by a circuit analog model (256, 257). Note that we use resistance because of challenges in simulating FEV1 directly; however the inclusion of the FEV1-like DI immediately prior to resistance measurement allows us to capture the crucial response to this maneuver.

Sensitivity analysis with respect to both the coefficient of variation of ASM force, and the parenchymal modulus μ was carried out; results presented are typical for large areas of parameter space. The quantitative results given are computed for 50% coefficient of variation of ASM force, though sensitivity analysis showed broadly similar results for coefficients of variation ranging from 10%-100%.

The radius distributions shown in the manuscript have been estimated from the samples by kernel density estimation, using `MATLAB`'s built-in `ksdensity()`.

Reference radii are taken to be $r_{ref}=R(P_{ref})$. Order dependent parameters are taken from (185), and the rest are given in Table A1.

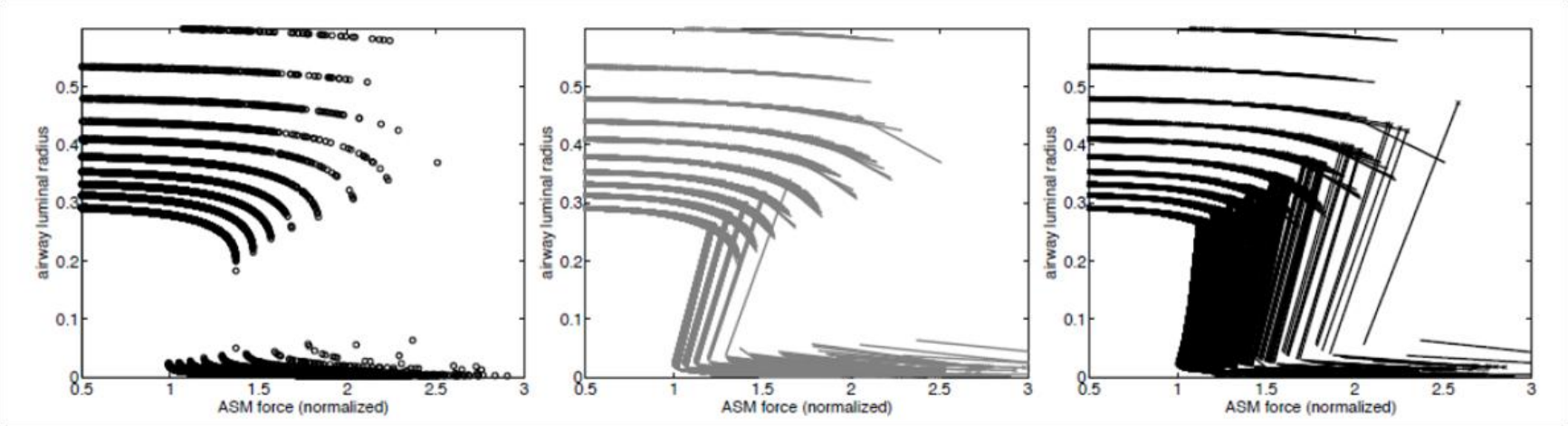

Figure A.1 ASM force and airway radii for the small airways. The three panels illustrate three states of the lung; the left panel is the challenged/constricted lung, with a clear bimodal distribution (with respect to radii). The center panel shows the response to DI (without prior DIs), with a number of airways being reopened, indicated by the grey lines taking a previously closed airway into an open position. The right panel shows the effect of a DI with prior DIs; here many more airways are reopened, primarily on account of the altered rate of force increase with stretch, due to altered ASM dynamics. The striations in each figure are a result of the discrete families of airways classified by Horsfield order

parameter	value
P_0	25 cmH_2O
μ	10 cmH_2O
P_{ref}	10 cmH_2O
L_0	0.9
p_1 (control)	4.1
p_2 (control)	-5.9
p_1 (prior DIs)	3.4
p_2 (prior DIs)	-5.3
ϱ	2 (1/s)

Table A.1 Model parameters

Appendix B

Supplementary to Chapter 5.

		Gene Counts				p-values	
Gene	**Description**	**Non-Asthmatic**	**Asthmatic**	**Fatal Asthmatic**	**Non-Fatal Asthmatic**	**Non-Asthmatic vs. Asthmatic**	**Non-Asthmatic vs. Fatal Asthmatic**
Structural Contractile Genes							
ACTA2	α-Smooth Muscle Actin	4774 ± 587.1	4626 ± 732.2	4130 ± 561.3	5619 ± 1983	0.874	0.505
ACTG1	Actin Gamma 1	13585 ± 1675.3	10473 ± 764.34	9946 ± 808.7	11528 ± 1678.9	**0.041**	**0.028**
ACTN1	Actinin 1	1006 ± 78.69	929 ± 72.7	915 ± 87.0	957 ± 150	0.454	0.425
ACTN4	Actinin 4	1846 ± 171.7	1350 ± 120.3	1376 ± 118.3	1297 ± 304.0	**0.025**	0.056
CALD1	Caldesmon 1	1286 ± 172.0	818 ± 125	756 ± 93.5	942 ± 350	**0.034**	**0.026**
CNN1	Calponin 1	268 ± 41.1	220 ± 38.6	222 ± 47.7	215 ± 75.7	0.404	0.480
CNN2	Calponin 2	1316 ± 117.1	1027 ± 86.86	1030 ± 116.3	1021 ± 141.0	0.065	0.100
CNN3	Calponin 3	3309 ± 431.2	2064 ± 197.4	2069 ± 201.1	2054 ± 489.6	**0.007**	**0.015**
MYH11	Myosin Heavy Chain 11	1564 ± 212.0	1328 ± 232.4	1402 ± 299.2	1179 ± 406.3	0.445	0.646
MYH15	Myosin Heavy Chain 15	8 ± 0.9	8 ± 0.9	7 ± 0.8	8 ± 2	0.627	0.423
TPM1	Tropomyosin 1	3430 ± 304.1	2791 ± 204.7	2737 ± 160.9	2898 ± 578.4	0.079	0.085
TPM2	Tropomyosin 2	5662 ± 656.7	5497 ± 441.7	5548 ± 578.0	5396 ± 763.2	0.824	0.891
TPM3	Tropomyosin 3	2103 ± 127.0	1826 ± 81.05	1777 ± 101.8	1923 ± 138.4	0.056	**0.041**
TPM4	Tropomyosin 4	2836 ± 373.2	2063 ± 213.4	2019 ± 214.0	2151 ± 532.5	**0.049**	0.059
Regulatory Contractile Genes							
ADBR1	Adrenoceptor Beta 1	262 ± 29.4	297 ± 56.2	361 ± 75.0	170 ± 22.4	0.551	0.145
ADBR2	Adrenoceptor Beta 2	321 ± 19.6	308 ± 32.6	342 ± 40.1	239 ± 42.9	0.735	0.611
ARAF	A-Raf Proto-Oncogene Serine/Threonine Kinase	242 ± 10.5	238 ± 10.5	240 ± 12.9	234 ± 20.4	0.793	0.909
ARHGEF1	Rho Guanine Nucleotide Exchange Factor 1	850 ± 65.1	941 ± 49.1	954 ± 55.3	914 ± 109	0.254	0.245
ARHGEF11	Rho Guanine Nucleotide Exchange Factor 11	179 ± 9.63	149 ± 10.2	156 ± 14.1	134 ± 10.3	**0.032**	0.132

		Gene Counts				p-values	
Gene	**Description**	**Non-Asthmatic**	**Asthmatic**	**Fatal Asthmatic**	**Non-Fatal Asthmatic**	**Non-Asthmatic vs. Asthmatic**	**Non-Asthmatic vs. Fatal Asthmatic**
ARHGEF12	Rho Guanine Nucleotide Exchange Factor 12	98 ± 7.2	77 ± 6.8	82 ± 9.0	68 ± 9.5	**0.040**	0.151
GNA11	Guanine Nucleotide Binding Protein Alpha 11	1616 ± 76.61	1457 ± 97.43	1593 ± 106.3	1184 ± 120.3	0.209	0.859
GNA12	Guanine Nucleotide Binding Protein Alpha 12	278 ± 16.0	247 ± 14.2	256 ± 19.0	231 ± 20.0	0.160	0.355
GNA13	Guanine Nucleotide Binding Protein Alpha 13	1032 ± 48.10	1004 ± 68.57	941 ± 77.7	1130 ± 125.1	0.736	0.293
GNAQ	Guanine Nucleotide Binding Protein Q	1513 ± 63.20	1312 ± 63.13	1348 ± 88.51	1241 ± 68.87	**0.027**	0.094
GNAS	GNAS Complex Locus	1368 ± 72.49	1297 ± 48.64	1364 ± 57.52	1162 ± 38.61	0.408	0.967
ILK	Integrin Linked Kinase	731 ± 35.2	753 ± 41.7	779 ± 48.9	701 ± 81.6	0.681	0.423
MAP2K1	Mitogen-Activated Protein Kinase Kinase 1	339 ± 30.8	284 ± 16.7	273 ± 17.9	306 ± 36.6	0.100	0.072
MAP2K2	Mitogen-Activated Protein Kinase Kinase 2	1459 ± 69.03	1480 ± 60.64	1475 ± 77.29	1488 ± 112.0	0.814	0.866
MAPK1	Mitogen-Activated Protein Kinase 1	1174 ± 58.62	893 ± 42.7	907 ± 47.2	865 ± 96.4	**0.001**	**0.002**
MAPK3	Mitogen-Activated Protein Kinase 3	568 ± 31.2	468 ± 28.1	490 ± 38.2	424 ± 29.5	**0.017**	0.082
MYLK1	Myosin Light Chain Kinase 1	2267 ± 227.7	1680 ± 246.8	1695 ± 278.3	1651 ± 554.9	0.106	0.158
MYLK2	Myosin Light Chain Kinase 2	9 ± 0.8	9 ± 0.8	10 ± 0.95	9 ± 1	0.570	0.430
MYLK3	Myosin Light Chain Kinase 3	123 ± 19.7	91 ± 18	114 ± 23.3	46 ± 9.9	0.233	0.772
PPP1CA	Myosin Light Chain Phosphatase Catalytic Subunit Alpha	1495 ± 115.9	1251 ± 55.44	1270 ± 61.50	1213 ± 124.2	0.063	0.123

		Gene Counts				p-values	
Gene	**Description**	**Non-Asthmatic**	**Asthmatic**	**Fatal Asthmatic**	**Non-Fatal Asthmatic**	**Non-Asthmatic vs. Asthmatic**	**Non-Asthmatic vs. Fatal Asthmatic**
PPP1CB	Myosin Light Chain Phosphatase Catalytic Subunit Beta	4750 ± 287.7	4234 ± 192.9	4401 ± 243.2	3900 ± 278.5	0.132	0.352
PPP1CC	Myosin Light Chain Phosphatase Catalytic Subunit Gamma	637 ± 24.6	567 ± 17.0	579 ± 20.6	544 ± 30.5	**0.018**	0.069
PPP1R12A	Myosin Light Chain Phosphatase Regulatory Subunit 12A (MYPT1)	601 ± 44.3	469 ± 38.1	457 ± 42.4	491 ± 85.3	**0.029**	**0.031**
PPP1R12B	Myosin Light Chain Phosphatase Regulatory Subunit 12B (MYPT2)	706 ± 46.7	626 ± 59.9	658 ± 75.9	564 ± 103	0.281	0.557
PPP1R14A	Myosin Light Chain Phosphatase Regulatory Subunit 14A (CPI-17)	278 ± 38.9	185 ± 15.6	186 ± 16.4	183 ± 37.7	**0.020**	**0.038**
PRKACA	Protein Kinase A cAMP-Dependent Catalytic Alpha	1221 ± 56.83	1045 ± 49.33	1020 ± 50.09	1095 ± 117.6	**0.020**	**0.016**
PRKACB	Protein Kinase A cAMP-Dependent Catalytic Beta	220 ± 19.6	176 ± 26.1	167 ± 23.6	194 ± 69.0	0.152	0.113
PRKACG	Protein Kinase A cAMP-Dependent Catalytic Gamma	33 ± 3.7	27 ± 4.3	31 ± 5.8	20 ± 4.5	0.351	0.785
PRKCA	Protein Kinase C Alpha	170 ± 9.81	133 ± 14.3	140 ± 19.6	120 ± 19.5	**0.041**	0.126
PRKCB	Protein Kinase C Beta	205 ± 19.7	267 ± 28.7	255 ± 41.9	291 ± 24.1	0.063	0.158
PRKCD	Protein Kinase C Delta	934 ± 37.6	902 ± 50.0	930 ± 63.6	845 ± 83.5	0.607	0.953
PRKCE	Protein Kinase C Epsilon	874 ± 46.4	634 ± 38.2	636 ± 48.9	630 ± 70.0	**0.001**	**0.002**
PRKCG	Protein Kinase C Gamma	9 ± 0.8	8 ± 1	9 ± 1	5 ± 1	0.557	0.674
PRKCH	Protein Kinase C Eta	773 ± 31.9	647 ± 47.0	651 ± 57.1	638 ± 94.9	**0.035**	0.066
PRKCQ	Protein Kinase C Theta	126 ± 6.75	143 ± 8.61	144 ± 11.4	142 ± 14.6	0.112	0.141

		Gene Counts				p-values	
Gene	**Description**	**Non-Asthmatic**	**Asthmatic**	**Gene**	**Description**	**Non-Asthmatic**	**Asthmatic**
PRKG1	Protein Kinase A cGMP-Dependent Type 1	174 ± 14.8	127 ± 14.9	133 ± 18.4	114 ± 28.2	**0.038**	0.106
PRKX	Protein Kinase A X-Linked	157 ± 10.7	171 ± 13.1	186 ± 13.8	140 ± 23.4	0.399	0.116
RAF1	Raf-1 Proto-Oncogene Serine/Threonine Kinase	668 ± 45.0	546 ± 25.2	543 ± 27.8	550 ± 58.1	**0.019**	**0.031**
RGS2	Regulator of G-Protein Signaling 2	820 ± 103	1052 ± 125.0	962 ± 138	1231 ± 258.6	0.137	0.376
RHOA	Ras Homolog Family Member A	720 ± 70.9	489 ± 38.8	501 ± 52.8	465 ± 57.6	**0.004**	**0.014**
ROCK1	Rho Kinase 1	1181 ± 55.80	976 ± 53.57	960 ± 73.30	1010 ± 77.02	**0.011**	**0.013**
ROCK2	Rho Kinase 2	1501 ± 77.12	1346 ± 69.63	1328 ± 80.29	1381 ± 150.4	0.135	0.134
TAS2R13	Taste Receptor Type 2 Member 13	38 ±3.9	40 ± 3.0	40 ± 4.2	39 ± 3.3	0.664	0.645
TAS2R14	Taste Receptor Type 2 Member 14	111 ± 7.63	99 ± 7.7	102 ± 11.4	91 ± 3.8	0.249	0.485
TAS2R19	Taste Receptor Type 2 Member 19	62 ± 5.1	54 ± 3.6	54 ± 4.7	55 ± 5.9	0.228	0.257
TAS2R38	Taste Receptor Type 2 Member 38	9 ± 0.7	8 ± 0.8	8 ± 1	6 ± 1	0.405	0.765
Structural Cytoskeletal Genes							
ACTB	Actin Beta	19309 ± 1504.7	16498 ± 876.93	15870 ± 952.33	17754 ± 1854.1	0.085	0.053
ACTG1	Actin Gamma 1	13585 ± 1675.3	10473 ± 764.34	9946 ± 808.7	11528 ± 1678.9	**0.041**	**0.028**
ATCG2	Actin Gamma 2	1916 ± 297.2	1997 ± 484.1	1617 ± 455.9	2756 ± 1149	0.893	0.612
ACTN1	Actinin Alpha 1	1006 ± 78.69	929 ± 72.7	915 ± 87.0	957 ± 150	0.454	0.425
ACTN4	Actinin Apha 4	1846 ± 171.7	1350 ± 120.3	1376 ± 118.3	1297 ± 304.0	**0.025**	0.056
ACTR2	Actin-Related Protein 2	3002 ± 119.0	2800 ± 138.3	2617 ± 132.7	3166 ± 247.8	0.258	**0.033**
ACTR3	Actin-Related Protein 3	2445 ±179.1	2010 ± 161.2	1838 ± 164.4	2355 ± 316.3	0.068	**0.015**
DAG1	Dystroglycan 1	396 ± 27.5	337 ± 20.3	355 ± 26.9	301 ± 22.6	0.094	0.287
DES	Desmin	1592 ± 258.9	1415 ± 345.1	1609 ± 492.0	1026 ± 324.8	0.677	0.972

		Gene Counts				p-values	
Gene	**Description**	**Non-Asthmatic**	**Asthmatic**	**Fatal Asthmatic**	**Non-Fatal Asthmatic**	**Non-Asthmatic vs. Asthmatic**	**Non-Asthmatic vs. Fatal Asthmatic**
DMD	Dystrophin	322 ± 27.4	272 ± 22.6	306 ± 26.0	203 ± 11.2	0.149	0.651
FILIP1	Filamin A Interacting Protein 1	326 ± 15.6	287 ± 19.2	300 ± 25.9	261 ± 24.4	0.124	0.348
FLNA	Filamin Alpha	5596 ± 597.8	4017 ± 455.4	3837 ± 432.2	4378 ± 1160	**0.039**	**0.035**
FLNB	Filamin Beta	1063 ± 93.89	656 ± 61.4	711 ± 71.1	547 ± 109	**0.002**	**0.011**
FLNC	Filamin Gamma	111 ± 16.2	107 ± 19.3	117 ± 26.9	87 ± 23	0.870	0.836
HSPB1	Heat Shock 27kDa Protein	847 ± 74.4	975 ± 133	1136 ± 171.1	653 ± 73.3	0.373	0.070
PARVA	Parvin Alpha	1327 ± 114.7	985 ± 67.2	1050 ± 77.19	855 ± 116	**0.014**	0.066
PARVB	Parvin Beta	169 ± 6.07	144 ± 9.31	131 ± 10.3	170 ± 11.4	**0.039**	**0.002**
PXN	Paxillin	476 ± 22.7	393 ± 18.4	392 ± 24.4	395 ± 30.8	**0.005**	**0.011**
SGCD	Sarcoglycan D	26 ± 2.0	28 ± 1.9	28 ± 2.8	28 ± 1.3	0.564	0.600
SMTN	Smoothelin	276 ± 24.9	350 ± 30.5	384 ± 32.3	282 ± 55.2	0.066	**0.019**
SNTB2	Syntrophin Beta 2	555 ± 24.2	498 ± 29.1	512 ± 29.2	468 ± 69.9	0.133	0.312
TAGLN	Transgelin	4422 ± 619.0	3527 ± 488.2	3179 ± 378.3	4223 ± 1308	0.242	0.124
TLN1	Talin 1	2994 ± 169.6	2329 ± 143.4	2291 ± 170.7	2405 ± 295.4	**0.005**	**0.007**
TLN2	Talin 2	89 ± 8.1	62 ± 6.3	64 ± 8.6	57 ± 8.7	**0.011**	**0.035**
VCL	Vinculin	1237 ± 142.6	880 ±120	861 ± 135	917 ± 270	0.064	0.078
VIM	Vimentin	8915 ± 354.0	7026 ± 509.3	6893 ± 548.3	7292 ± 1189	**0.008**	**0.010**
WASL	Wiskott-Aldrich Syndrome-Like Protein	457 ± 29.3	361 ± 27.3	381 ± 34.1	319 ± 44.0	**0.029**	0.115
ZYX	Zyxin	4385 ± 421.0	5375 ± 420.9	5288 ± 581.4	5548 ± 597.1	0.092	0.162
Regulatory Cytoskeletal Genes							
ARAF	A-Raf Proto-Oncogene	242 ± 10.5	238 ± 10.5	240 ± 12.9	234 ± 20.4	0.793	0.909
ARHGEF1	Rho Guanine Nucleotide Exchange Factor 1	850 ± 65.1	941 ± 49.1	954 ± 55.3	914 ± 109	0.254	0.245
ARHGEF11	Rho Guanine Nucleotide Exchange Factor 11	179 ± 9.63	149 ± 10.2	156 ± 14.1	134 ± 10.3	**0.032**	0.132

		Gene Counts				p-values	
Gene	**Description**	**Non-Asthmatic**	**Asthmatic**	**Fatal Asthmatic**	**Non-Fatal Asthmatic**	**Non-Asthmatic vs. Asthmatic**	**Non-Asthmatic vs. Fatal Asthmatic**
ARHGEF12	Rho Guanine Nucleotide Exchange Factor 12	98 ± 7.2	77 ± 6.8	82 ± 9.0	68 ± 9.5	**0.040**	0.151
GNA11	Guanine Nucleotide Binding Protein Alpha 11	1616 ± 76.61	1457 ± 97.43	1593 ± 106.3	1184 ± 120.3	0.209	0.859
GNA12	Guanine Nucleotide Binding Protein Alpha 12	278 ± 16.0	247 ± 14.2	256 ± 19.0	231 ± 20.0	0.160	0.355
GNA13	Guanine Nucleotide Binding Protein Alpha 13	1032 ± 48.10	1004 ± 68.57	941 ± 77.7	1130 ± 125.1	0.736	0.293
GNAQ	Guanine Nucleotide Binding Protein Q Polypeptide	1513 ± 63.20	1312 ± 63.13	1348 ± 88.51	1241 ± 68.87	**0.027**	0.094
GNAS	GNAS Complex Locus	1368 ± 72.49	1297 ± 48.64	1364 ± 57.52	1162 ± 38.61	0.408	0.967
MAP2K1	Mitogen-Activated Protein Kinase Kinase 1	339 ± 30.8	284 ± 16.7	273 ± 17.9	306 ± 36.6	0.100	0.072
MAP2K2	Mitogen-Activated Protein Kinase Kinase 2	1459 ± 69.03	1480 ± 60.64	1475 ± 77.29	1488 ± 112.0	0.814	0.866
PRKCA	Protein Kinase C, Alpha	170 ± 9.81	133 ± 14.3	140 ± 19.6	120 ± 19.5	**0.041**	0.126
PRKCB	Protein Kinase C, Beta	205 ± 19.7	267 ± 28.7	255 ± 41.9	291 ± 24.1	0.063	0.158
PRKCD	Protein Kinase C, Delta	934 ± 37.6	902 ± 50.0	930 ± 63.6	845 ± 83.5	0.607	0.953
PRKCE	Protein Kinase C, Epsilon	874 ± 46.4	634 ± 38.2	636 ± 48.9	630 ± 70.0	**0.001**	**0.002**
PRKCG	Protein Kinase C, Gamma	9 ± 0.8	8 ± 1	9 ± 1	5 ± 1	0.557	0.674
PRKCH	Protein Kinase C, Eta	773 ± 31.9	647 ± 47.0	651 ± 57.1	638 ± 94.9	**0.035**	0.066
PRKCQ	Protein Kinase C, Theta	126 ± 6.75	143 ± 8.61	144 ± 11.4	142 ± 14.6	0.112	0.141
PRKG1	Protein Kinase, Cgmp-Dependent, Type I	174 ± 14.8	127 ± 14.9	133 ± 18.4	114 ± 28.2	**0.038**	0.106
RAF1	Raf-1 Proto-Oncogene Serine/Threonine Kinase	668 ± 45.0	546 ± 25.2	543 ± 27.8	550 ± 58.1	**0.019**	**0.031**
RGS2	Regulator of G-Protein Signaling 2	820 ± 103	1052 ± 125.0	962 ± 138	1231 ± 258.6	0.137	0.376

		Gene Counts				p-values	
Gene	**Description**	**Non-Asthmatic**	**Asthmatic**	**Fatal Asthmatic**	**Non-Fatal Asthmatic**	**Non-Asthmatic vs. Asthmatic**	**Non-Asthmatic vs. Fatal Asthmatic**
RHOA	Ras Homolog Family Member A	720 ± 70.9	489 ± 38.8	501 ± 52.8	465 ± 57.6	**0.004**	**0.014**
ROCK1	Rho Kinase 1	1181 ± 55.80	976 ± 53.57	960 ± 73.30	1010 ± 77.02	**0.011**	**0.013**
ROCK2	Rho Kinase 2	1501 ± 77.12	1346 ± 69.63	1328 ± 80.29	1381 ± 150.4	0.135	0.134
Calcium Handling Genes							
CALM1	Calmodulin 1	575 ± 61.7	348 ± 48.2	371 ± 66.3	301 ± 63.1	**0.007**	**0.030**
CALM2	Calmodulin 2	7216 ± 757.9	4079 ± 429.5	4209 ± 537.3	3818 ± 805.0	**0.001**	**0.005**
CALM3	Calmodulin 3	749 ± 30.5	789 ± 22.7	818 ± 19.8	732 ± 47.0	0.302	0.112
CD38	Cyclic ADP Ribose Hydrolase	996 ± 74.0	633 ± 39.8	646 ± 57.7	608 ± 40.0	**<0.001**	**0.001**
ITPR1	Inositol 1,4,5-Trisphosphate Receptor 1	427 ± 27.0	335 ± 23.7	322 ± 25.7	363 ± 52.0	**0.011**	**0.008**
ITPR2	Inositol 1,4,5-Trisphosphate Receptor 2	214 ± 9.24	197 ± 9.42	184 ± 7.28	224 ± 19.0	0.194	**0.021**
ITPR3	Inositol 1,4,5-Trisphosphate Receptor 3	1539 ± 100.8	1612 ± 120.1	1686 ± 162.8	1463 ± 154.8	0.630	0.389
Growth and Proliferation Genes							
AKT1	V-Akt Murine Thymoma Viral Oncogene Homolog 1	2929 ± 124.6	2852 ± 143.5	2847 ± 176.2	2863 ± 285.7	0.680	0.692
AKT2	V-Akt Murine Thymoma Viral Oncogene Homolog 2	808 ± 30.4	771 ± 34.9	808 ± 42.2	697 ± 48.1	0.422	0.992
AKT3	V-Akt Murine Thymoma Viral Oncogene Homolog 3	1176 ± 61.86	912 ± 57.3	937 ± 59.5	862 ± 135	**0.005**	**0.019**
BRAF	B-Raf Proto-Oncogene, Serine/Threonine Kinase	535 ± 12.1	488 ± 26.1	476 ± 29.8	511 ± 55.7	0.101	0.063
CD38	Cyclic ADP Ribose Hydrolase	996 ± 74.0	633 ± 39.8	646 ± 57.7	608 ± 40.0	**<0.001**	**0.001**
MAPK1	Mitogen-Activated Protein Kinase 1	1174 ± 58.62	893 ± 42.7	907 ± 47.2	865 ± 96.4	**0.001**	**0.002**

		Gene Counts				p-values	
Gene	**Description**	**Non-Asthmatic**	**Asthmatic**	**Fatal Asthmatic**	**Non-Fatal Asthmatic**	**Non-Asthmatic vs. Asthmatic**	**Non-Asthmatic vs. Fatal Asthmatic**
MAPK2	Mitogen-Activated Protein Kinase 3	568 ± 31.2	468 ± 28.1	490 ± 38.2	424 ± 29.5	**0.017**	0.082
MYOCD	Myocardin	74 ± 3.8	78 ± 11	86 ± 15	61 ± 13	0.746	0.305
Housekeeping Genes							
GNB2L1	Guanine Nucleotide-Binding Protein Subunit β-2-Like 1	8866 ± 1629	9826 ± 1483	9801 ± 1525	9877 ± 1622		
GUSB	β-Glucuronidase	191 ± 34.1	205 ± 23.1	206 ± 20.1	202 ± 31.7		
POLR2A	RNA Polymerase R2A	1085 ± 156.8	1175 ± 102.9	1207 ± 80.4	1112 ± 126.2		
RPL19	Ribosomal Protein L19	23289 ± 4077.9	21683 ± 2063.9	21483 ± 1226.7	22081 ± 3433.6		
TBP	TATA Box Binding Protein	253 ± 36.6	207 ± 36.1	202 ± 38.6	217 ± 33.5		

Table B.1 Gene expression counts for all genes in data set.

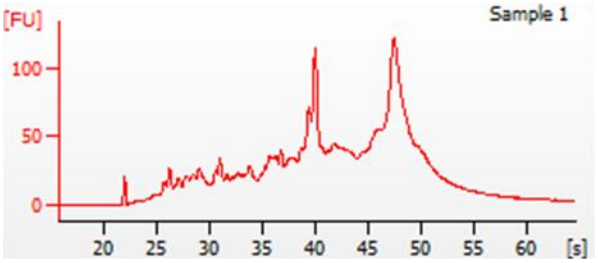

Figure B.1 RNA integrity from frozen lung section. RNA isolated from 20 serially cut frozen lung sections. RIN value was 7.40. Y-axis shows intensity while x-axis is time.

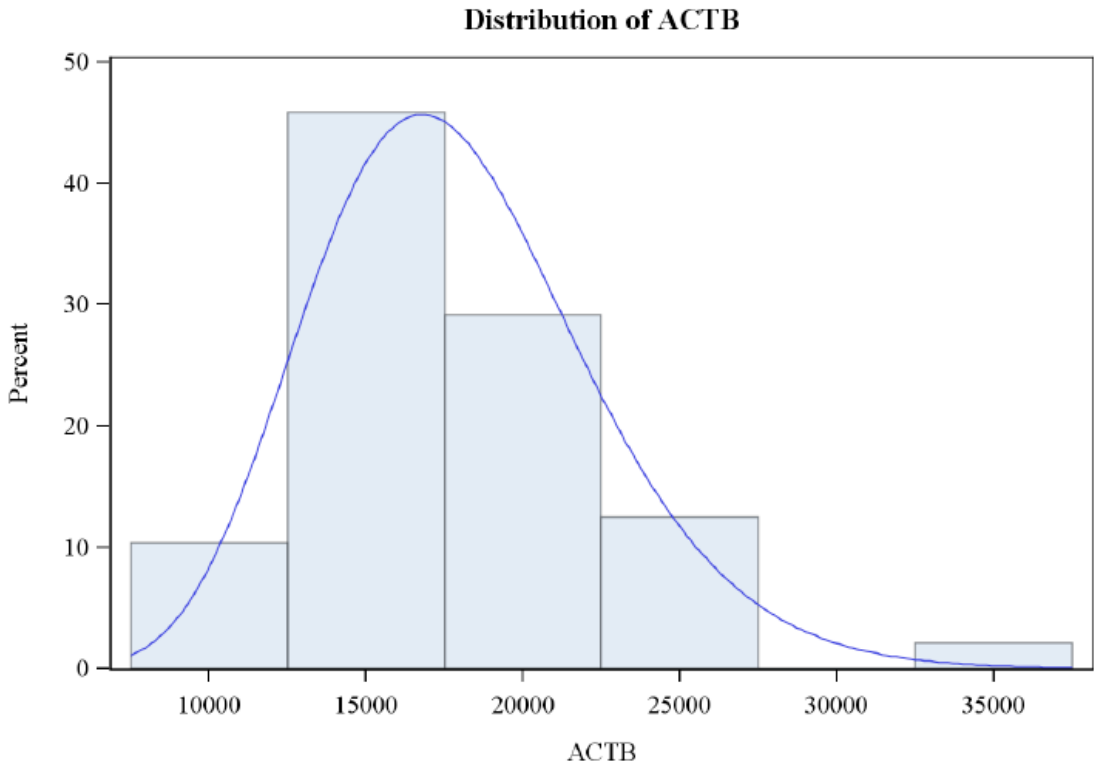

Figure B.2 ACTB gene counts fitted with a gamma distribution.

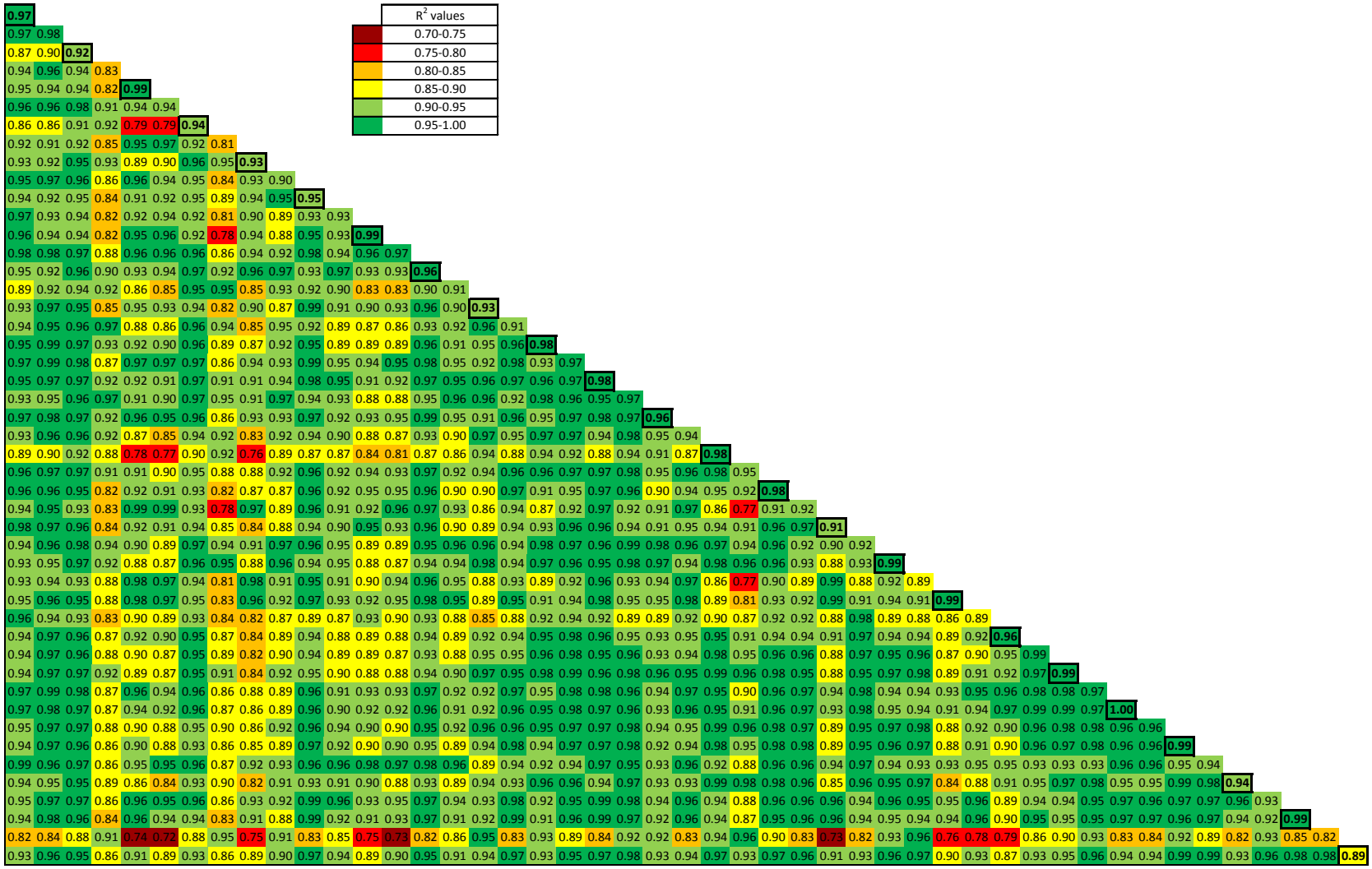

Figure B.3 Correlation of gene expression between sample cores. Values represent the R^2 correlation value. Colours represent strength of correlation (see legend). Values outlined in a dark box represent cores from the same subject. Values not outlined in a dark box represent cores from different subjects.

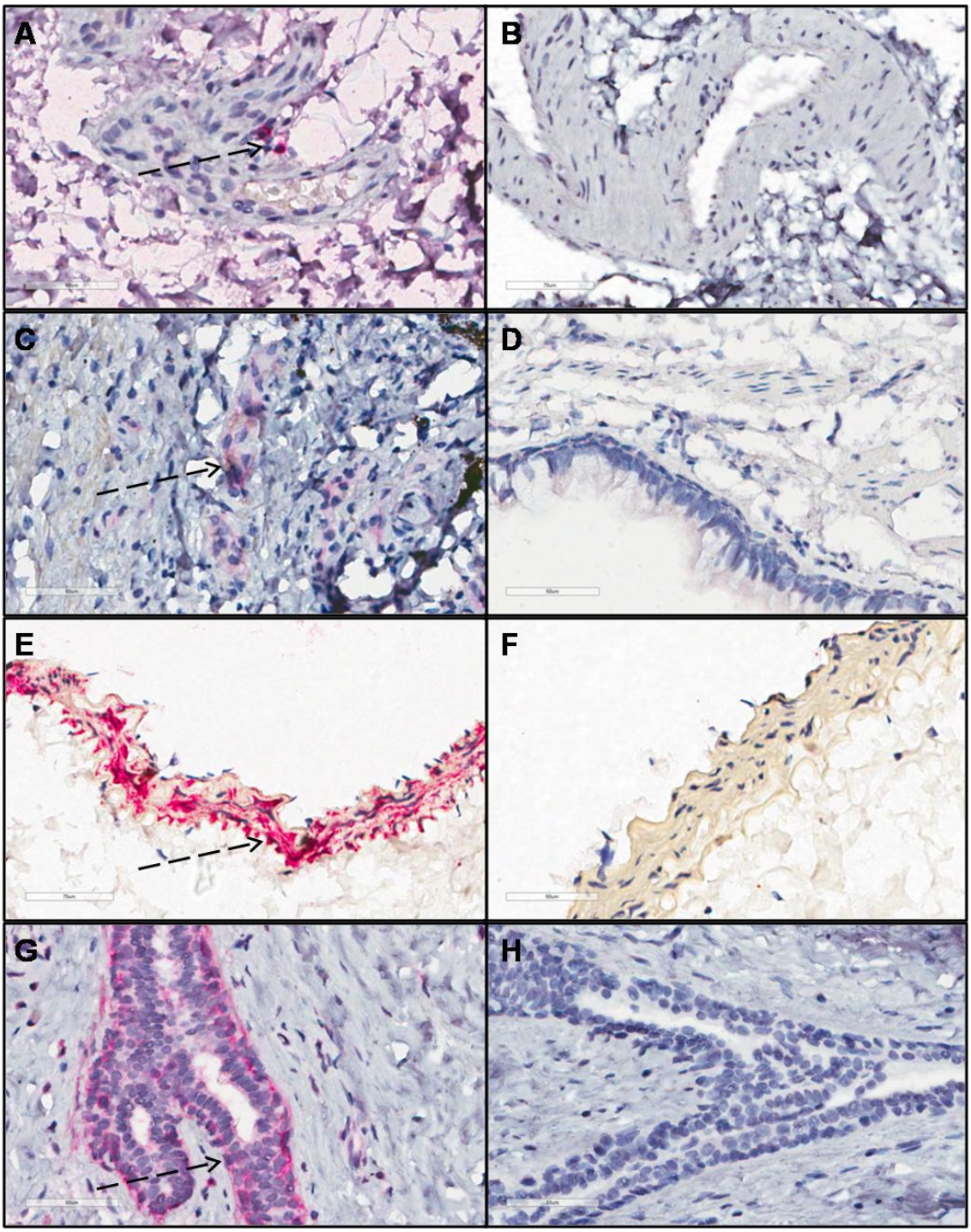

Figure B.4 Positive and negative stains. CD38 positive (A) and negative (B) stained sections of lung cancer. FLNB positive (C) stained section of lung cancer and negative (D) stained section of airway epithelium. SMTN positive (E) and negative (F) stained sections of vascular smooth muscle. ZYX positive (G) and negative (H) stained sections of breast tissue. Dashed arrows point to positive areas.